GAZİ ÜNİVERSİTESİ

1926

TEMPORAL FLOOD RISK ASSESSMENT BY REMOTE SENSING AND GIS: THE CASE STUDY OF ISTANBUL- ESENYURT

A THESIS SUBMITTED TO
THE GRADUATE SCHOOL OF NATURAL AND APPLIED SCIENCES
OF
GAZİ UNIVERSITY

BY

Buse ÖZER

IN PARTIAL FULFILLMENT OF THE REQUIREMENTS
FOR
THE DEGREE OF MASTER OF SCIENCE
IN
CITY AND REGIONAL PLANNING

AUGUST 2023

ETHICAL STATEMENT

I hereby declare that in this thesis study I prepared in accordance with thesis writing rules of Gazi University Graduate School of Natural and Applied Sciences;

- All data, information and documents presented in this thesis have been obtained within the scope of academic rules and ethical conduct,
- All information, documents, assessments and results have been presented in accordance with scientific ethical conduct and moral rules,
- All material used in this thesis that are not original to this work have been fully cited and referenced,
- No change has been made in the data used,
- The work presented in this thesis is original,

or else, I admit all loss of rights to be incurred against me.

Buse ÖZER

09/08/2023

TEMPORAL FLOOD RISK ASSESSMENT BY REMOTE SENSING AND GIS: THE CASE STUDY OF ISTANBUL-ESENYURT

(M. Sc. Thesis)

Buse ÖZER

GAZİ UNIVERSITY

GRADUATE SCHOOL OF NATURAL AND APPLIED SCIENCES

August 2023

ABSTRACT

Floods are one of the natural induced disasters that cause the most loss of life and property in the world with increasing urbanization. In the last decade, there was a series of floods occurred in Haramidere Basin covering the part of Esenyurt district in İstanbul. These floods can indicate the presence of existing flood risk. Therewithal, the dense urbanization in this region increases flood risks. High urbanization in the study area has occurred due to the shared involvement of the rapid population growth and the urban planning resulting from the intensity of buildings. Due to these factors, the Haramidere Basin within Esenyurt district has been regarded as valuable to examine. The objective of this thesis is to reveal the historical effects of the urbanization on the flood risks by considering spatial and temporal changes in the study area. It is essential to detect building imprints to assess the impacts of urbanization on flood risk. For this purpose, Landsat-8 satellite data has been utilized to examine NDVI (Normalized Difference Vegetation Index), NDBI (Normalized Difference Building Index) and BU (Built-up Index) due to their operational interval and high spectral resolution, respectively. In this way, historical backgrounds of the buildings (i.e., the start of construction) have been revealed for the temporal risk calculations. As a result of the historical background analysis of the buildings, it was concluded that the urbanization rate increased suddenly in 2016, 2017 and 2021. In order to calculate flood risk, the flood inundation depth and flood inundated areas generated for 100-year return period in 2014 has been used. Moreover, the economic loss, the population affected by flood and depth-damage function were considered in the risk analysis. After all, the values were normalized and combined to reach the total flood risk for each building. According to the results obtained, from 2014 to 2022, it has been identified that high urbanization increased the population affected by the flood by 32,9%, the economic damage by 22,3% that would occur in case of a flood, and the total flood risk by %13,6.

Science Code	:	80208
Key Words	:	Flood risk, urbanization, background analysis of buildings, remote sensing, GIS, Bibliometric Analysis, Istanbul, Esenyurt, Haramidere
Page Number	:	142
Supervisor	:	Prof. Dr. Özge YALÇINER ERCOŞKUN

UZAKTAN ALGILAMA VE CBS İLE ZAMANSAL TAŞKIN RİSK DEĞERLENDİRMESİ: İSTANBUL-ESENYURT ÖRNEĞİ

(Yüksek Lisans Tezi)

Buse ÖZER

GAZİ ÜNİVERSİTESİ

FEN BİLİMLERİ ENSTİTÜSÜ

Ağustos 2023

ÖZET

Taşkınlar artan kentleşme ile dünyada en fazla can ve mal kaybına neden olan doğa kaynaklı afetlerden biridir. Son on yılda İstanbul ili Esenyurt ilçesinin bir bölümünü kapsayan Haramidere Havzası'nda bir dizi taşkın meydana gelmiştir. Bu taşkınlar mevcut taşkın riskine işaret etmektedir. Yapılaşma yoğunluğu bakımından hızlı nüfus artışı ile şehir planlamasının karşılıklı etkileşimi nedeniyle yoğun kentleşme meydana gelmiştir. Bunlarla birlikte bu bölgedeki yoğun kentleşme taşkın risklerini artırmaktadır. Bu nedenlerle Esenyurt İlçesi içerisinde yer alan Haramidere Havzası incelemeye değer görülmüştür. Bu tezin amacı, çalışma alanındaki mekânsal ve zamansal değişimlerin dikkate alınarak kentleşmenin taşkın riskleri üzerindeki tarihsel etkilerinin ortaya konulmasıdır. Kentleşmenin taşkın riski üzerindeki etkileri için bina izlerinin tespit edilmesi esastır. Bu işlem için NDVI (Normalized Difference Vegetation Index), NDBI (Normalized Difference Building Index) ve BU (Built-up Index) sırasıyla çalışma aralığı ve yüksek spektral çözünürlüğü nedeniyle Landsat-8 uydu verileri aracılığıyla incelenmiştir. Bu sayede risk hesaplamaları için yapıların tarihsel arka planları (inşaatın başlangıcı) ortaya çıkarılmıştır. Bina geçmiş durum analizi sonucunda kentleşme oranının 2016, 2017 ve 2021 yıllarında aniden arttığı sonucuna ulaşılmıştır. Taşkın riskinin hesaplanmasında 2014 yılında 100 yıllık tekerrür aralığı için oluşturulan taşkın alanları ve derinlikleri kullanılmıştır. Ayrıca ekonomik zarar, taşkından etkilenen nüfus ve derinlik-hasar fonksiyonu da risk analizlerinde dikkate alınmıştır. Analiz sonuçları normalize edilerek bir araya getirilmiş ve bina özelinde toplam taşkın riskine ulaşılmıştır. Elde edilen sonuçlara göre 2014 yılından 2022 yılına kadar yaşanan şehirleşme etkisi ile taşkından etkilenen nüfusun %32,9, taşkın yaşanması durumunda oluşacak ekonomik zararın %22,3 ve toplam taşkın riskinin %13,6 arttığı görülmüştür.

Bilim Kodu	:	80208
Anahtar Kelimeler	:	Taşkın riski, kentleşme, bina geçmiş durum analizi, uzaktan algılama, GIS, Bibliyometrik Analiz, İstanbul, Esenyurt, Haramidere
Sayfa Adedi	:	142
Danışman	:	Prof. Dr. Özge YALÇINER ERCOŞKUN

ACKNOWLEDGEMENT

Foremost, I would like to express my deepest gratitude to my research supervisor Prof. Dr. Özge YALÇINER ERCOŞKUN for her guidance and patience, who provided me a tremendous opportunity to work with her. I would also like to thank members of the examining committee, Assoc. Prof. Dr. Meltem ŞENOL BALABAN and Assoc. Prof. Dr. Hayri ULVİ for their visionary contributions.

I want to express my gratitude to my father, mother and sister for their unconditional love, moral support, and for always believing in me, even when times were tough and the end seemed far away. This accomplishment would not have been possible without them. I would like to say a special thanks to my lovely sister Gülse ÖZER, who has always been by my side with her love and understanding throughout this long process.

I would also like to thank friends for their companionship, patience, shared knowledge, and memorable moments during my journey.

Also, I would like to thank my colleague Egemen FIRAT, who has always supported me with his knowledge and experience from the beginning to the end of this study.

TABLE OF CONTENTS

Page

LIST OF TABLES

Table **Page**

LIST OF FIGURES

Figure **Page**

Figure **Page**

LIST OF MAPS

Map **Page**

LIST OF SYMBOLS AND ABBREVIATIONS

The symbols and abbreviations used in this study are presented below with their explanations.

Symbols	Explanations
$	US Dollar
km^2	Square kilometers
m^2	Square meters
m^3/s	Cubic meters per second
TL	Turkish Lira
TL/m^2	Turkish lira per square meter
µm	Micrometer (Band Wavelengths)

Abbreviations	Explanations
BU	Built-up Index
EU	European Union
FLEMO	Flood Loss Estimation Model
GEE	Google Earth Engine
GIS	Geographical Information Systems
HAND	Height Above Nearest Drainage
HV	Hazard, vulnerability
HVE	Hazard, vulnerability, exposure
IBI	Index-based Built-up Index
İSKİ	İstanbul Water and Sewerage Administration
JRC	European Commission’s Joint Research Centre
LULC	Land use/ land cover
NbS	Nature-based solutions
NDBI	Normalized Difference Building Index
NDVI	Normalized Difference Vegetation Index
NIR	Near Infrared
R	Visible Red

Abbreviations	**Explanations**
SLEUTH	Slope, Landuse, Excluded area, Urban extent, Transportation and Hillshade
SWIR	Shortwave Infrared
SYGM	General Directorate of Water Management
TEM	Trans European Motorway
VAT	Value added tax
WoS	Web of Science

1. INTRODUCTION

Throughout the years, the dynamics between precipitation and flow have shifted significantly due to increased urbanization. The effects of urbanization create differences in the urban water cycle and cause urban floods by affecting numerous parameters. According to The Emergency Events Database, the averages of the number of floods, loss of life, and the amount of economic damage that occurred between 2002-2021 are quite low compared to the floods that occurred in 2022. This situation suggests an increase in the frequency and impact of floods as of 2022. Annually floods are on the rise globally, and this trend is also applicable to Turkey. According to the 2017 data released by General Directorate of Water Management, the Republic of Turkey Ministry of Agriculture and Forestry, when comparing the periods 1975-2002 and 2003-2015, it is seen that the number of floods increased 1.5 times (Taşkın Yönetimi, 2017:25).

Cities with intense populations are quite prone to increasing floods. Because the damage and loss of life in floods are not insignificant and are difficult to repair. In this context, the increasing flood risk due to increasing urbanization and rapid growth has become a major problem for cities. Therefore, the objective of this research is to evaluate the flood risk on the basis of urbanization historically. Thus, the effects created by both temporal and spatial changes were determined.

The aim of this study has been shaped around the following questions:

1. How much does increasing urbanization affect flood risk in a time interval? Additionally, how does the economic damage and the population affected by the flood change with increasing urbanization?
2. To what extent could economic damage have been mitigated by factoring flood risk into urban planning? In this scenario, how many people would not have been affected by the flood?

The factors influencing the selection of Esenyurt as the study area in line with this purpose and research questions are:

- It is the most populous district of Istanbul with approximately 1 million inhabitants.
- Rapid population increases were observed when examining changes in the population over the past years.
- There is a significant density of construction due to the coexistence of industrial and residential areas.
- In 2022, floods occurred in Esenyurt, resulting in loss of life.

For these reasons, the part of Esenyurt district affected by Haramidere River was determined as the study area. Historical flood risk analyses were conducted in the determined study area between 2014 and 2022.

Flood risk occurs with the spatial combination of hazard, degree of vulnerability, and exposure. In this context, the flood risk components evaluated within the framework of HVE (Hazard, Vulnerability, Exposure) used in the thesis, are as seen in Figure 1.1. The adopted methodology was created within the HVE framework.

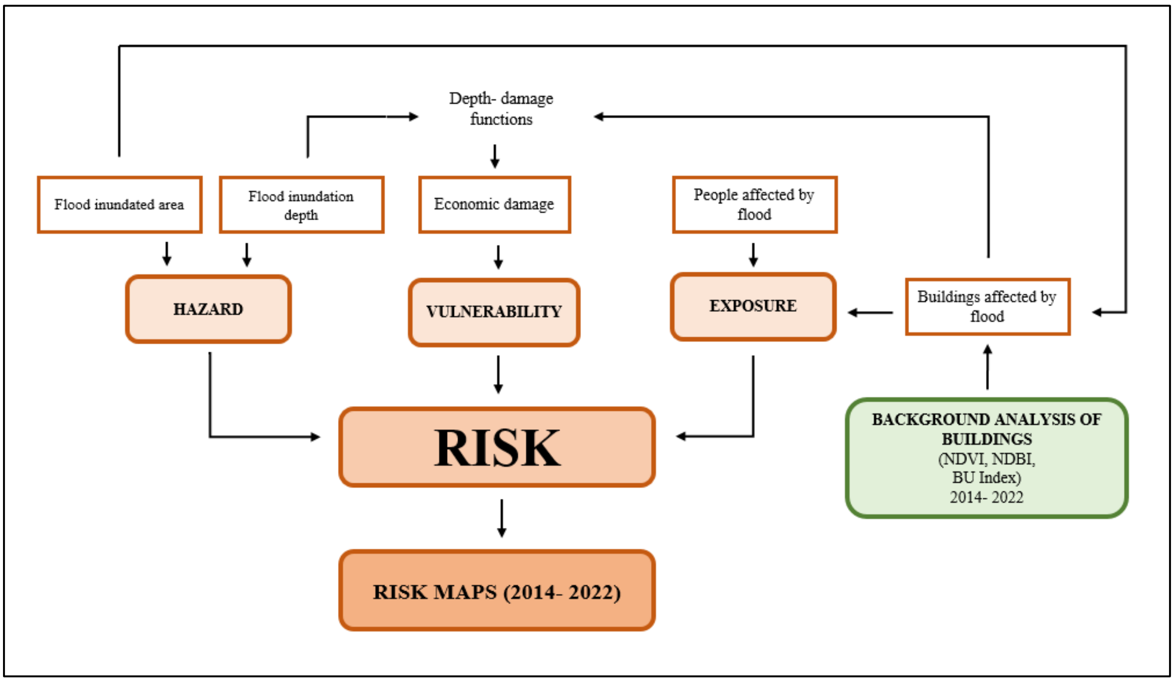

Figure 1.1. Thesis methodology flow diagram

The flood risk framework of HVE (Hazard, Vulnerability, Exposure) holds great significance for assessing and managing flood risks in urban planning and disaster management. This framework provides a comprehensive and systematic approach to understanding and addressing flood-related issues. Here are the key reasons for the importance of the HVE framework:

- Holistic risk assessment: by encompassing various dimensions, the HVE framework enables a comprehensive evaluation of flood risks. It considers hazard, which signifies the potential for flood; vulnerability, which assesses the susceptibility of exposed elements like buildings, infrastructure, and communities to flood impacts; and exposure, which accounts for the affected people by flood and value of assets located in flood-prone regions. Integrating these three components offers a more comprehensive understanding of flood risk compared to solely focusing on hazards.
- Identifying hotspots: The HVE framework aids in identifying areas with high flood risk, where hazards, vulnerabilities, and exposures converge. As these hotspots represent areas with the highest potential for flood damage and affected people, they are guides in emergency response, urban planning, risk reduction strategies.
- Informed decision-making: It helps decision makers as it plays an important role in identifying factors and hotspots that contribute to flood risk. Especially in terms of urban planning, these features are of great importance because they enable informed decision-making.

Study methodology comprises two interrelated components for the calculation of building-based flood risk over the years. The first of these is the identification of flood-affected buildings, and the second is the calculation of flood risk in a way that is compatible with the methodology used in Flood Management Plans, using the identified buildings. These components are not distinct from each other; both parts are interrelated and mutually supportive.

Within the scope of the study, buildings physically exposed to flood were determined to detect intense construction. Landsat-8 satellite data was used for detecting background of buildings due to its working range and high spectral resolution. Breakpoints were determined for each structure according to the indexes using Normalized Difference Vegetation Index (NDVI), Normalized Difference Building Index (NDBI), and Built-up Index (BU), and the historical background of each structure (construction year) was obtained through Google Earth Engine (GEE). The accuracy of the obtained data was verified with the help of Google

Earth. Through this process, background of buildings exposed to flood were determined by years.

Flood risk analysis was historically performed using the determined background of buildings. The methodology applied in the Flood Management Plans conducted by the Republic of Turkey Ministry of Agriculture and Forestry, General Directorate of Water Management was applied using the ArcGIS program in the risk analysis. This methodology is selected due to its suitability to the field scale, field characteristics, and its applicability as per the existing data. This methodology was applied in this thesis in a smaller basin and in more detail than the Flood Management Plans applied in Turkey.

Two fundamental assumptions were formulated when performing risk analysis. One of these is related to flood inundated and inundatin depth. Within the scope of the thesis, the results of the "Haramidere Basin Flood Modeling Project" commissioned by İSKİ (General Directorate of Istanbul Water and Sewerage Administration) were utilized. The flood inundated area and inundation depth of the 100-year return period in this project, which was carried out in 2014, was based on for this thesis. Over time, rehabilitation work was carried out on the Haramidere River in the study area. However, to eliminate the effects of these rehabilitation works, the results of the model implemented in 2014 were taken as the basis. It has been assumed that there has been no structural intervention in the river network since 2014 and the flood areas and depths remain constant. Therefore, historical risk accounts were analyzed from 2014 to 2020.

The other assumption made is that when determining the economic damage of the buildings, it is assumed that the Building Approximate Unit Costs, which represent the economic cost of one square meter of the building, is consistent across all the analyzed years. This can be explained by the rapid price increases experienced in Turkey, which result in different costs each year. As the costs increasing every year would also increase the risk, a comparison could not be made between the years in this case. To ensure that urbanization was the sole variable for comparing flood risk, the costs for 2022 used as a reference for the approximate unit cost of buildings for each year.

Risk analyses were conducted between 2014 and 2022 using the methodology specified in the HVE framework. The results of the analyses were mapped for each year. Flood risk maps play a critical role in spatial planning by identifying flood-prone areas and high-risk zones. When selecting the locations for areas such as designated settlement areas, infrastructure and basic facilities are developed through a proper and effective planning, flood exposure decreases. This situation can reduce both the number of people affected by the flood and the economic damage. Flood risk maps are vital for estimating potential economic losses and guiding investments in flood protection measures. At the same time, the population at risk is determined by risk maps and even the population at risk can be reduced by effective urban planning. This enables for the identification of vulnerable populations for emergency situations and evacuation plans. As a result, flood risk maps contribute significantly to urban planning efforts in ensuring the safety and well-being of communities in flood-prone areas.

As a result, it was concluded that flood risk increased between 2014-2022 due to urbanization and building density. In addition to the risk that could occur in the 100-year return period as a result of this analysis, economic damage and affected population were also determined. Alongside the findings obtained, the original value of this thesis is to present the flood risk as a historical process in all its dimensions with background analysis of buildings, hydrodynamic processes, depth-damage curves, and a methodology specific to the field. At the end of this process, the historical increase in economic damage, affected population, and flood risk has revealed the significance of urban planning. Urban planning ensures that potential flood damage is minimized and the impact on the urban population is reduced.

The introduction was included in the first chapter of the thesis, and the relationship between flood and urbanization risk was discussed in the second chapter. This relationship was examined in a process context in the form of urbanization causing flood by affecting the water cycle and then the emergence of damage as a result of flood. In addition, in this chapter, a literature review was mentioned with the help of Bibliometric Analysis. In the third chapter, the field of study was introduced and the methodology consisting of two main parts was explained in detail. In the same section, flood analysis maps and economic damage, population affected by flood, flood risk results was demonstrated. Finally, the results of the analysis and the relationship between the flood risk and urban planning was discussed.

2. FLOOD- URBANIZATION- RISK CONCEPTS

This section primarily explains the effects of urbanization on the water cycle based on the literature. Then, the relationship between urbanization and the flood occurrence process is examined, and the impacts of urbanization on this process resulting in damage are evaluated. Finally, the risk of flood is discussed in terms of urbanization, and the literature is comprehensively presented with the help of Bibliometric Analysis.

2.1. Relation Between Flood and Urbanization

According to the World Bank, approximately 56% of the world's population - 4,4 billion people - live in cities in 2023. The urban population is expected to more than double its current size by 2050 (URL-1). The majority of the world's population lives in cities, and the urban population is increasing every year.

As in the rest of the world, the urban population in Turkey is higher than the rural population. According to the Turkish Statistical Institute (TÜİK), in 2014, 91,8% of the population of 71 286 182 lived in cities and districts, while 8,2% lived in towns and villages. In 2022, 93,4% of the population of 85 279 553 lived in cities and district centers, while 6,6% lived in towns and villages (URL-2). The number of people living in cities increased by 11,7% from 2014 to 2022. While one reason for this significant increase is rapid urbanization, another reason is related to urban-rural status. In Turkey, the boundaries of metropolitan municipalities have been determined as the administrative boundaries of provinces since 2014 by Law No. 6360, and the villages within the boundaries of metropolitan municipalities have been transformed into urban neighbourhoods through the removal of their legal personality. For this reason, villages with urban neighbourhood status were included in the city population. According to statistics, although 93,4% of the population lives in cities in 2022, this rate is actually lower due to the change in urban-rural status.

The rapid growth in the urban population over the last decade has led to many changes in cities. With these changes, the occurrence of natural induced disasters in cities has been triggered and the number of people affected has naturally increased. One of these natural induced disasters is flood and flood is one of the most common disasters in the world (Li et al., 2022).

According to the data obtained from The Emergency Events Database (EM-DAT, CRED), there was an annual average of 168 floods between 2002-2021, while a total of 176 floods occurred in 2022 (URL-3). During the floods that occurred between 2002-2021, an annual average of 5 195 lives were lost, whereas the number of fatalities reached 7 954 in 2022. Floods between 2002-2021 caused an annual average economic damage of 41,6 billion US dollars, whereas the economic damage rose to 44,9 billion US dollars in 2022. Among the global disasters in 2022, floods that affected a total of 33 million people in Pakistan rank first (Table 2.1). Floods in Pakistan, where 1 739 people lost their lives, were identified as the third most damaging disaster globally in 2022 with economic damages of 15 billion US dollars. In India, floods that occurred in 2022 claimed the lives of 2 035 people and caused 4,2 billion dollars in economic damage.

Table 2.1. The top 10 countries most affected by disasters in terms of population-2022 (URL-3)

Rank	Country	Disaster	Total affected people
1	Pakistan	Flood	33.0 million
2	Congo (Democratic Rep.)	Drought	26.0 million
3	Ethiopia	Drought	24.1 million
4	Nigeria	Drought	19.1 million
5	Sudan	Drought	11.8 million
6	Bangladesh	Flood	7.2 million
7	China	Drought	6.1 million
8	Niger	Drought	4.4 million
9	Burkina Faso	Drought	3.5 million
10	Philippines	Storm ‘Nalgae’	3.3 million

Floods are among the natural induced disasters causing the most significant economic loss in Turkey. According to Taşkın Yönetimi (2017:25), the floods occurring each year cause approximately 300 million TL in damage. The total number of floods between 1975 and 2002 was 487, with a total death toll of 493. The total number of floods evaluated in the period of 2003-2015 was 722, with a total death toll of 227 (Table 2.2). The number of floods in the period of 2003-2015 increased approximately 1,5 times compared to the floods seen between 1975 and 2002.

Table 2.2. Flood statistics in Turkey (Taşkın Yönetimi, 2017:25)

	1975-2002	2003-2015
The total number of floods	487	722
The total loss of life	493	227

Along with the floods, issues related to the ecosystem - such as access to natural resources, availability of resources, and quality problems - are experienced. At the same time, these floods also cause physical, social, and economic impacts. In this section, initially, the city and water cycle were examined, followed by the exploration of the relationship between urbanization and flood, and the outcomes arising from this relationship were analyzed.

2.1.1. Impacts of urbanization on the water cycle

The relationship between cities and water has been endured for centuries, and they have always been interconnected. However, with increasing urbanization, the rainfall-runoff relationships have changed greatly from their natural state. The process involves the evaporation of water from water bodies, soil, or plants, which then accumulates temporarily in the atmosphere, creating clouds. When the atmospheric conditions reach saturation, this stored water transforms into precipitation, such as rain, snow, or hail, which ultimately falls back onto the soil, water bodies, or plant surfaces. Runoff refers to the movement of the precipitation water that reaches the soil's surface or infiltrates into the soil structure. Most of the precipitation that reaches the soil surface undergoes infiltration, increasing the soil's moisture content. In essence, this recurring cycle represents the rainfall-runoff process (Tarboton, 2003; Ward and Trimble, 2003).

With urbanization, artificial and impermeable surfaces and structural density have enhanced. Thus, the difference between the natural water cycle and the urban water cycle has been widened. Despite increasing differences, the urban water cycle incorporates both artificial and natural elements (Salvadore, Bronders, Batelaan, 2015).

According to Salvadore et al. (2015), the urban water cycle was as shown in Figure 2.1. Accordingly, in some parts of the cycle, water follows its natural course. Soil infiltration, which only occurs on permeable surfaces and appropriate geological units, can be given as an example. Also, storm drainage and sewer flow can be given as examples of the areas of the water cycle where there is human interference.

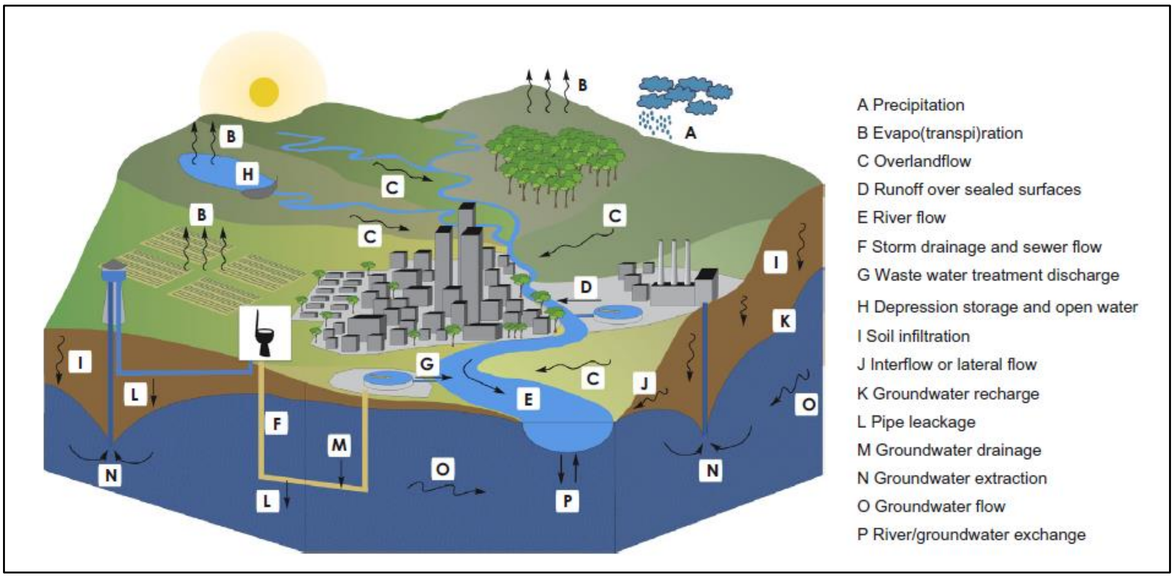

Figure 2.1. Urban water cycle (Salvadore et al., 2015)

As in the water cycle shown in Figure 2.1, changes in land use affect temperature and evaporation. With this balance changing, the occurrence and intensity in precipitation is changing (Salvadore et al., 2015). Precipitation can turn into runoff in the following ways:

- It can be collected in water collectors,
- It can join water bodies,
- It can transition to runoff from impermeable surfaces.

A significant part of the urban water cycle is also formed by the water collector system. This system constitutes a large and effective part of the water cycle to serve the citizens (Marsalek et al., 2008). With urbanization, the drainage system needs to be well-designed and a solution to the city's needs when planning the city. Otherwise, it creates problems rather than serving the city. If there is poor drainage system planning, changes in land use increase the possibility of disasters such as flood (Zhou, Leng, Su and Ren, 2019).

Urban soil covers usually have near-zero permeability and increase as a natural result of urbanization. Therefore, impermeable surfaces are much more common in urban areas than in rural areas. As a result, while the rate of precipitation transitioning to runoff increases, groundwater recharge decreases (Leopold, 1968; Miller et al., 2014). The precipitation turning into runoff increases the possibility of flood. Impermeable surfaces consist of different elements such as residential areas, industrial areas, asphalt roads. In residential areas, impervious surfaces exceed 50%, while this situation can be 70-80% in industrial areas (Salvadore et al., 2015). Therefore, the type of impermeable surfaces in the city is of great importance, followed by their density and location.

Urbanization affects many parameters that have an impact on the water cycle. These parameters both are affected by urbanization and also affect each other. For instance, as in the study conducted by Verbeiren et al. (2013), it was seen that increases in impervious surfaces affected peak discharges. Huang (2019) examined the effects of urbanization on flood and concluded that urbanization increases the flow volume. Moreover, in addition to the increased volume, the flow reaches its maximum value in a shorter period of time. Impermeable surfaces affect hydrological parameters such as "flow velocity, magnitude, and volume of surface runoff" (Salvadore et al., 2015; Walsh et al., 2005: 706-723; Dams et al. 2013).

The relationship between urbanization, the water cycle, and hydrological parameters resulting in flood is revealed in the next section.

2.1.2. Impacts of urbanization on flood

Accelerated urbanization negatively affects the city in many ways, such as economically, socially, culturally, and health-wise, increasing its vulnerability (Kuddus, Tynan and McBryde, 2020:1-4). The spatial reflections of the growing population density in the city and land use changes become inevitable. As a result, the city's urbanization increases, and this can happen in two ways:

- The density of existing residential areas may increase.
- The city expands, and urban sprawl can occur. When these spatial changes are not well managed, especially in developing countries, it can lead to poorly planned and rapid

urbanization (Jha et al., 2011). Settlements start to form in areas unsuitable for settlement and these areas include flood-prone areas and flood plains.

In light of these results, the water cycle is affected by the rapid growth in urbanization. This impact leads to flood depending on many parameters in the water cycle, which is a complex system.

Figure 2.2 provides a hydrograph, a time-dependent graph of discharge. This figure shows the change in the hydrograph before and after urbanization. With urbanization, the land cover changes and the impervious surface certainly increases. Natural and green areas decrease, and these areas turn into impervious surfaces like built-up areas and asphalt roads. Accordingly, less evapotranspiration and more soil infiltration occur. This leads to the precipitation turning into surface runoff. This change affects runoff rates and surface runoff volume (Salman and Li, 2018; Chen, Xie and Xu, 2019), and also increases peak flow due to urbanization (Huang, 2019; Miller et al., 2014; Du et al., 2012; Li and Wang, 2009).

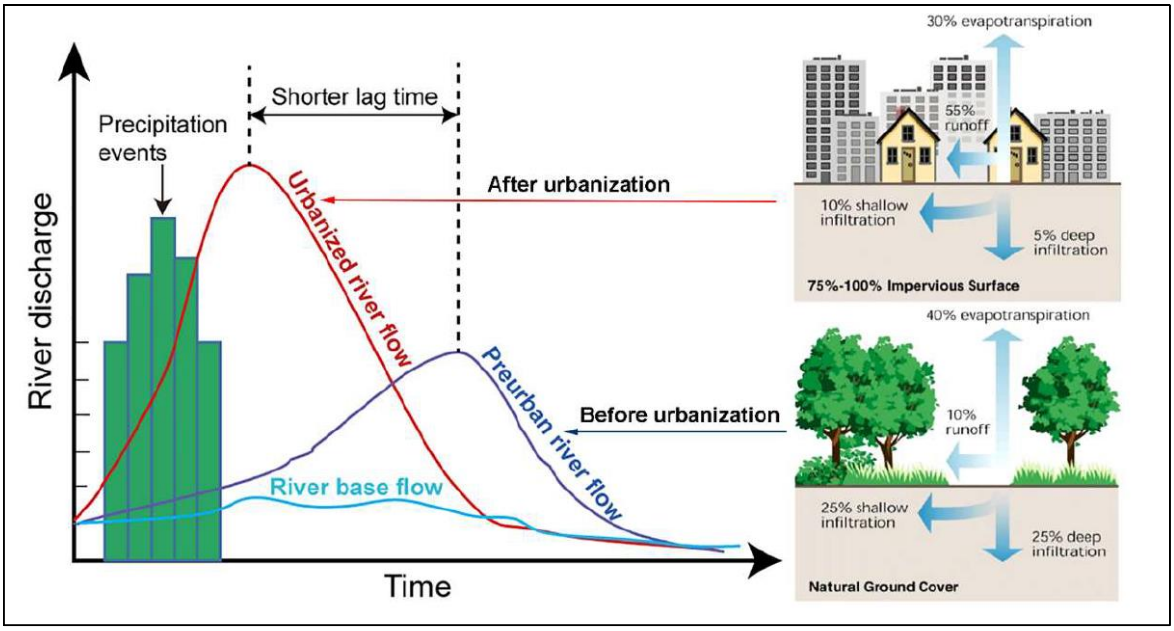

Figure 2.2. Impacts of urbanization on surface on hydrological parameters (Ding, Wu, Tang, Chen, and Xu, 2022)

Another consequence of the increase in impervious surfaces is the shortening of lag time, defined by Meals, Dressing and Davenport (2010) as "the amount of time between an action and the response to that action", along with the reduction of roughness. Thus, precipitation turns into surface runoff in a shorter time (shorter lag time) (Ding et al., 2022; Leopold, 1968).

When all the features are examined, urbanization also increases rainfall to runoff conversion rate, the duration of the flood and the frequency of the flood occurrences. The shortening of the lag time and the increase in the amount of flow, the less infiltration, the stream exceeds its channel (fluvial flood) or the drainage systems are overloaded (pluvial flood) (Jha, 2011; McGrane, 2016). In this thesis, floods caused by a decrease in river storage capacity are considered.

The flood has long been associated with the effects of increasing urbanization. Many researchers began to contacted the urbanization-flood relationship from the period when urbanization began to increase (Anderson, 1970; Hollis, 1975; Sheng and Wilson, 2009; Du et al., 2012; Miller et al., 2014; Huang, 2019). Different methods and different parameters have long been used to reveal the relationship between urbanization and floods. Many studies have been conducted in this field, and the subject has been examined with various methods from different perspectives.

The first studies in which the urbanization and flood relationship were contacted belong to Anderson (1970), Leopold (1968), Johnson, and Sayre (1973:50), and Hollis (1975). Significant findings were obtained in the study conducted by Hollis (1975) and it became a reference for many studies. It was emphasized that with the rapid increase in urbanization, floods could increase up to 10 times and the intensity of 100-year return periods could double. Anderson (1970) conducted his study in a forested rural state in Northern Virginia. In this area, residential areas started to become new development areas. Statistical analyses were performed using precipitation and streamflow, drainage area and length, and slope data. The most notable outcome of the study was that the parameter most affected by urbanization was the lag time. This implies that one of the significant parameters causing floods is the lag time.

In their study, Sheng and Wilson (2009) revealed the relationship between floods and urbanization in Los Angeles using GIS and statistical methods. They revealed that the flood risk increases with urbanization, and the flood duration shortens. In urban basins, approximately 90% of precipitation turned into flow depending on the distribution of impervious surfaces, while in non-urban basins, the rate of precipitation turning into flow was lower.

Miller et al. (2014) compared a highly urbanized area and a recently developed peri-urban area in the United Kingdom. The most significant difference between these areas was their permeability rates, and they proved that there was a difference in "peak flows and the duration of floods."

In China, the urbanization rate is approximately 60%, and in 2018, a total of more than 55,76 million population was affected by floods in 83 cities (Du et al., 2012). Therefore, China is the country where the most research has been conducted on the relationship between urbanization and flood.

Du et al. (2012) found that when the impervious surfaces in a province of China increased from 3% (1988) to 31% (2018), the annual runoff, daily peak flow, and flood volume also increased. They particularly emphasized that small floods were more sensitive to urbanization and "peaks flow and flood volumes" were directly related to impervious surfaces.

According to Huang (2019), urbanization changes the parameters of flood peak, peak timing and total volume, which affect flood damage. The rapid occurrence of flood peak is emphasized as the most apparent effect of urbanization. In addition, it was found that urbanization could also affect flood inundation depth; thus, even small-scale precipitation could create more impact than expected.

In their study on Java Island, Indonesia, Handayani, Chigbu, Rudiarto and Putri (2020) first extracted the Land-Use-Land Cover (LULC) map for 2009 and 2018 from satellite images. In this study, when built-up areas were compared by combining urban-rural classification, flood events, and land-use change, it was concluded that there were more floods in urban areas.

Beshir and Song (2021) used a GIS, remote sensing, and statistical analysis together in their study in Ethiopia. In this area, urbanization increased from approximately 80 km^2 in 1984 to

288 km^2 in 2020. The analyses revealed that urbanization increased the runoff depth and doubled the flood susceptible areas.

Liu, Huang and Yang (2022) developed a new assessment model. They evaluated the subsystems of urbanization and flood within the same model on a national scale in China. What distinguish this model from the rest was their examination of multiple factors that affect the relationship between urbanization and flood, and their analysis of the spatiotemporal distribution of these factors.

2.1.3. Damage as a result of urban flood

The growing urban population, along with rapid urbanization, affects many parameters in the hydrological cycle. The affected parameters cause flood disasters in the city. Rapid urbanization, when not well managed, increases vulnerability. According to Liselotte (2022), when this situation is flooded, it causes damage, which is briefly defined as "reparable harm", and loss, which is defined as "irreversible damage". Bae and Chang (2019) used 30 years of flood damage and landcover data in their study. They aimed to establish a relationship between the factors affecting urbanization and flood damage. Using GIS, spatial analysis, and spatial regression analysis, they emphasized in their study that flood damage increases with increasing urbanization over the years. Considering the escalating urbanization each year, the risk of flood, as well as the damage and loss caused by flood, are also on the rise. The annual global economic loss caused by flood, which was about $6 billion per year in 2005, is expected to be $52 billion by 2050 (Hallegatte, Green, Nicholls, and Corfee-Morlot, 2013). This striking increase makes the examination of the relationships between flood and damage/loss valuable in flood risk calculations.

Damage caused by floods can be divided into 2 categories: direct and indirect damages (Salman and Li, 2018; Merz, Kreibich, Thieken, and Schmidtke, 2004). Indirect damages can occur not only at the time of flood but also long after the flood. Indirect damages include the financial assistance needed as a result of a flood, as well as social and psychological effects (Merz et al., 2004). Direct damages are physical damages that occur during and immediately after the flood due to physical contact. Direct damages include physical destruction, such as damage to buildings, infrastructure, and roads (Smith and Ward, 1998).

Both types are classified as tangible and intangible. These classes depend on the monetary equivalent of the damage (Smith and Ward, 1998). If there is a monetary equivalent and it is calculated, it is classified as tangible damage, if not and it is difficult to transfer to monetary values, it is classified as intangible damage. Although this classification can be interpreted differently by different scholars, the general structure of classification is given in Table 2.3.

Table 2.3. Classification of flood damages (adapted from Merz et al.,2004; Salman and Li, 2018; Meyer et al., 2013)

Damage Classification	Direct Damage	Indirect Damage
Tangible	Physical damage to asset such as buildings, infrastructure	Necessary financial aid
Intangible	Loss of life, health issues, negative effects on ecosystems, damage to historic and cultural heritage	Hygiene problems, social psychology effects, job losses

Calculating direct tangible damage is much easier compared to the others. Therefore, according to Merz et al. (2004), a large part of the literature consists of studies related to direct tangible damage. It is much easier to calculate temporally compared to other types of damage because it occurs during and immediately after the flood. Also, since it consists of physical damage, it can be identified spatially and calculated economically.

Traditionally, damage is associated with inundation depth. It is based primarily on the linear relationship between depth and damage (Chinh, Dung, Gain, and Kreibich, 2017; Pistrika, 2010). It assumes that the damage is greater in areas where the depth is higher. The foundations of depth-damage functions date back to the depth-damage curve studies in the USA in the 1960s. This approach has been accepted as the international standard approach (Smith, 1994; Pistrika, 2010; Thieken, Muller, Kreibich, and Merz, 2005). Pistrika (2010) showed that although depth-damage functions are an important and widely used method, more parameters should be considered. There is another significant dimension to the depth and damage relationship. Besides the influence of depth on damage, the elements of land use and building use carry substantial significance as well. In addition to inundation depth, building use has also been used in studies (Merz et al., 2004; Jongman et al., 2012; Penning-Rowsell et al., 2005). Because the economic losses caused by flood are different due to the monetary values of commercial areas, industrial areas, infrastructure structures, communication systems, residential areas etc.

Merz et al. (2004) diversified the parameters used in damage calculation in their study because they found that the total damage was affected by different parameters in addition to the inundation depth. A database called HOWAS, which includes flood damage data, was used in Germany. This database contains 4 000 flood damage records and information about the location of the flood, building use, water stage, and past damage. The results of the studies supported the need to use other factors in addition to inundation depth and building use. It was suggested to detail the economic sectors and building types (timber structure, concrete buildings, etc.) for additional factors.

Chinh et al. (2017) noted that additional factors could also be hydrological parameters such as flood duration, in addition to land use and building use. These parameters have been attempted to be determined by many scholars. Hydrological parameters can include flow velocity (Citeau, 2003; Pistrika and Jonkman, 2009), duration of inundation (USACE, 1996; Penning-Rowsell et al., 2005) in addition to inundation depth.

One of the most important parts of flood risk is loss modeling. Different methods have been developed for this purpose. Highly urbanized areas become important when putting forth the loss. Because the loss in floods occurring in highly urbanized areas is more and costly (Jha et al., 2011). The methods developed vary according to the characteristics of the study area, the scale of analysis, and data limitations. It is known that models using multi-parameters such as inundation depth, land use depth give more accurate results among these methods (Jongman et al., 2012). Within the scope of this study, models that use multi-parameters, namely FLEMO (Germany), HIS-SSM Model (The Netherlands), The Flemish Model (Belgium), Multi-Coloured Manual (United Kingdom), HAZUS-MH (United States), the JRC Model (European Commission) were examined.

FLEMO (Germany)

Flood Loss Estimation Model is a model developed by the German Research Center for Geosciences to address flood scenarios. It has two different types: FLEMOps reveals the damage in residential buildings, while FLEMOcs reveals the direct damage in the commercial and industrial sector.

FLEMOps and FLEMOc both use the same data for calculating damage: inundation depth, contamination, and private precaution. In addition to these, FLEMOps uses the building type, building quality for residential damage, while FLEMOc uses economic sectors, company size data for commercial and industrial damage (Thieken et al., 2008; Kreibich et al., 2010; Apel et al., 2009). It can be used both at a local and national scale in Germany (Jongman et al., 2012).

HIS-SSM Model (The Netherlands)

In the Netherlands, the standard model used for flood damage is HIS-SSM (Kok et al., 2004). It is used by state agencies for national and regional flood damage detection. When calculating the damage, it relies on depth-damage functions. In national and regional calculations, maximum damage values determined at the national scale are used, and in addition to this, indirect losses are calculated by adding 5% on top of the direct loss (Jongman et al., 2012).

The HIS-SSM model uses detailed data about building use and other urban structures for damage detection. As these data can not be obtained at a national or regional scale, the Damage Scanner model has been developed (Klinj et al., 2007, as cited in Jongman, 2012). This model differs from HIS-SSM by using land data instead of detailed data.

The Flemish Model (Belgium)

It was developed by the Flemish Environmental Agency in Belgium (Vanneuville et al., 2007, as cited in Jongman, 2012). It resembles the model used in the Netherlands. Damage is calculated at a national and regional scale based on land use. Maximum damage values have been calculated at the national scale. Unlike other models, it is assumed that damage to residential content constitutes 50% of structural losses (Jongman et al., 2012). In contras to, the HIS-SSM Model, indirect losses are added to the direct loss depending on the type of agriculture (may vary by 10%) and industry (may vary by 40%).

Multi-Coloured Manual Model (United Kingdom)

The Multi-Coloured Manual Model, unlike other models, uses the material equivalent of depth instead of damage-depth functions. At the same time, the determined material equivalent varies according to the building use. Another feature that distinguishes this model from others is that it includes details such as affected roads, infrastructure losses, damaged vehicles (Penning et al., 2005: 38).

HAZUS-MH (United States)

HAZUS-MH is used for risk estimates, hazard, and loss detection (Haque, Mahmud, and Walker, 2022). It was developed by the Federal Emergency Management Agency (FEMA) of the USA. Its usage area is limited to the USA and Canada. It uses building data from the national database and in this aspect, it is similar to the Multi-Coloured Manual Model, but different from other models. The damage-depth curve is used for damage detection.

The JRC Model (European commission)

The approach reflecting European policy on flood risk management is by the European Commission's Joint Research Centre. It uses depth-damage functions and maximum damage values when calculating damage. Normalized damage functions have been developed for each continent (Huizinga, De Moel, and Szewczyk, 2017:6). To customize the functions, it includes five different damage classes: residential, commercial, industrial, roads, and agriculture (Huizinga et al., 2017:3).

The characteristics of the damage models examined in Table 2.4 were compiled. In terms of hydrological characteristics, all models use inundation depth, and in addition, HAZUS-MH uses the most parameters. When the scales of the models are examined, FLEMO, Multi-Coloured Manual, and HAZUS-MH are the most advantageous as they can be applied at a local level, but other models can also be adapted to the local scale. When examined in terms of the unit of analysis and number of unit classes, it was seen that the most detailed analyses could be conducted by the Multi-Coloured Manual and HAZUS-MH. However, HAZUS-MH has advantages in all aspects, its only disadvantage being its applicability in limited areas.

Table 2.4. Properties of the damage models (adapted from Jongman et al., 2012)

Damage model	Hydrological characteristics	Scale of application	Units of analysis	Number of unit classes
FLEMO	Depth Contamination	Local Regional National	Surface area (Land use)	5-10
HIS-SSM Model	Depth	Regional National	Surface area (Land use)	5-10
The Flemish Model	Depth	Regional National	Surface area (Land use)	5-10
Multi-Coloured Manual	Depth	Local Regional	Individual objects	> 20
HAZUS-MH	Depth Duration Velocity Debris Rate of rise Timing	Local Regional	Individual objects Surface area	> 20
The JRC Model	Depth	Regional National	Surface area (Land use)	5-10

Although the damage functions revealed by JRC are different for each country, they are the same in the whole country where the model is applied at national scale. However, the maximum damage values may vary depending on the characteristics of the regions. Nevertheless, it is efficient in countries like Turkey, which do not have sufficient data from past floods. Damage functions determined by JRC were used in many Flood Management Plans made by the General Directorate of Water Management, Republic of Turkey Ministry of Agriculture and Forestry. The flood management plans where these methodologies have been applied are in the following basins: North Aegean Basin (2019), Eastern Mediterranean Basin (2019), Akarçay Basin (2019), Lake Van Basin (2020), Asi (2020), and East Black Sea Basin (2020). Examples of economic damage maps created under the Eastern Mediterranean Basin Flood Management Plan and Van Lake Basin Flood Management Plan are given in Map 2.1 and Map 2.2, respectively.

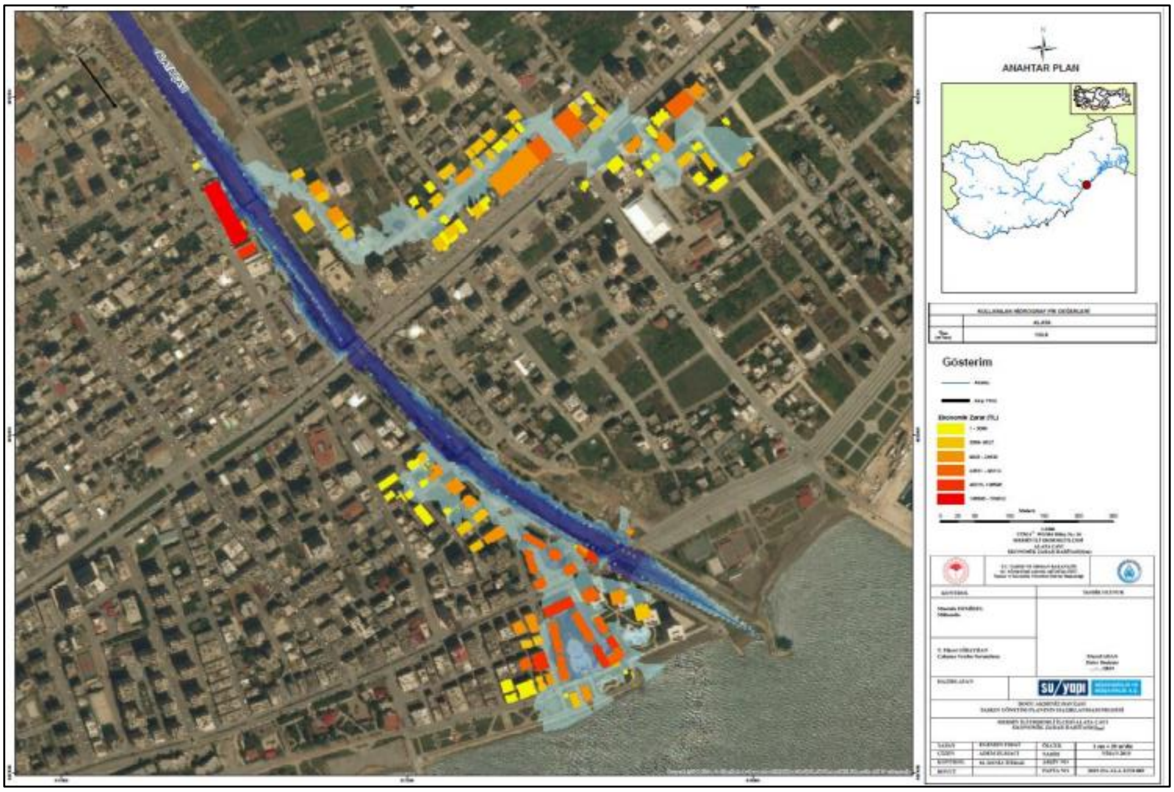

Map 2.1. A sample economic damage map from Eastern Mediterranean Basin Flood Management Plan (SYGM, 2019)

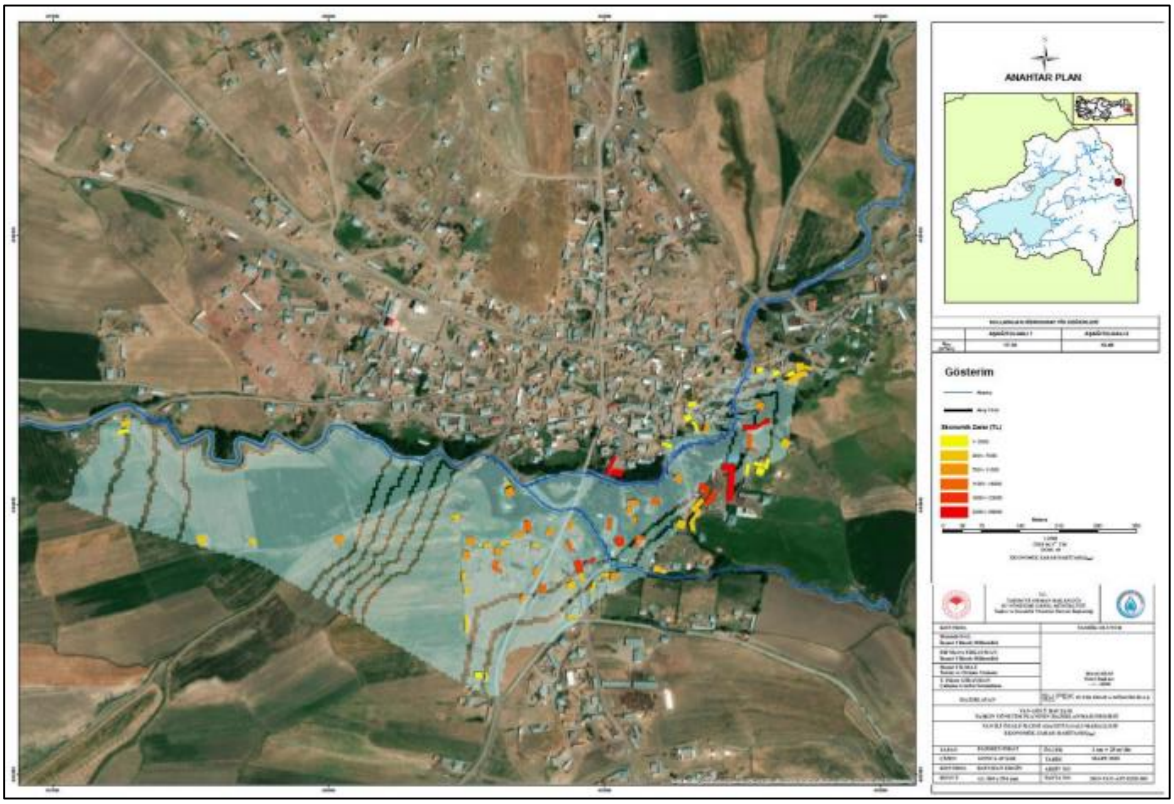

Map 2.2. A sample economic damage map from Van Lake Basin Flood Management Plan (SYGM, 2020)

2.2. Flood Risk in the Scope of Urbanization

Risk is defined as "the expected loss (of lives, persons injured, property damaged, and economic activity disrupted) due to a particular hazard for a given area and reference period" (UN, 1992). The EU Flood Risks Directive (2007) defined flood risk as follows: "the combination of the probability of a flood event and of the potential adverse consequences for human health, the environment, cultural heritage and economic activity associated with a flood event".

The most important common point in flood risk definitions is its association with potential adverse consequences. According to Kron (2005) in the literature, it is widely accepted that risk is a product of a hazard and its consequences. There are many areas where these consequences can occur. Especially when an urban flood occurs, it negatively affects many areas such as society, economy, ecosystem, and urban structures. To minimize the negative effects of flood and flood risk is going to be analyzed first. There are various evaluations and components of flood risk analysis using different methods. Among these, to analyze the flood risk in a way that is close to reality, it needs to be designed with a holistic process involving flood scenarios, extreme events and their probabilities of occurrence, and their physical effects. In this process, the components of flood risk are identified for a comprehensive analysis of its consequences. These components are mostly expressed in the literature with the following two different expressions.

$$\text{Risk} = \text{Hazard} \times \text{Vulnerability} \qquad (2.1)$$

$$\text{Risk} = \text{Hazard} \times \text{Vulnerability} \times \text{Exposure} \qquad (2.2)$$

There are many studies that approach flood risk from the framework of HV (Hazard, Vulnerability) (Apel et al.,2008; Kron, 2005; Meyer, Haase, and Scheuer, 2009; Li, Ahuja and Padgett, 2012; Pistrika and Tsakiris, 2007). Hazard is expressed as "the probability of occurrence" (URL-4) or according to Pistrika and Tsakiris (2007) as "a source of potential harm". In order to identify the hazard, the main physical characteristic features (especially the size of the flood inundated areas, inundation depth, and flood duration) need to be determined (Guerriero et al., 2018; Apel et al., 2008; Aerts et al., 2018). These features are specified in flood hazard analyses. Díez-Herrero and Garrote (2020) found in their Bibliometric Analysis study that the hydrologic-hydraulic method was most commonly used in hazard analysis. Modeling studies are carried out with this method to simulate flood areas. These analyses can be prepared according to certain flood frequencies or return periods (25 years, 100 years or different scales). The meaning of these scales is as follows: for example, when considering a 100-year return period, it represents a flood with a one percent chance of occurring in any given year (Jha et al., 2012: 71-74).

Vulnerability refers to the degree to which a system, which could be individuals or assets, is susceptible to or unable to cope with the negative impacts of natural induced disasters (Jha et al., 2012: 173). Vulnerability, a component of risk, can be evaluated from different perspectives, such as social, economic, and environmental. Damage functions, which describe the relationship between flood hazard and vulnerability, are used to make these evaluations (Aerts et al., 2018). These methods were previously explained under the title "Damage as a result of urban flood".

Studies that approach from the framework of HVE (Hazard, Vulnerability, Exposure) emphasized the need to include exposure in flood risk analysis (Aerts et al., 2018; Kron, 2005; IPCC, 2012). Fundamentally, exposure analysis is measured with people and assets (IPCC, 2012). In this respect, it significantly affects flood risk. In the Bibliometric Analysis study by Díez-Herrero and Garrote (2020), it was seen that population and land use were most often taken as the basis in the exposure analysis of the studies examined. This is because the population and assets affected by these two features are determined according to land use. For this reason, exposure analysis becomes particularly important in urban areas where the population is high and land use changes rapidly.

There are many different methods in flood risk assessments, which consist of hazard, vulnerability, and exposure components. According to Diaconu, Costache, and Popa (2021), there are 1 326 studies in the literature between 1979-2020 that focus solely on flood and methodology. There are many different methods in flood risk assessments, which consist of hazard, vulnerability, and exposure components. Accordingly, 24% of the flood assessment methods in these studies have used modeling and simulation, which consist of hydrological, hydraulic, and hydrodynamic modeling. The next most commonly used methods are statistical analysis at 20% and GIS techniques at 17%. In addition to these, remote sensing techniques (analyzed via GIS) constitute 8% of all methods. According to this study, the most frequently used methods are modeling- simulation, statistical analysis, and GIS techniques. The methods first used in the literature were mathematical and statistical analyses. In addition to these methods, surveys and interviews were also employed. Later on, with the development of technology, different methods were developed to obtain results closer to reality and to understand the risk in all its dimensions. With these methods, more flood parameters can be used, enabling real-time and spatial analyses.

Statistical methods can be used to estimate future years by looking at the trend of past years using data from flood disaster events. Li et al. (2022) and Diaconu et al. (2021) emphasized that this method is an early method and has been a pioneer in flood risk assessments. For this method, it was stated that there should be detailed and long-term data such as frequency, depth, and loss, so that the trend of past years can be determined more accurately (Quan, 2012, as cited in Li et al., 2022). It was used to determine flood frequency along with statistical methods, and then it began to be used with spatial methods as other methods developed. However, Van Steenbergen, Ronsyn and Willems (2012) proved in their study that the predictive uncertainty in the forecasts can be calculated by analyzing past floods to predict future floods.

In the literature, the most commonly used method for determining the hazard component of flood risk is a dynamic process based on hydrological and hydrodynamic models. Its use has been increasing since the end of the 20th century (Li et al., 2022). While the hydrological model consists of the mathematical expression of hydrological processes, the hydrodynamic model, according to Diaconu et al. (2021), is "used to show water flows' evolution to simulate water movement during floods, along waterways, reservoirs, and hydraulic structures".

Hydrodynamic models are critical tools in flood modeling, offering crucial understanding of the dynamics and patterns of water flow under varying circumstances. These models are instrumental in forecasting the range, depth, speed, and period of flood. The two primary forms of hydrodynamic models are the 1-dimensional (1D), 2-dimensional (2D) models and and 3-dimensional (3D) models (Lin, Wicks, Falconer, and Adams, 2006; Bürgler, Vetsch, Boes, and Vanzo, 2023; Gharbi, Soualmia, Dartus and Masbernat, 2016). The main features of the models are as follows:

- 1-Dimensional hydrodynamic models: Such models capture water flow along a single dimension, typically the flow direction. They are commonly applied in modeling flow in river courses or pipelines. They forecast the river's water level and discharge using different parameters such as inflow, outflow, channel shape, and roughness. The Hydrologic Engineering Center's River Analysis System (HEC-RAS), developed by the U.S. Army Corps of Engineers, is a notable example of a frequently used 1D model.
- 2-Dimensional hydrodynamic models: These models consider flow in two dimensions (generally horizontal), facilitating a more detailed depiction of flow patterns, particularly across floodplains and in urban areas. 2D models are more proficient in representing intricate hydraulic events, like alterations in flow direction, compared to 1D models. Some of the 2D models include LISFLOOD-FP, MIKE 21, and FLO-2D. MIKE 21 is a frequently used 2-dimensional (2D) hydrodynamic model developed by the Danish Hydraulics Institute (DHI).
- With the Delft3D model, FLOW-3D model, the flow field simulation can be modeled in three dimensions and realistic results can be obtained.

In certain scenarios, 1D and 2D models may be integrated to create a composite model, maximizing the benefits of both types. These hybrid models (often labeled as 1D/2D or 1,5D models) are utilized when the region of study comprises both distinct channels and floodplains, a common scenario in urban flood modeling. These models need various input data like topography, river/channel shape, land use data, and rainfall or flow information, and their results typically manifest as flood depth, range, speed, and flood onset time maps.

Among the frequently employed methods is geographic information systems. This method is also used in conjunction with remote sensing methods. Flood areas and river networks are detected with remote sensing technologies, and geographic information technologies are analyzed. Diaconu et al. (2021) emphasized that these are the methods with the greatest advantages in creating and analyzing spatial data. One of these advantages is the ability to detect hydrological processes worldwide using remote sensing technologies. This eliminates issues related to data deficiency and data accuracy. In the study of hydrological processes, while the remote sensing method gives better results in large-scale flood areas, it has temporal and spatial limitations for small floods (Li et al., 2022). Continuity with the same accuracy is also ensured in the detection of these processes.

In addition to these, a multi-criteria index system is implemented with the help of GIS. It was developed by Thomas L. Saaty in the 1970s and has been extensively studied and refined since then. Essentially, the Analytical Hierarchy Process (AHP) focuses on decision-making and ranking. It facilitates the simplification of intricate issues by organizing them into a series of smaller, more understandable sub-issues (Saaty, 1980). The purpose of this analysis is to bring together a large number and variety of criteria. Analytical Hierarchy Process is the most frequently used method.

According to Li et al. (2022), the choice of methods is usually dependent on the spatial scale and the presence of fundamental data. According to these methods, the parameters forming the flood risk, hazard, vulnerability, and exposure, also have significant importance on the resulting risk. With the advancements in technology and accumulation of methodology, different methods can be used together. Through this means, the flood risk can be addressed in all its dimensions, and risk assessment can be determined in the closest way to field reality. There are many studies in the literature where these determinations are made. As mentioned above, these differ in terms of the method and the framework in which they address the risk.

2.2.1. Overview and search rules of Bibliometric Analysis

Bibliometric Analysis is a method used in the analysis of large data, which easily enables reaching many results at the same time and identifying knowledge gaps. With this analysis, the effects of important studies were monitored and analyzed. Therefore, Bibliometric Analysis was used during the literature review. One of the prominent features of this analysis is that it can carry out extensive reviews, thereby making a lot of input meaningful. It reveals the foundation of a field with meaningful results (Zupic and Cater, 2015). These features increase the use of the analysis in recent years. At the same time, Donthu, Kumar, Mukherjee, Pandey, and Lim (2021) emphasize in their study that the development of software like Gephi, Bibexcel, VOSviewer, and scientific databases contributes to the frequent use of Bibliometric Analysis. Among these software, VOSviewer stands out with its graphic representation of outputs. Thus, it was used in this study as it provides a comprehensive perspective. VOSviewer is a software tool developed by Van Eck and Waltman (2010). The analysis results can be displayed with different visualization types. In this study, it was given as network visualization, and in this representation, the analysis results (items) were expressed with the sizes of nodes, cluster colors, and the closeness of circles. Items of higher importance are shown more prominently than those of less importance with these features. In the analysis, items are assigned to clusters. The relationship between clusters becomes easier to understand, and different subgroups can be revealed (Wang and Yang, 2019). Thus, relationships become easier to understand.

During the analysis, the workflow suggested by Zupic and Cater (2015) in their study was followed. Firstly, the research question and scope were determined. Then, Web of Science (WoS) was chosen as the bibliometric database, and studies filtered according to the determined criteria were exported. Thus, a database was created within the scope of this study. VOSviewer was chosen as the bibliometric software and the analysis was conducted. Then, the analyses were visualized, mapped, and explained. The customized version of these stages according to the study was given in Figure 2.3.

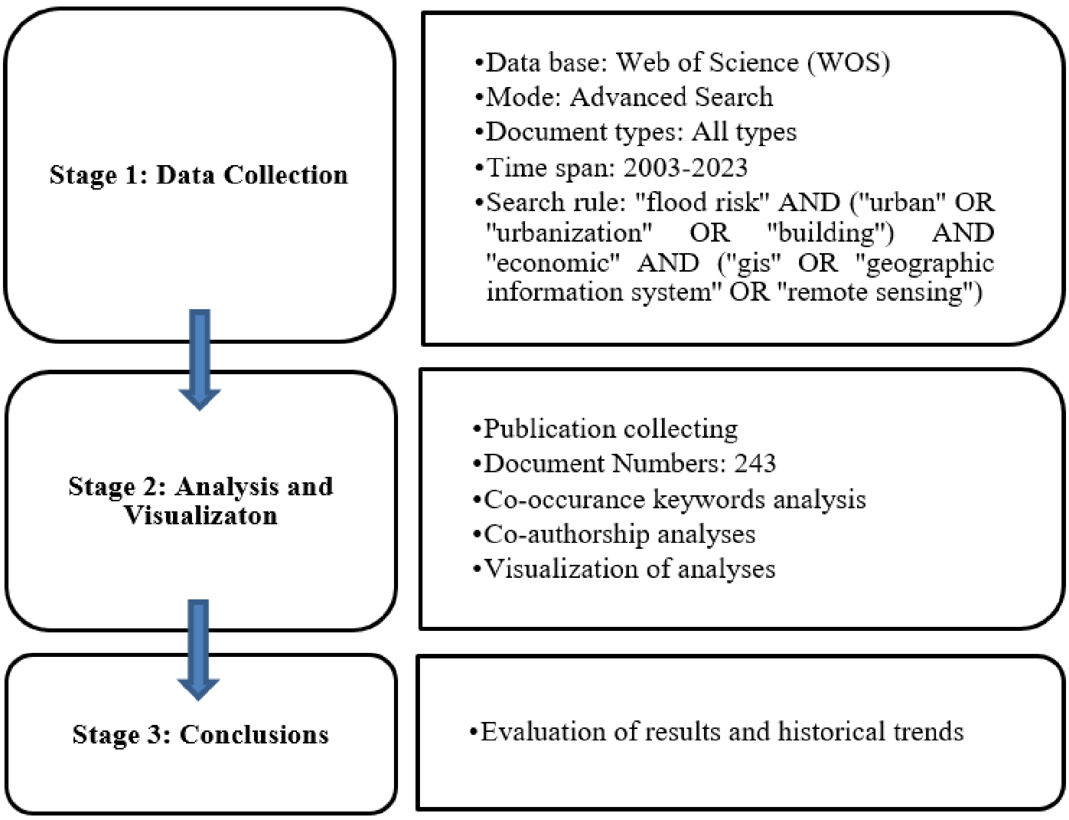

Figure 2.3. Stages of Bibliometric Analysis (the Wos core collection was last updated on Jan 1, 2023) (adapted from Guo et al., 2019)

Due to the fact that the necessary articles cannot be reached without the correct choice of keywords, care was taken in the selection of keywords (Polat, Alkan, Paulsson, Paasch and Kalogianni, 2022). As the theme of this study, flood risk was prioritized. It was narrowed down with words having similar meanings to the research subject. In the scope of this study, direct and tangible damage was used for risk analysis. This study does not consider the risk that occurs in the social and ecosystem; it is based on the risk arising from physical, economic factors and the number of people affected. Therefore, in conducting the Bibliometric Analysis, the word "economic" was added to the search rule to demonstrate this difference. Additionally, geographic information system, remote sensing were added to specify the study method, and the research rule was determined.

The search rules "flood risk" AND ("urban" OR "urbanization" OR "building") AND "economic" AND ("gis" OR "geographic information system" OR "remote sensing") were used as the All Fields Search criterion in the Web of Science Core Collection database. Document types were not selected and all documents were considered. No date selection was made, and it was observed that the date range of the documents was between 2003 and 2023, and documents from all dates were considered.

A total of 243 papers were retrieved. Of the 243 papers, the number of articles was 192, which accounts for 79,01% of the total number of papers, followed by proceedings papers 46 (18,93%) and review articles (3,9%). In Figure 2.4, the documents count between the years 2003 and 2023 is given. Since the analysis results were obtained at the beginning of 2023, the number of publications made in this year was not considered as it would be misleading. According to the graph, it was observed that there was an increasing trend over the years and there has been a significant increase since 2015. This trend emphasizes the increasing importance in the assessment of flood risk. The highest number of publications was in 2022, and accordingly, it can be said that there will be a similar situation in 2023 with the increasing trend.

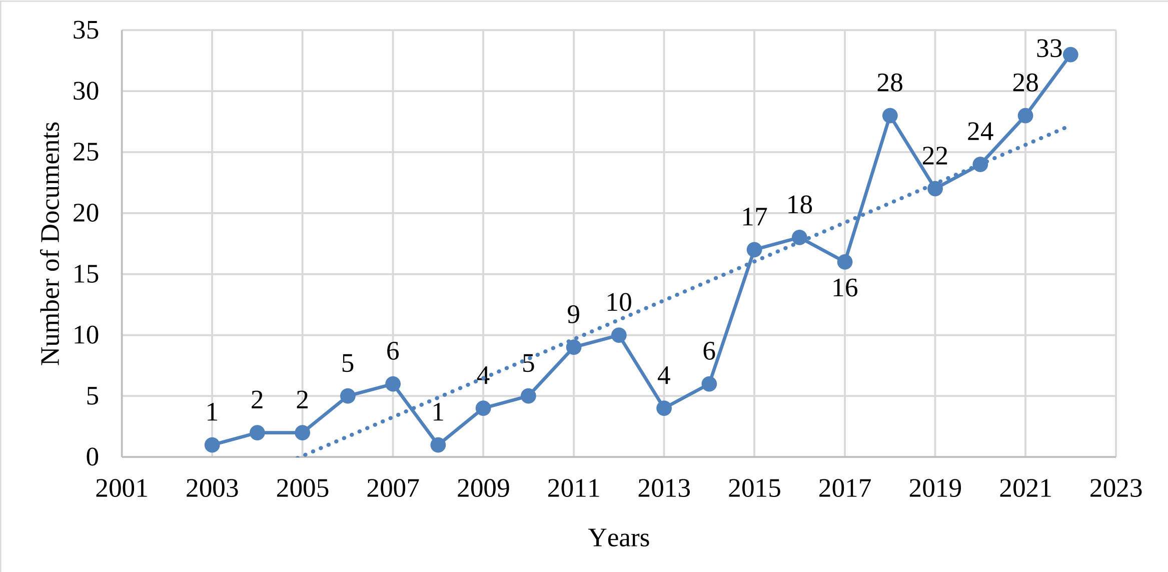

Figure 2.4. Number of documents from 2003 to 2023

2.2.2. Results of Bibliometric Analysis

This section includes the results of the Bibliometric Analysis. First of all, the relationship between the countries, then the results of co-author analysis and keyword analysis were given. Through this analysis, the most prominent features were deduced as a result of keyword analysis. Around 2015, the focus was on broader concepts like natural hazards, floods and urbanization. However, as the years progressed, there was a shift towards emphasizing risk assessment and its methodologies.

Countries and regions

A co-authorship analysis was conducted to identify common researches among different countries. Co-authoring of papers was considered an indicator of collaboration (Zupic and Cater, 2015), and an analysis was performed based on the countries of the authors included in the bibliometric data. Thus, joint researches at the country level were revealed.

In the field of economic evaluation of flood risk, authors from a total of 65 countries have contributed. The top ten countries with the most contributions by authors among these countries were given in Table 2.5. Accordingly, the countries that have made the most contributions (the largest numbers of documents) are China, the USA, and Italy.

Shi and Kasperson (2015: 73) calculated the expected annual economic loss risk of flood. Accordingly, the United States is the country with the highest economic loss, the other countries in the top 10% are China, Japan, the Netherlands, India, Germany, France, Argentina, Bangladesh, Brazil, United Kingdom, Thailand, Myanmar, Cambodia, Canada. In this study, the expected annual mortality risk of flood was also calculated. Accordingly, the countries with the highest mortality rate are Bangladesh, China, India, Cambodia, Pakistan, Brazil, Nepal, the Netherlands, Indonesia, United States, Vietnam, Burma, Thailand, Nigeria, Japan. China, USA, Canada, England, India and Japan are among the countries that contributed the most to the literature, which can be attributed to their exposure to floods. It can be concluded that China, USA, Canada, England, India and Japan, as the countries contributing the most, have given significance to these studies in line with their experiences. At the same time, it is seen that the conduct of these studies is also related to the development levels of the countries.

Table 2.5. The ten countries/regions that contribute the most to flood risk

Countries/Regions	Record count	% of total
China	41	16.87
Usa	26	10.70
Italy	19	7.81
Australia	13	5.35
Canada	13	5.35
England	13	5.35
India	11	4.52
Romania	11	4.52
Iran	9	3.70
Japan	9	3.70

The co-authorship between countries and regions was analyzed and those that contributed to at least five documents were selected. The network visualization map is given in Figure 2.5. VOSviewer divided these 68 items into 4 different clusters. In this map, while the red cluster contains 8 countries, the green and blue clusters each contain 5 countries, and the yellow cluster contains 4 countries. The countries represented by nodes depicted in larger size have more international collaboration compared to those represented in smaller size. Countries within the same cluster have collaborated to a greater extent. Of the top three contributing countries, China and the USA have largely collaborated with each other, whereas Italy is located in a different cluster.

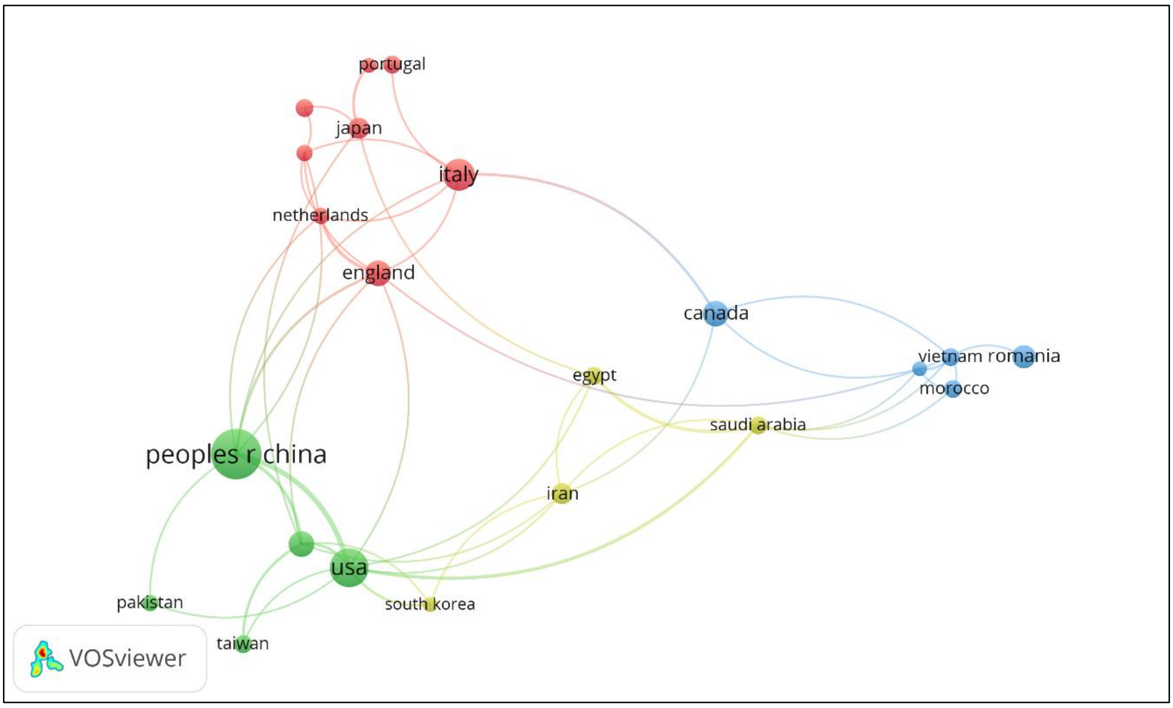

Figure 2.5. Co-authorship networks between countries

<u>Co-author Analysis results</u>

The primary purpose of conducting a co-author analysis is to identify collaboration between authors. When authors work together, a relationship is established between them, which is identified through the analysis (Lu and Wolfram, 2012). This way, the leading authors who have worked in the researched field and the connections between them are identified (Acedo, Barroso, Casanueva and Galán, 2006).

In total, 921 authors have contributed to the economic evaluation of flood risk. Among these authors, the list of most important contributing authors is provided in Table 2.6.

Table 2.6. List of most important contributing authors

Authors	Number of papers	% of papers	Citations
Critto, A.	4	0.43	90
Marcomini, A.	4	0.43	90
Torresan, S.	4	0.43	90
Zhang, Y.	4	0.43	106
Gallina, V.	3	0.33	48
Herath, S.	3	0.33	72
Kumar, P.	3	0.33	52
Lyu, H.M.	3	0.33	309
Sole, A.	3	0.33	39
Youssef, A.M.	3	0.33	122
Zabeo, A.	3	0.33	77

The co-authorship relationships among the authors were tried to be visualized. The following criteria were established considering the number of articles: the authors contributing to at least two documents and the authors having the greatest total link strength. Accordingly, 42 out of 921 authors met the thresholds. Figure 2.6 had shown the relationships of authors in terms of contribution. It was seen that the collaborations were not international and were very limited in number. The largest set of connected items among 42 authors consisted of 6 authors, these were Andrea Critto, Valentina Gallina, Antonio Marcomini, Jonathan Rizzi, Silvia Torresan, and Alex Zabeo. Among these authors, it was observed that Andrea Critto, Antonio Marcomini, and Silvia Torresan were the prominent contributors with numerous studies in the field. These authors, who were in the red cluster, collaborated more than those outside the cluster and when the years were examined, it was determined that this collaboration occurred in 2016.

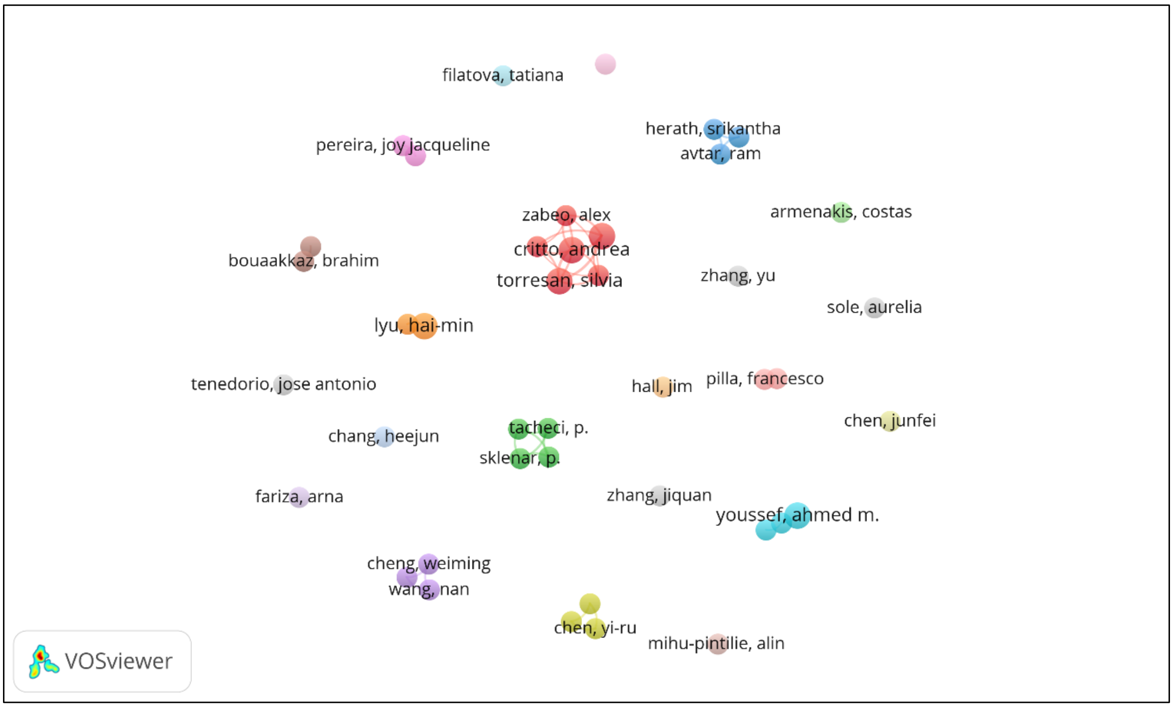

Figure 2.6. The author co-authorship network

Keyword Analysis results

The purpose of performing a co-word analysis is to emphasize that words used together are related and additionally that the concepts formed by these words are also related (Zupic and Cater, 2015). There is a direct link between the relationships because common words in different studies directly reflect the content of the study (Lu and Wolfram, 2012). The main topics, areas that need improvement, and historical development were identified by determining the content of the study. The analysis both provided an idea about the content of the studies and identified current trends. With this feature, keyword analysis significantly distinguished from other analyses (Polat et al., 2022; Donthu et al., 2021).

A co-word analysis was performed to gain insight into the content of the studies. It was found that a total of 1 163 keywords were used, of which 70 keywords that were repeated at least 5 times met the threshold. The network analysis was visualized as in Figure 2.7, the larger the circle size in the network visualization map, the more it is related to other keywords (Wang and Yang, 2019). Accordingly, the most remarkable keyword in Figure 2.7 and the keyword most frequently connected with other keywords is "GIS" (was linked with other keywords more frequently). The most used five keywords were "GIS", "vulnerability", "climate-change", "model", "flood risk" (record count: 87, 51, 31, 31 and 29 times, respectively).

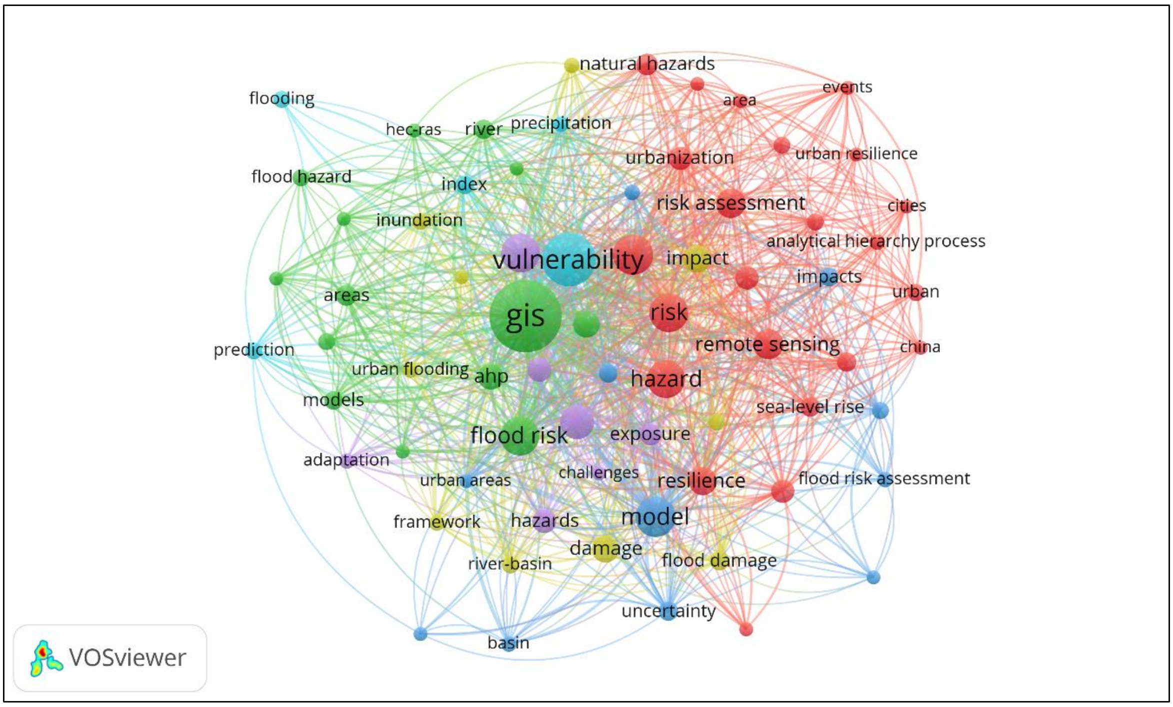

Figure 2.7. Keyword co-occurrences network

In the network visualization map in Figure 2.7, the larger the size (or node), the more it is connected to other keywords. The six clusters formed with these keywords were given in Table 2.7. Accordingly, "GIS" was the word that was most used and connected, which also appeared in the search rule. It was located in the second of the six clusters on the network visualization map, was green, and consisted of 14 items. Keywords related to flood risk calculation methods and spatially related keywords were associated with GIS. Cluster 1 mainly focused on the relationship between flood risk and climate change. This relationship was established through risk and hazard. Cluster 3, which is dark blue, focused on systematic approaches and models used to calculate flood risk. The yellow Cluster 4 was related to the damage and impact of the flood, while Cluster 5 (purple) was built on flood and management issues related to adaptation and challenges. Cluster 6 (light blue) mainly focused on the second most used word, vulnerability.

Table 2.7. Cluster keywords and the most frequent keywords

Cluster	Keywords	The most frequent keywords (occurences)
Cluster 1	remote sensing, risk assessment, resilience, climate change, floods, urbanization, natural hazards, sea-level rise, vulnerability assessment, land-use, urban, urban flood, analytical hierarchy process, area, china, cities, disaster, events, simulation, urban resilience.	climate-change (31), risk (29), hazard (28)
Cluster 2	ahp, areas, river, models, flood hazard, susceptibility, disasters, hazard assessment, hec-ras, spatial prediction, systems	gis (87), flood risk (29), risk-assessment (15)
Cluster 3	system, analytic hierarchy process, basin, flash floods, flood risk assessment, flood risk management, geographic information system, urban areas	model (31), uncertainty (9), impacts (8)
Cluster 4	decision-making, inundation, river-basin, framework, rainfall, urban flooding, impact assessment	damage(16), impact (16), flood damage (9)
Cluster 5	social vulnerability, exposure, adaptation, challenges	management (29), flood (24), hazards (13)
Cluster 6	prediction, precipitation	vulnerability (51), index (8), flooding (7)

After identifying the current contents of the studies with co-word analysis, Figure 2.8 was prepared for its temporal development. This figure shows the historical development of keywords in different time periods. With this examination, the development in terms of content of studies in the field of flood risk and urbanization was identified. It was found that there was a continuity in the increase of studies in this field since 2015, and for this reason, temporal change was examined from 2015 onwards.

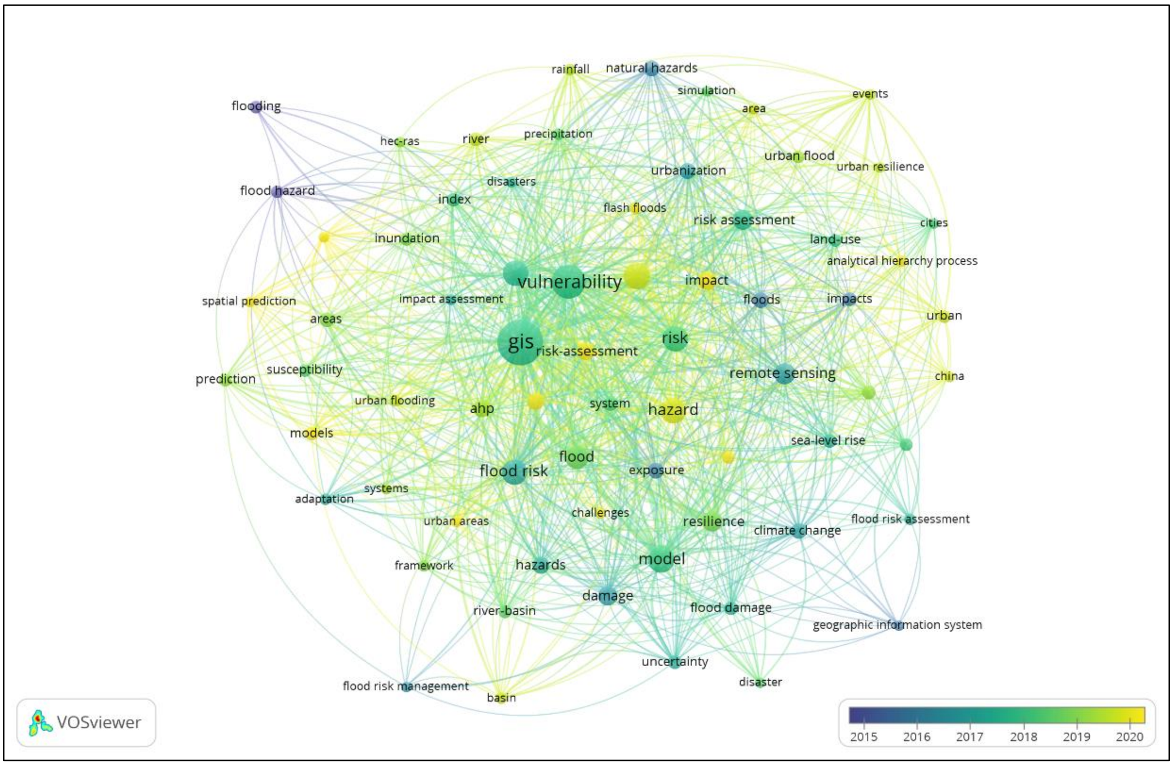

Figure 2.8. Keyword networks with a timeline (2015-2020)

In the early years of the increase in studies, there were more keywords in general concepts like natural hazards and flood. In later years, risk assessment and its methods came to the forefront. Key words such as "GIS", "vulnerability" and "management", which are located in the center and have a high connection, showed development in 2017-2018. Along with these concepts, spatial concepts such as cities and basins and a relationship with resilience were established. By 2020, it was observed that climate change and the concepts it is related to came to the forefront.

2.2.3. Literature review results

The urban flood system consists of many parameters, and these parameters are also related to each other. To determine these relationships, the spatial and temporal analysis of the system needs to be performed through parameters. Flood risk analyses evaluated under urbanization in the literature exhibit variations. This discrepancy can stem from the scale, method, flood risk components, or the framework in which the flood risk is addressed. To identify these differences, flood risk analysis studies conducted within the scope of urbanization were examined.

Luino, Turconi, Petrea, and Nigrelli (2012) conducted their research in a town in Italy with a population of 30 000, known for its significant industrial areas and located along a river. Structural measures like concrete walls and floodway channels were taken against flood risk in this area named Alba, but no decrease in flood risk was observed. The historical development of the town, historical floods were examined, and vulnerable areas from the past to the present were determined. As a result, the urban area that has been flooded increased from approximately 4% to 48% from 1852 to 1994.

A process of change occurs at a pace parallel to the increase in urbanization. Flood risk analyses conducted by Waghwala and Agnihotri (2019) in Surat City- India, and Bahrawi, Ewea, Kamis, and Elhag (2020) in East Ern Jeddah- Saudi Arabia support this fact. According to the studies, changes in Land Use/Land Cover (LULC) caused by rapid urbanization increase flood risk.

Changes in the urban area, city expansion, alterations in existing city density, and modifications in Land Use/Land Cover (LULC) can occur. The encountered changes affect the water cycle; therefore, studies in the literature have evaluated the hydrological process and land use together. In Nguyen et al.'s (2021) study, The Tra Khuc River basin in Vietnam was analyzed by combining urban flood risk, land use, and hydraulic modeling (1D and 2D). Land use for 1995 and 2019 was obtained by classifying satellite images and used to predict 2040 land use. Then, with the help of the Analytic Hierarchy Process method, the building-based flood risk was handled from the HVE perspective, and flood risks for the years 1995, 2019, and 2040 were compared. The Analytic Hierarchy Process method is one of the methods frequently used in flood risk analysis. The advantage of this method is to obtain a flood risk map showing the spatial distribution and intensity level of flood risk from very high risk to very low risk (Chen, Yeh and Yu, 2011; Gigović, Pamučar, Bajić, and Drobnjak, 2017; Rincón, Khan, and Armenakis, 2018).

Zope, Eldho and Jothiprakash (2016) estimated the land use change between 1966, 2001, and 2009 in an urban basin in Mumbai, India. Satellite images were used during this process. It was observed that urbanization developed faster after 2001. The HEC-RAS program was used to model the river to determine the change in land use. As a result, it was concluded that the areas under flood in a 100-year return period increased by approximately 6%. It was seen that the total risk increased by approximately 22% along with the changing land use.

In flood risk studies according to scenarios, Mustafa et al. (2018) determined 24 different urbanization scenarios that could occur by the year 2100 in the Wallonia region of Belgium using past land use data. Hydraulic modeling was conducted for these scenarios during 25, 50, and 100-year return periods. A spatial agent-based model was used while determining future urbanization scenarios; WOLF 2D was used during hydraulic modeling, and FLEMO was used in the loss model during flood risk analysis. It was found that the flood risk could increase by 5,5% to 11% every decade compared to 2010 from 2030 to 2100. One of the most significant outcomes of this study is that it also uses urban intensity in flood risk leading more realistic results.

Do, Do, and Tran (2022) studied urbanization trends in a city in northern Vietnam using remote sensing (utilizing 30-meters resolution Landsat 5 and Landsat 8), and Urbanization Index analysis with GIS data. It was determined that urban intensity has been more than 43% in the last 35 years. Then, artificial intelligence methods were used to determine the flood risk. According to the obtained results, the areas with the highest flood risk were areas where intense urbanization was observed. According to the studies, not only is the impact of urbanization important, but also its size and intensity.

Nigussie and Altunkaynak (2019) conducted their research at Ayamama Creek in Istanbul's Esenler district. Urbanization was first modeled using the SLEUTH (Slope, Landuse (optional), Excluded area, Urban extent (at least four), Transportation (at least two) and Hillshade) model with different land use policies, and future predictions were made. The results of this stage were used in the 2-dimensional hydrodynamic model. In the model results, it was noticed that in the scenario where dense development is present, flood areas and therefore risk increased.

In the studies of Yu, Park, and Lee (2021), flood risk was handled from the HVE perspective. High-resolution building-based flood risk assessment was conducted in Ulsan Metropolitan City in Korea, and physical risk and index-based risk assessment methods were used together. In risk calculations, the uses of the facilities, and where high-risk buildings are concentrated gained importance in the evaluations. It was especially determined that the risk was high around the river where urban development was rapid, but there was no risk in planned settlements. Handayani, Chigbu, Rudiarto, and Putri (2020) supported the relationship that poorly planned urban planning causes an increase in flood-prone areas in

Indonesia. Moreover, it was stated that urbanization would increase the flood risk in the coming years as a result of urban plans made without considering flood risk due to the increase in population and infrastructure (Mustafa et al., 2018).

Table 2.8 gives a general summary of the literature assessed within the scope of urban flood risk assessment. As a result of the literature review, many studies on urban flood risk analysis and the effect of urbanization on flood risk were examined. However, in this section, studies that make risk assessment and that are methodologically or conceptually similar to the study area were evaluated.

Table 2.8. Summary of the literature assessed within the scope of urban flood risk

Authors	Years	Findings
Luino et al.	2012	The urban area that has been flooded increased from approximately 4% to 48% from 1852 to 1994 in Italy.
Zope et al.	2016	It was concluded that the areas under flood in a 100-year return period increased by approximately 6% in India. It was seen that the total risk increased by approximately 22% along with the changing land use.
Mustafa et al.	2018	They determined 24 different urbanization scenarios that could occur by the year 2100 in Belgium. It was found that the flood risk could increase by 5.5% to 11% every decade compared to 2010 from 2030 to 2100.
Nigussie and Altunkaynak	2019	They conducted their research at Ayamama Creek in Istanbul's Esenler district. In 2-dimensional hydrodynamic model results, it was noticed that in the scenario where dense development is present, flood areas and therefore risk increased.
Waghwala and Agnihotri	2019	Changes in Land Use/Land Cover (LULC) caused by rapid urbanization increase flood risk in India.
Handayani et al.	2020	They concluded that poorly planned urban planning causes an increase in flood-prone areas in Indonesia.
Yu et al.	2021	Flood risk was handled from the HVE perspective in Korea in this study. It was especially determined that the risk was high around the river where urban development was rapid, but there was no risk in planned settlements.
Nguyen et al.	2021	Land use for 1995 and 2019 was obtained by classifying satellite images and used to predict 2040 land use in Vietnam. Then, with the help of the Analytic Hierarchy Process method, the building-based flood risk was handled from the HVE perspective, and flood risks for the years 1995, 2019, and 2040 were compared.
Do et al.	2022	It was determined that urban intensity has been more than 43% in the last 35 years with the help of remote sensing and GIS in Vietnam. According to the obtained results, the areas with the highest flood risk were areas where intense urbanization was observed.

As a result of the literature review, many studies on urban flood risk analysis and the effect of urbanization on flood risk were examined. Changes in land use and rapid urbanization affect the water cycle, and studies have assessed hydrological processes and urbanization together. Different studies from Vietnam, India, Indonesia and Belgium explored the impact of urbanization scenarios on flood risk, indicating an increase in risk over time. Studies in northern Vietnam and Istanbul showed how urban intensity influences flood risk. The use of remote sensing and geographical information technologies provided valuable insights into flood risk assessment in urban areas. Overall, urbanization without proper flood risk consideration leads to increased flood-prone areas, emphasizing the importance of urban planning for mitigating flood risks.

3. CASE STUDY

In this section, firstly, the study area is introduced, then the methodology applied in the study is explained. Finally, the risk analysis and results created as a result of the applied methodology are included.

3.1. Study Area

Esenyurt is a district of Istanbul on the European side, located to the west of Büyükçekmece Lake and to the south of Küçükçekmece Lake. It is bounded by the Trans European Motorway (TEM) to the north and the D-100 highway to the south. In addition, the roads connecting these important arteries are also within the boundaries of the district (Map 3.1).

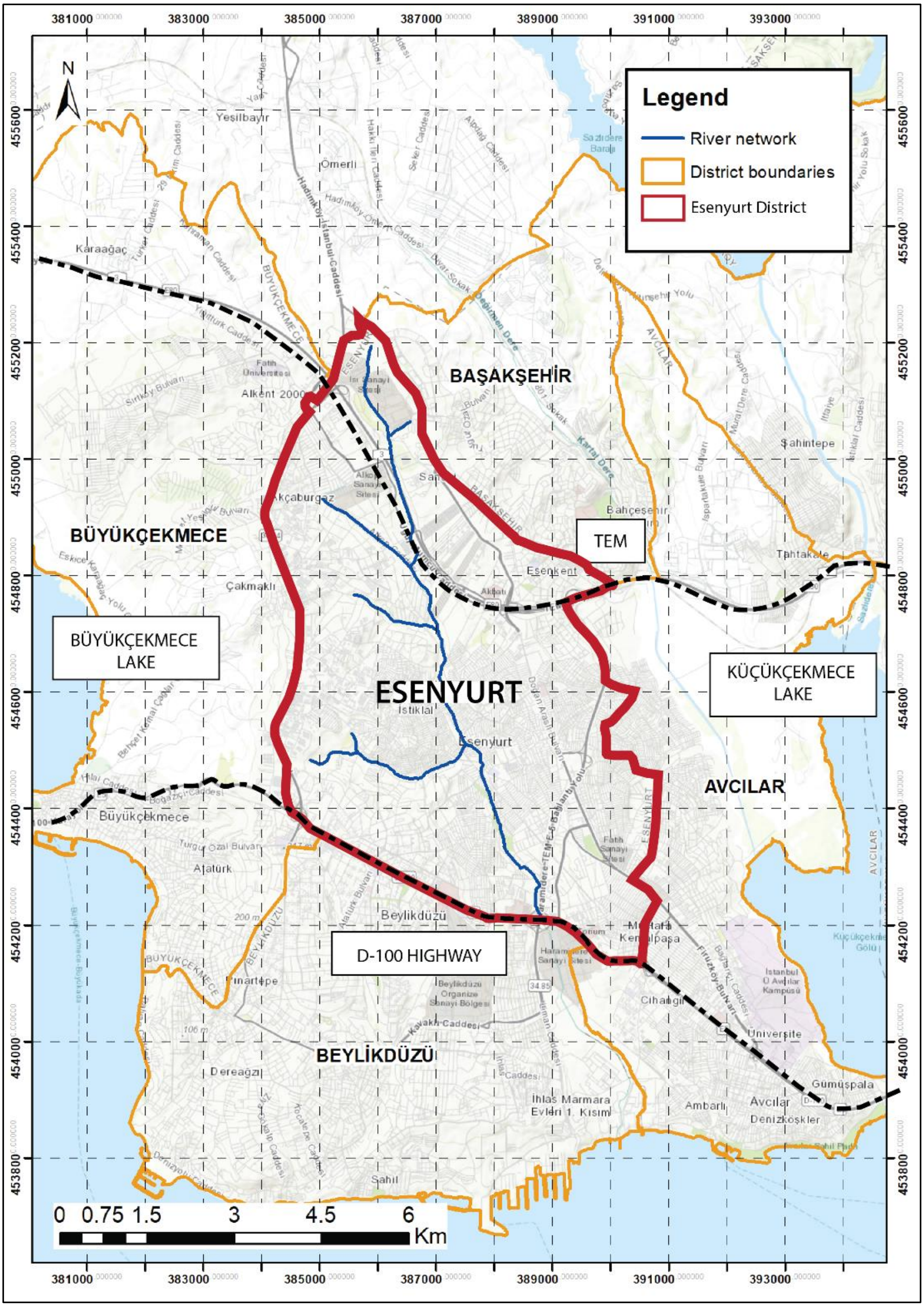

Map 3.1. Esenyurt district (created by the author)

Due to its location at the intersection of major transportation arteries, in 1970 it was a village dominated by agriculture and livestock with a population of 2 066 (URL-5). According to

Ayhan's (2019) study on the population development of Esenyurt, industrialization and population increased significantly in the 1980s with the rise in industrial facilities and Esenyurt's strategic location at the intersection of major transport routes. In 1980, the population was 7 180 (URL-5). By the 1990s, mass housing constructions had begun. Esenyurt started to become a more popular district due to cheap land prices and the relocation of industrial facilities out of the city. In 1990, the population was 72 519 (URL-5). The effects of growth in the construction sector began to be seen in the 2000s, as it was across all of Turkey. The structures built in the 2000s, characterized by rapid and unplanned construction, make up the majority of Esenyurt's building stock. In 2000, the population was 173 198 (URL-5). Over the years, with the development it provided, it gained district status in 2008. This period also marks an acceleration in both industrialization and vertical construction. After 2008, although the rate of population growth in the district varied, it continued to show a consistently increasing trend. Esenyurt district has the highest population in Istanbul in 2022. With a district population of 983 571 in 2022, it makes up 6,18% of the population of Istanbul (URL-2). Historical change of Esenyurt district is given in Figure 3.1 and population evolution by years given in Figure 3.2. When the change in the population of the district of Esenyurt over time was analyzed using figures, it was found that the population was on an upward trend. It was determined that the population increased rapidly with the changes experienced over the years.

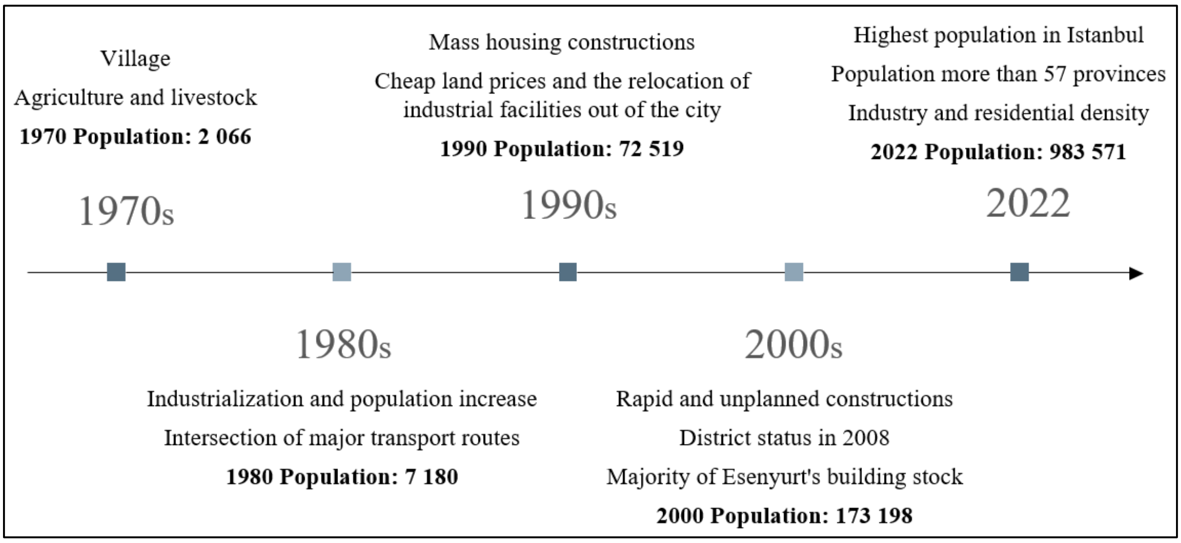

Figure 3.1. Historical change in the population of Esenyurt district

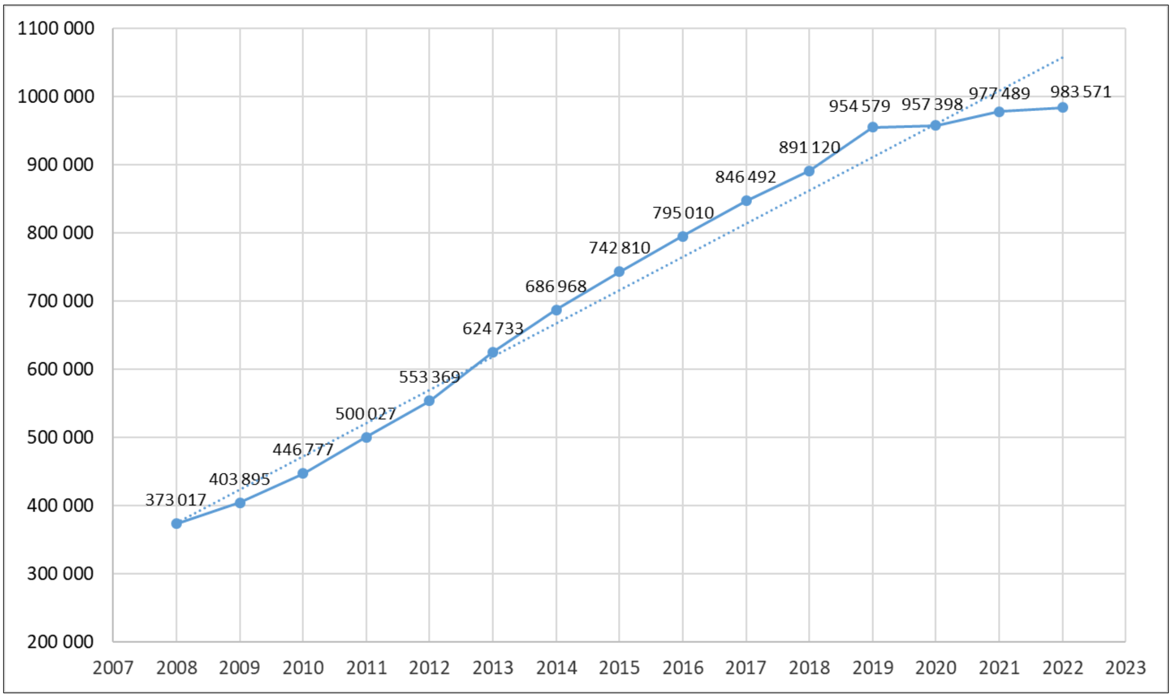

Figure 3.2. Population of Esenyurt by years (URL-2)

In the 1/100 000 scale Environmental Master Plan approved in 2009, it was decided to establish a multi-centered and linear macroform in Istanbul, and accordingly, Esenyurt was determined as a secondary center (Environmental Master Plan, 2009). It is expected to relieve the burden of the city center. At the same time, it is foreseen to have specialized trade and service functions within its own hinterland. In the Environmental Plan, thanks to its transportation advantage, it has been stated that it has become an attraction point for large-scale industries. About 30 years ago, it was stated that it turned into an unplanned and unhealthy area due to industrial facilities, while it was a village dominated by the agriculture and livestock sector with a population of 2 066.

The changes Esenyurt district has experienced over the years are visible. Examples for observing these changes are given in Figure 3.3, Figure 3.4, and Figure 3.5. These examples are Google Earth images from 2002, 2010, and 2022 of residential areas where Seyis Stream flows into Haramidere River within the Esenyurt district, given in Figure 3.2, Figure 3.3, and Figure 3.5. According to these, the building and population density increased each year, and especially when looking at the year 2022, it was seen that the residential buildings was very dense. By examining the satellite images, it can be seen that the unstructured areas are gradually decreasing from the past to the present.

Figure 3.3. The area where Seyis Creek is downstream from Haramidere River, 2002

Figure 3.4. The area where Seyis Creek is downstream from Haramidere River, 2010

Figure 3.5. The area where Seyis Creek is downstream from Haramidere River, 2022

Haramidere is a river that originates from the Esenyurt district and forms a watershed of approximately 47,5 km^2. The stream passes through important main artery roads (TEM and D-100 highway), densely populated residential areas, and industrial areas. The basin it forms mainly consists of Esenyurt (74,1%), along with Büyükçekmece (1,3%), Başakşehir (1,7%), Beylikdüzü (15,7%), and Avcılar (7,2%) districts. The basin area is shown in Map 3.2. This map also includes the floods that occurred in the years 2020-2022. These floods were identified from internet news and assigned to their approximate locations (APPENDIX-1). According to this data, all the floods occurred in the Esenyurt district.

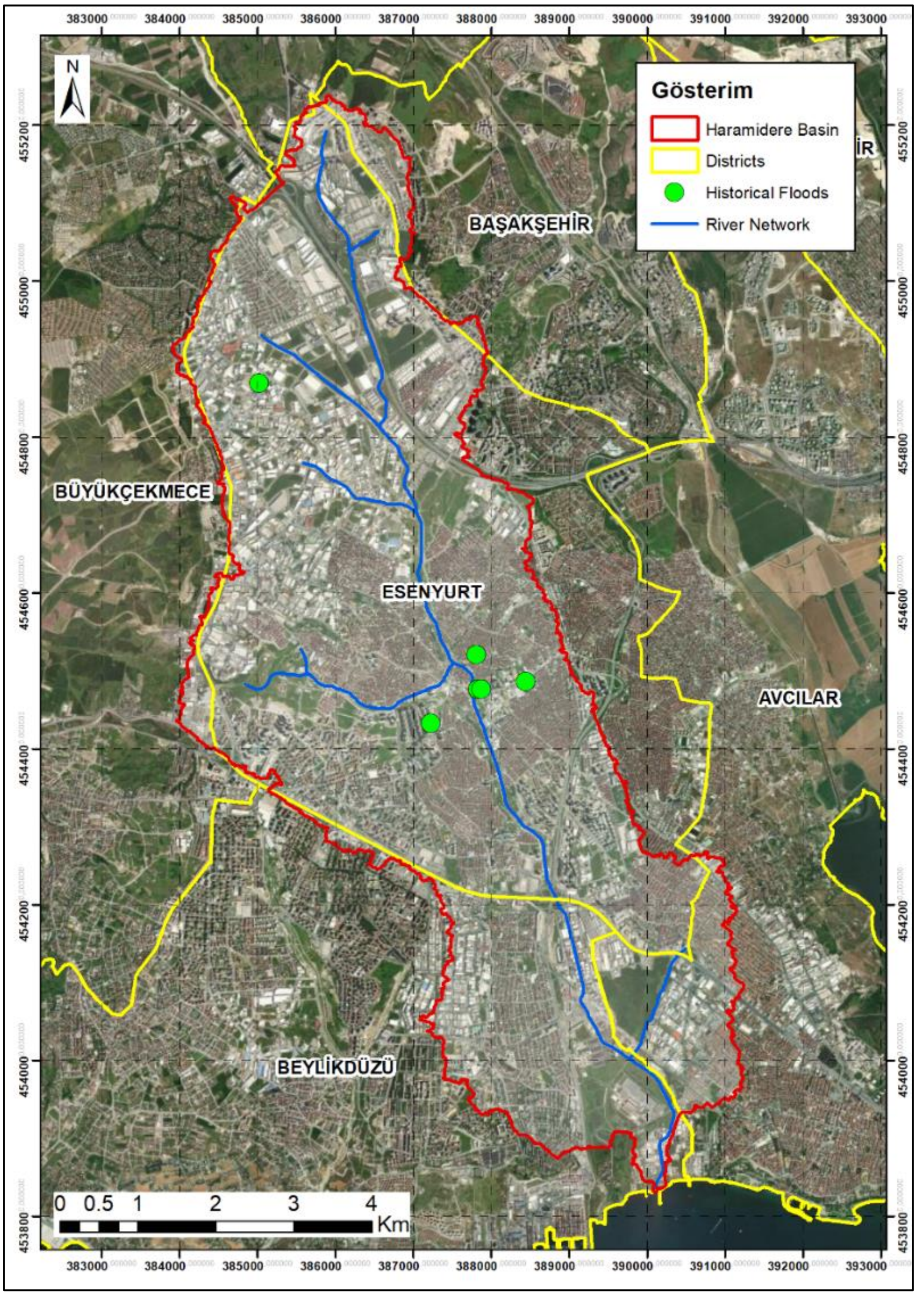

Map 3.2. Haramidere Basin and districts (created by the author)

As a result of these processes, Esenyurt district has become an area where industrial facilities are concentrated in the north and residential areas are dense in the south. The distribution of industrial facilities and residential areas in the basin is given in Map 3.3.

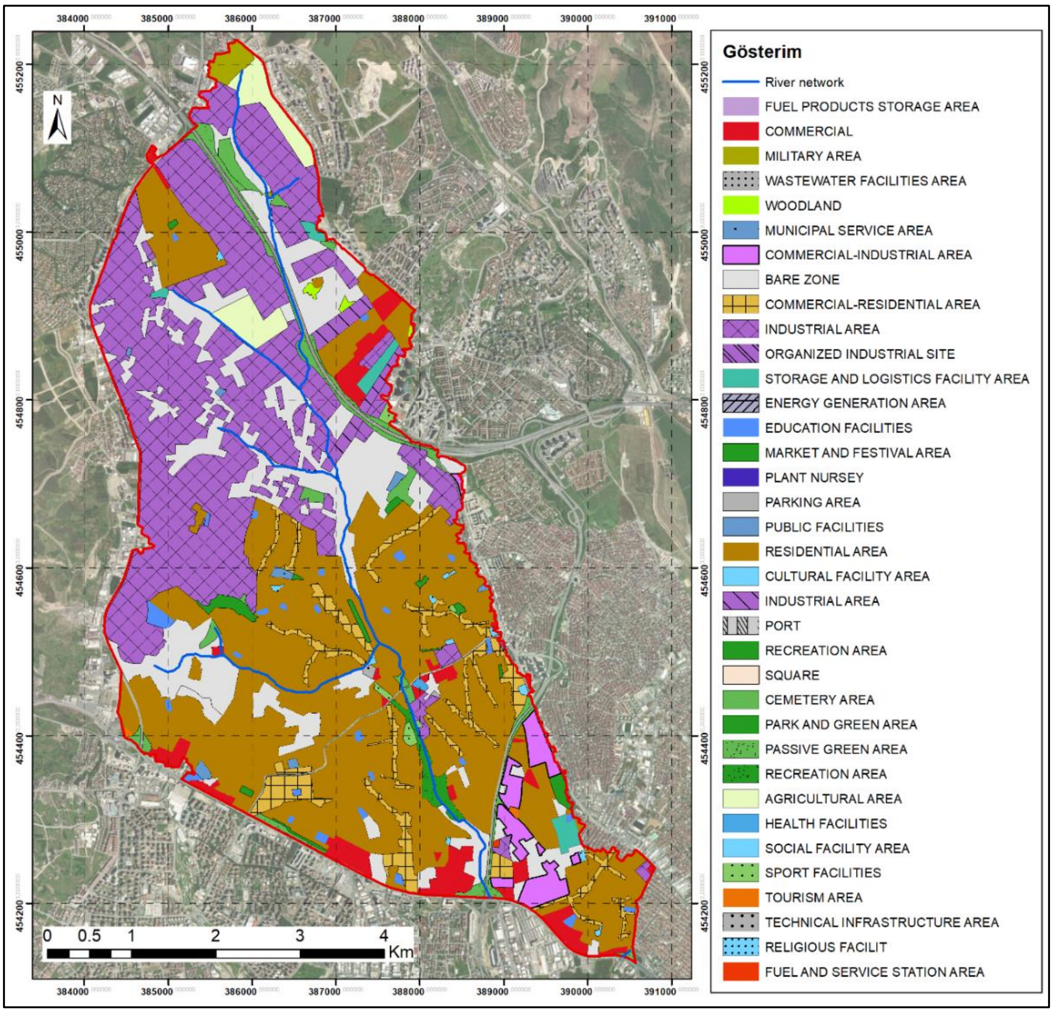

Map 3.3. Esenyurt district land use (URL-6) (created by the author)

The part of Esenyurt district affected by Haramidere River was determined as the study area (Map 3.4). The reasons behind the selection of this area are as follows:

- When the floods in the basin were examined, it was seen that they all occurred in the Esenyurt district (APPENDIX-1).
- Esenyurt district constitutes the vast majority of the basin, with 74.1%.
- It is the most populous district of Istanbul with approximately 1 million inhabitants. This district experienced rapid population growth and intense urbanization.

- This area consists of both industrial and residential areas. In this way, the difference in risk in different areas could be revealed.

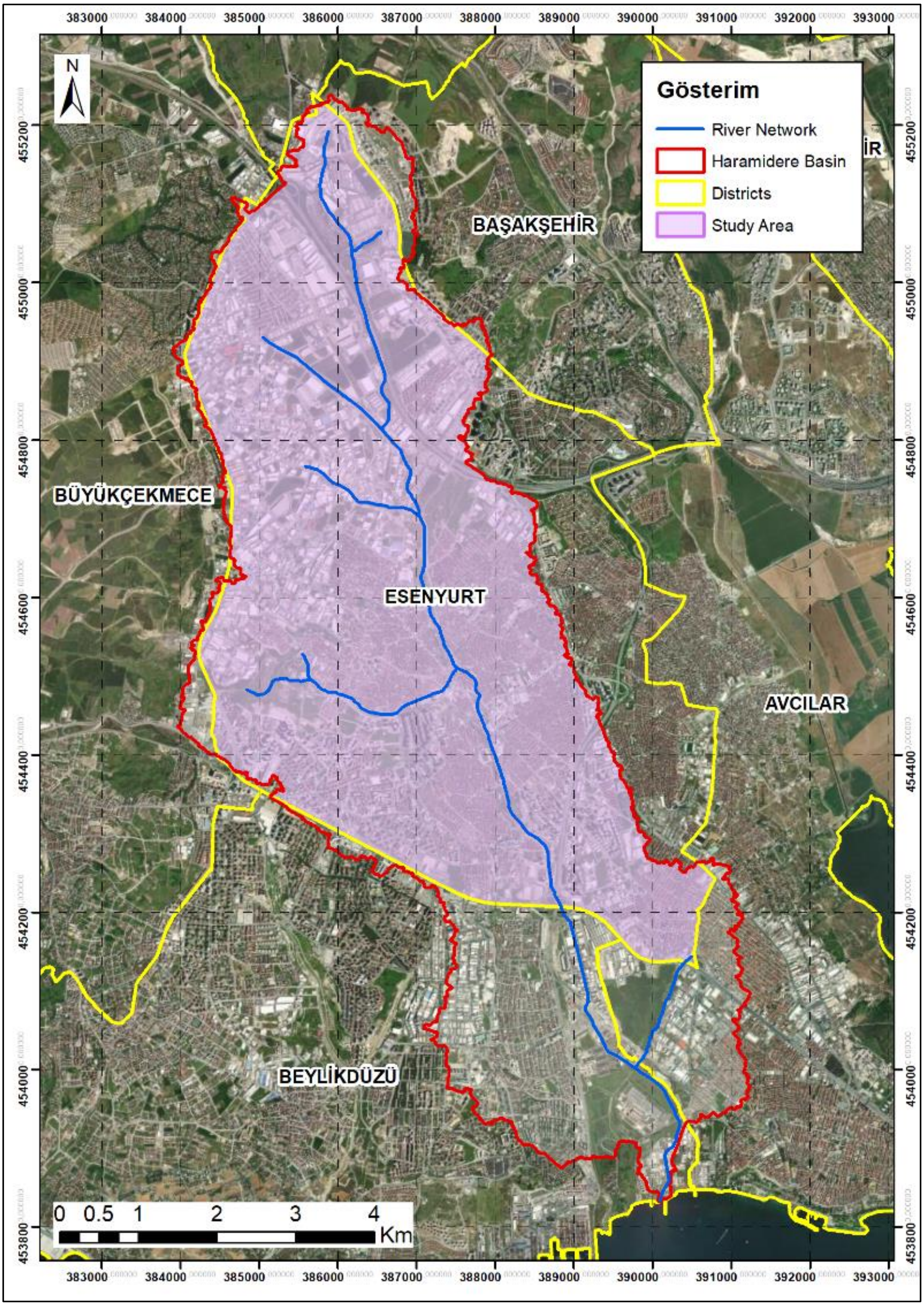

Map 3.4. Study area (created by the author)

Photographs to help identify the study area are given in APPENDIX-2.

3.2. Material and Method

Flood risk occurs with the spatial combination of hazard, degree of vulnerability, and exposure. In this context, the flood risk components evaluated within the framework of HVE (Hazard, Vulnerability, Exposure) used in the thesis, are as seen in Figure 3.6.

The followed methodology consists of two interrelated parts for the calculation of building-based flood risk over the years. The first of these is the identification of flood-affected buildings, and the second is the calculation of flood risk in a way that is compatible with the methodology used in Flood Management Plans, using the identified backgrounds of buildings. These parts are not separate from each other; both parts are interrelated and mutually supportive. The method used in the thesis was explained in detail in this section.

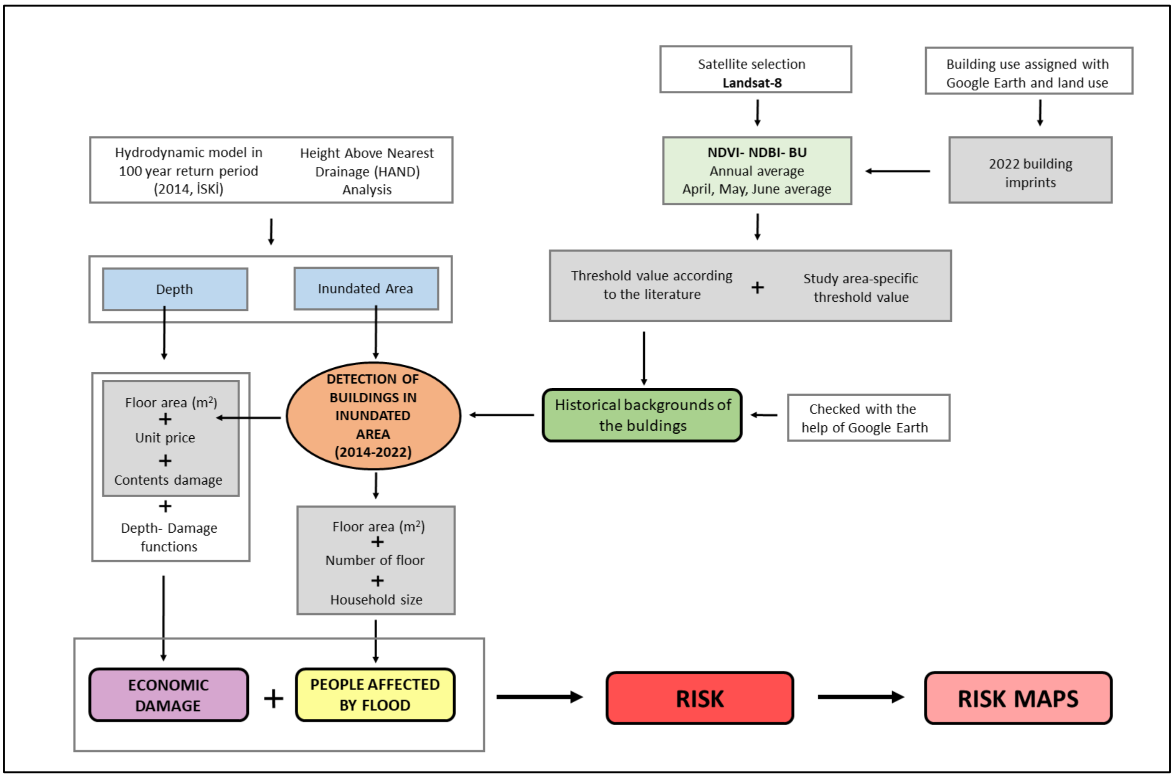

Figure 3.6. Thesis methodology flow diagram

3.2.1. Background Analysis of buildings

In order to calculate the historical flood risk within the scope of the study, it is necessary to know when the buildings were built. The study area is highly urbanized, soil was considered more practical to determine the past status of the building through remote sensing techniques, rather than examining them individually. Initially, the essential base conditions were determined.

These conditions are:

- The coverage years of the relevant satellites should cover the years 2014-2022.
- In terms of temporal resolution, it should take measurements at least once a month.
- It should be frequently used in international studies.
- It should possess bands that enable the differentiation of water, green spaces, and soil on the earth's surface.
- It should have the highest possible spatial resolution (<30m).

Remote sensing data are primary sources for analyzing environmental processes on a local or global scale (Kshetri, 2018). There are different methods in the literature for one of the basic conditions mentioned above, which is to differentiate water, green spaces, and soil. One of these methods is remote sensing techniques, where the behaviours at different wavelengths, as seen in Figure 3.7, are examined.

Soil, vegetation and water behave differently at different wavelengths in the electromagnetic spectrum (Figure 3.7). Using these behaviors, these three components can be distinguished from each other. The goal here is to differentiate buildings from other components. Therefore, NDVI, NDBI and BU, which can easily identify these components, were used. NDVI is considered to decrease in value when a previously vegetated area turns into a building area, while the other two indices, NDBI and BU, are considered to increase in value vice versa.

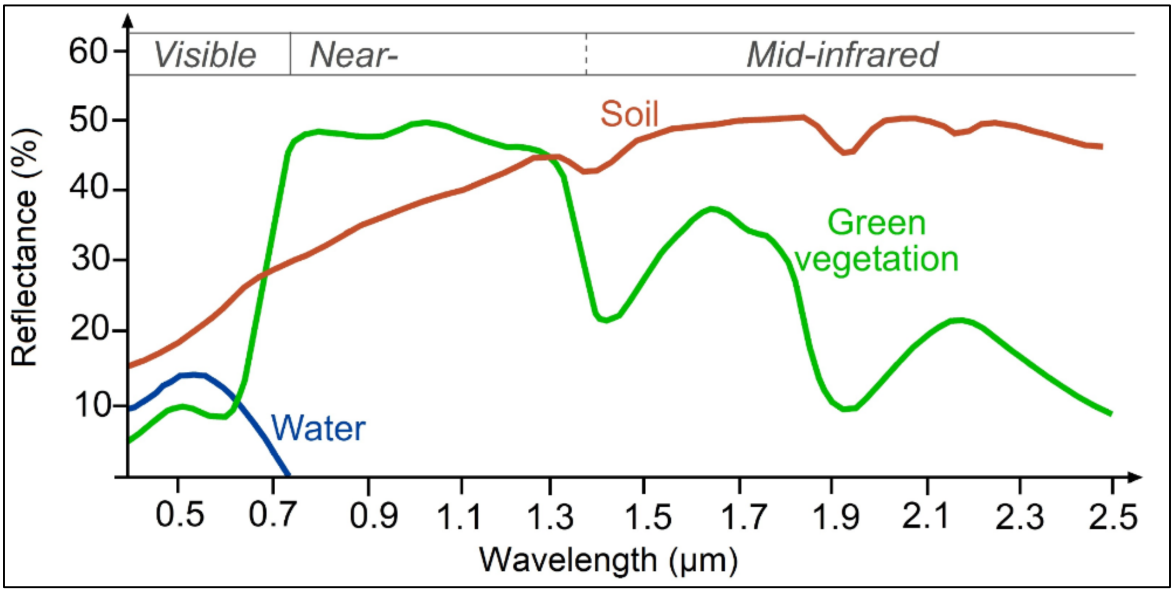

Figure 3.7. Reflectance of water, soil and vegetation at different wavelengths (URL-7)

In this thesis, it is similarly intended to investigate the Normalized Difference Vegetation Index (NDVI), the Normalized Difference Built-Up Index (NDBI), and the Built-Up Index (BU) to be used in the study area. These three indices were calculated using the Visible Red, Near Infrared (NIR), and Shortwave Infrared (SWIR) ranges required in different wavelengths (Table 3.1). The vegetation and built-ups for the buildings located in the flood inundated area have been examined. In this way, it has been aimed to determine the construction years of the buildings retrospectively. Another benefit of this study is that the effect of urbanization on NDVI, NDBI, and BU was analyzed. The aim here has been to determine the values used in the classification of these indices in terms of building construction years. Therefore, it has been aimed to determine the threshold values of the indices that will distinguish buildings from the ground and green areas specific to the thesis area.

Table 3.1. Wavelengths of electromagnetic spectrum

Wavelength (nm)	Spectral Range Name
400–500	Blue
500–600	Green
600–700	Red
700–1 100	Near Infrared (NIR)
1 100–3 000	Shortwave Infrared (SWIR)

Normalized Difference Vegetation Index (NDVI)

With the advancement of technology, Remote Sensing methods are increasingly being used to conduct observations and analyses in various fields, enabling situational assessments based on the derived information.

Several methods are frequently employed to identify vegetation using satellite imagery. Within the scope of this thesis, the Normalized Difference Vegetation Index (NDVI) is deemed appropriate for evaluation among these methods. NDVI results allow for understanding the changes in vegetation presence in the region over years or months (Internet: Measuring Vegetation, 2000). Furthermore, the images enable users to perform this evaluation spatially.

The NDVI calculation method essentially involves the joint evaluation of Near-Infrared (NIR) and Visible Red (R) wavelengths in the electromagnetic spectrum (Figure 3.8). The reflectance properties of vegetation, due to the chlorophyll pigment it contains, are high in the near-infrared wavelengths and low in the visible red wavelength. This distinction allows for a comparison, as can be seen in Figure 3.8.

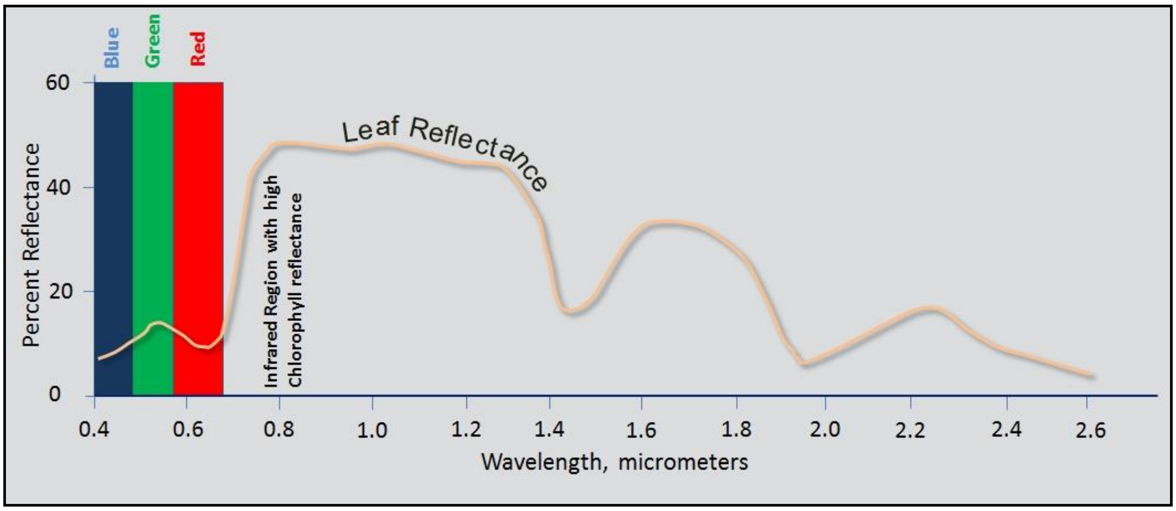

Figure 3.8. Leaf reflectance – wavelength (URL-8)

NDVI is calculated by the following formula:

NDVI = (NIR-VR)/(NIR+VR) (3.1)

NIR: Near Infrared

VR: Visible Red

The results obtained from the NDVI calculation vary in the range of -1 to +1. According to these results, as we move from -1 to +1, vegetation increases (URL-9).

Upon examining the studies in the literature;

- Holben (1986) classified -0,257 as water, -0,046 as snow and ice, 0,002 as cloud, 0,025 as bare non-vegetated area, and 0,7 as intense vegetation.
- Weier and Herring (2000) indicated that values less than 0,1 represent water, snow, ice, and bare rock areas, 0,20 – 0,30 represent grassland and shrub, and 0,6 – 0,8 represent dense stable forest areas (URL-9).
- Anim et al. (2013) classified values less than -0,1 as areas covered with water, -0,10 – 0,15 as non-vegetated areas, 0,15 – 0,25 as grassland and shrub, 0,25 – 0,32 as open (low density) forests, and 0,32 – 0,40 as closed (dense) forest areas.

Taking into consideration the aforementioned studies, it is necessary to classify the NDVI values to understand how the vegetation status of the basin has changed using NDVI values within the scope of the study. For this purpose, considering these studies, the NDVI values have been classified as seen in Table 3.2.

Table 3.2. NDVI Classification

NDVI Values	Description
<0	Water, Water Structures, Snow, Ice
0-0,15	Bare Area, Bare Rock, Settlement
0,15-0,25	Sparse Vegetation
0,25-0,35	Sparse-Moderate Vegetation
0,35-0,40	Moderate Vegetation
0,40-0,50	Moderate-Intense Vegetation
0,50-0,60	Intense Vegetation
>0,60	Very Intense Vegetation

Adapting from studies in the literature, the NDVI values have been divided into eight classes. Through this classification, the aim is to more effectively reveal how the vegetation and soil presence in the basin change over different time periods.

Normalized Difference Built-Up Index (NDBI)

There are numerous indices employed in the analysis of developed areas. The most frequently used among these are the Normalized Difference Built-up Index (NDBI), Built-up Index (BU), Urban Index (UI), Index-based Built-up Index (IBI) etc. Each of these indices has a unique formula and method of calculation. A pivotal feature of NDBI is its proficiency in distinguishing between built-up territories, barren land, and vegetative regions. This is made possible by exploiting the reflective properties of various surfaces in the Shortwave Infrared (SWIR) and Near Infrared (NIR) spectra. Habitually, built-up and barren zones reflect more SWIR than NIR, which makes them distinctive in NDBI computations as given below.

The Normalized Difference Built-Up Index (NDBI) has gained substantial recognition in numerous studies due to its utility in delineating and monitoring urbanized spaces. The Normalized Difference Build-up Index (NDBI) is considered as a rapid and appropriate method for mapping built-up areas (Karanam and Neela, 2018). The core advantage of NDBI stems from its capability to segregate built-up zones from other land cover types such as vegetation and aquatic bodies.

The process of image classification is lengthy and complicated, requiring multiple operations on a composite band to produce the final result. The accuracy of this technique depends on the analyst and the methodology they use. Yet, calculating NDBI is comparatively straightforward and simple. It has the following formula similar to NDVI:

NDBI=(SWIR – NIR)/(SWIR+ NIR) (3.2)

SWIR: Shortwave Infrared
NIR: Near Infrared

The value of the Normalized Difference Build-up Index ranges from -1 to +1. Negative NDBI values signify water bodies, while higher values correspond to built-up areas. It has low value for the vegetation.

NDBI values can be specific to the study area. Therefore, instead of giving classification table gathered from the literature, lower and upper limits specific to the study area have been determined, and building threshold values have been created.

Built-Up Index (BU)

For optimal results, consider utilizing the Built-up Index (BU). The Built-Up Index (BU) has emerged as a crucial resource in the field of urban planning and land use studies, largely due to its proficiency in detecting developed or built-up regions employs both NDBI and NDVI in given below. The Built-up Index generates a binary image where higher positive values signify built-up and barren areas, enabling the BU to map these regions automatically (Kshetri, 2018).

BU = NDBI – NDVI (3.3)

Furthermore, NDBI has been utilized in conjunction with other indices, like the Normalized Difference Vegetation Index (NDVI), to develop comprehensive land cover maps. The Built-Up Index (BU), calculated by subtracting NDVI from NDBI, has been validated as an effective tool for urban pattern mapping.

Built-Up Index (BU) holds considerable potential for urban studies, significantly enriching our comprehension of urban patterns, changes in land use, and urban heat islands.

Satellite selection

There are satellites that provide data for remote sensing for various purposes. These satellites have different features according to their intended uses. Some of the main ones can be listed as spatial and temporal resolution, bandwidth, band number, band type covering spectral range (spectral resolution), etc.

Within the scope of this thesis, satellites with bands for Visible Red, Near Infrared (NIR), and Shortwave Infrared (SWIR) wavelengths are required to calculate the indices mentioned in the previous sections. The main satellites that contain the wavelengths necessary to calculate these indices, which will be used to examine the past construction statuses of buildings, can be mentioned as Landsat 5-7-8, Sentinel-2, MODIS Aqua/Terra, etc. In this study, many satellites have been examined and the satellites mentioned in the previous sentence have been compared (Table 3.3).

The comparison criteria for these satellites have been determined as follows:

a) Having a resolution that can cover almost the building area (<30m),
b) Coverage years: 2014-2022,
c) Having a temporal resolution of at least one month.

Table 3.3. Comparison of satellites

Satellite	Spatial Resolution (m)	Temporal Resolution (Days)	Coverage Years	Band Types	Band Wavelengths (μm)
Landsat 5	30, 120 (TIR)	16	1984 - 2013	Multi-spectral	7 bands (0,45 – 2,35)
Landsat 7	15 (pan), 30, 60 (TIR)	16	1999 - 2021	Multi-spectral, Panchromatic	8 bands (0,45 – 2,35), Pan (0,52 – 0,90)
Landsat 8	15 (pan), 30, 100 (TIR)	16	2013 - Present	Multi-spectral, Panchromatic, Thermal	11 bands (0,43 – 2,51), Pan (0,50 – 0,68), TIR (10,60 - 12,51)
Sentinel-2A	10, 20, 60	5	2015 - Present	Multi-spectral	13 bands (0,443 – 2,19), including atmospheric bands
MODIS Aqua	250, 500, 1000	1-2	2002 - Present	Multi-spectral, Thermal	36 bands (0,405 – 14,385)
MODIS Terra	250, 500, 1000	1-2	1999 - Present	Multi-spectral, Thermal	36 bands (0,405 – 14,385)

As seen in Table 3.3, although the MODIS satellite meets all conditions, it was not selected due to its comparatively low spatial resolution. Moreover, although Sentinel-2A has a high resolution, its measurement range is not suitable for the scope of this study. Similarly, the operational ranges covered by Landsat-5 and Landsat-7 are not appropriate for evaluation in this study. For these reasons, it has been deemed appropriate to work with data from the Landsat-8 satellite.

Calculation of indices and evaluation of results for historical background of buildings

The Google Earth Engine (GEE) scripts have been utilized to process the Landsat-8 library for the study. As such, instead of individually downloading each of data, all analyses have been carried out on the GEE platform.

The dataset is precisely titled “LANDSAT/LC08/C02/T1_L2”. This dataset contains atmospherically corrected surface reflectance and land surface temperature derived from the data produced by the Landsat 8 OLI/TIRS sensors (Google-GEE, 2023). For this dataset, imagery with cloud coverage exceeding 20% have not been included in the study. Besides the annual average values of the indices, the three-month averages for the months of April, May, and June, when vegetation is dense, have been examined to exclude snow, ice, etc.

NDVI, NDBI, and BU calculations were carried out using 1 051 building polygons within the flood zone obtained for 2022. For each building, the annual and three-month (April, May, June) average NDVI, NDBI, and BU were calculated for the years between 2014-2022.

The calculations were finalized in 4 stages (Figure 3.9):

1) For the values obtained as time series, the years where the index values break were identified by using the percentage cumulative of yearly average values and the months covering April-May-June for the related year.
2) Subsequently, threshold values for the building present in the classification obtained from the literature for NDVI were studied.
3) However, considering that the dynamics of the study area might differ, area-specific building threshold values were also determined. The method was to take the lower and upper values of the indices (NDVI, NDBI, and BU) calculated for all the buildings in the study area since 2014 as the building threshold value. Then, the years that are not within these values for the buildings constructed after 2014 were identified.
4) For some buildings within the flood inundated area, the findings obtained from the 1st, 2nd, and 3rd items listed above were validated with Google Earth historical images to determine the most suitable method.

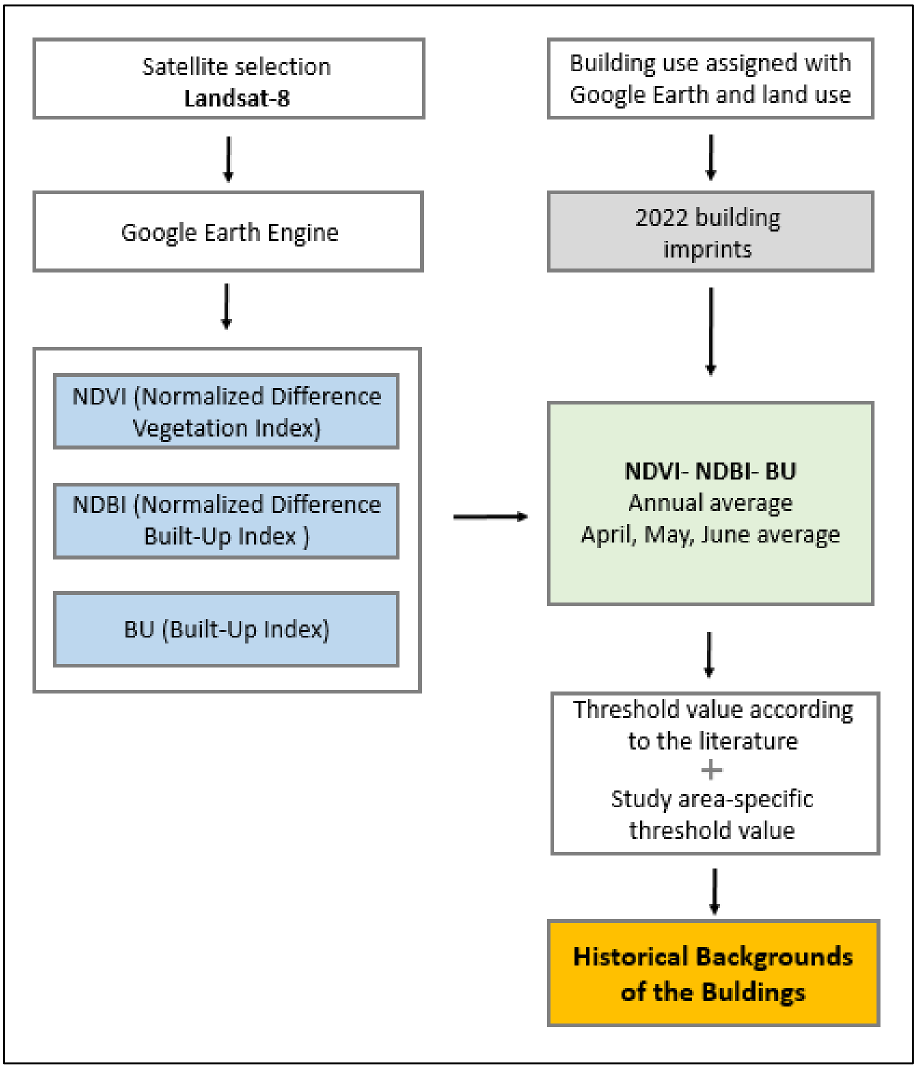

Figure 3.9. Background analysis of buildings flowchart

According to Figure 3.10, Figure 3.11, Figure 3.12, Figure 3.13, Figure 3.14 and Figure 3.15, the break line of the indices can be easily differentiated. All figures indicate that urbanization rate is suddenly increased in 2016, 2017 and 2021. The same methodology was applied for all individual buildings for the determination of their historical background in terms of existing or not.

Taking the average value of the 12 months of the year may lead to indices being affected by seasonal variations. For this reason, the averages of the index values of April, May and June, when vegetation is relatively high, were also evaluated (Figure 3.11, Figure 3.13, Figure 3.15).

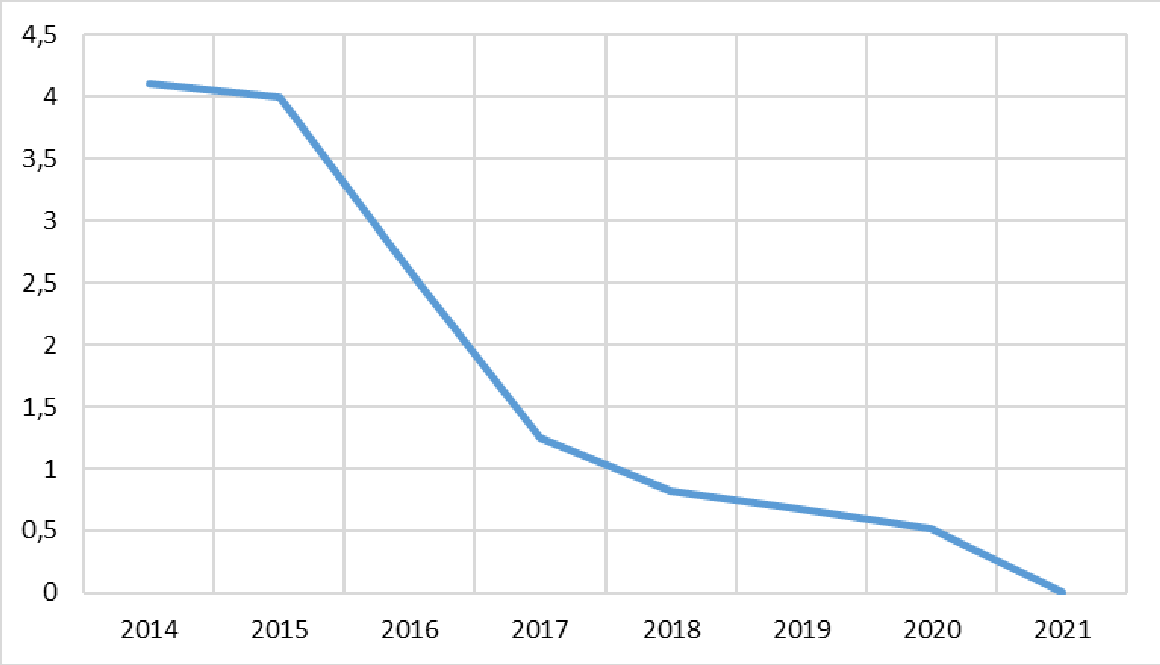

Figure 3.10. Percentage cumulative of yearly average NDVI values for all months

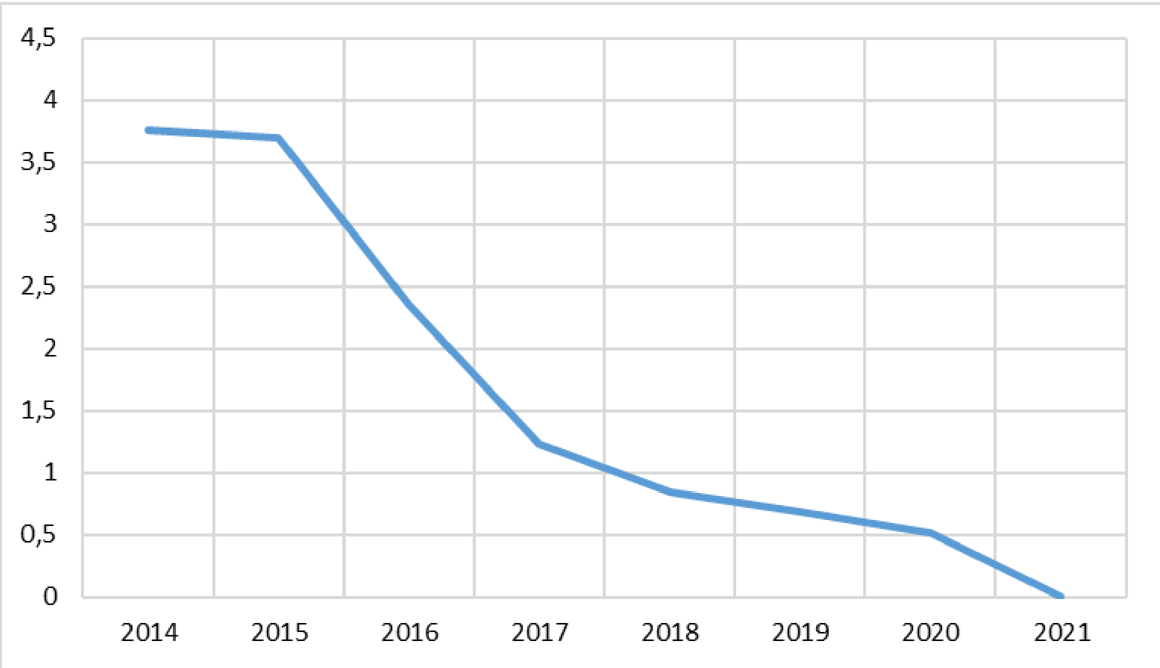

Figure 3.11. Percentage cumulative of yearly average NDVI values for 3 months (April-May- June)

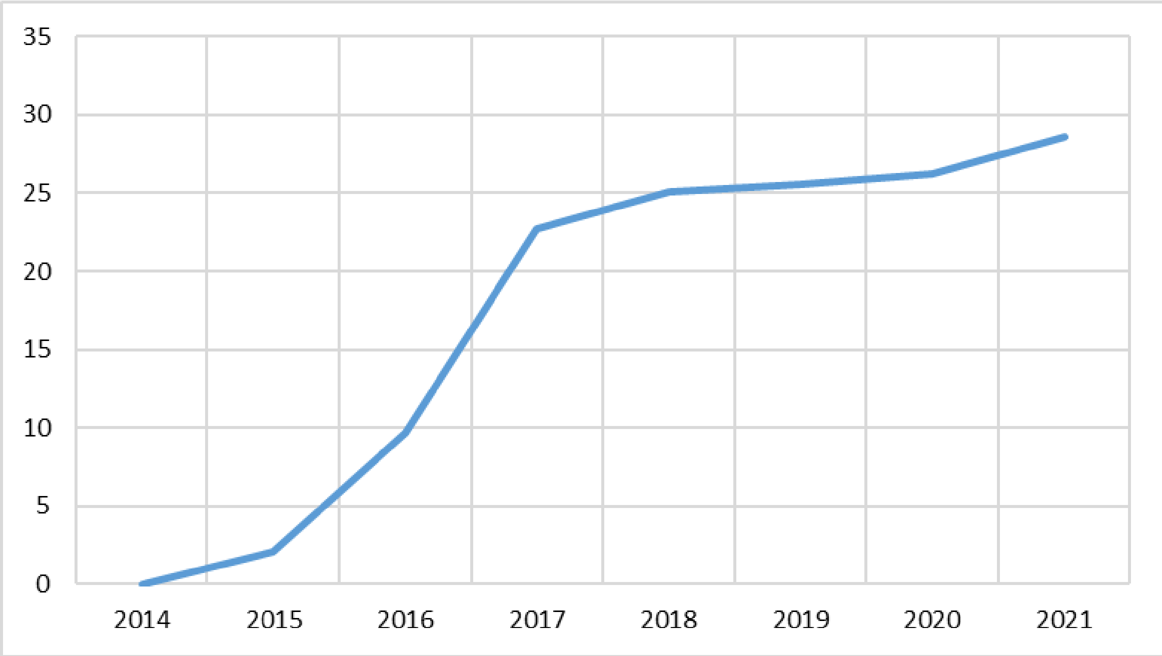

Figure 3.12. Percentage cumulative of yearly average NDBI values for all months

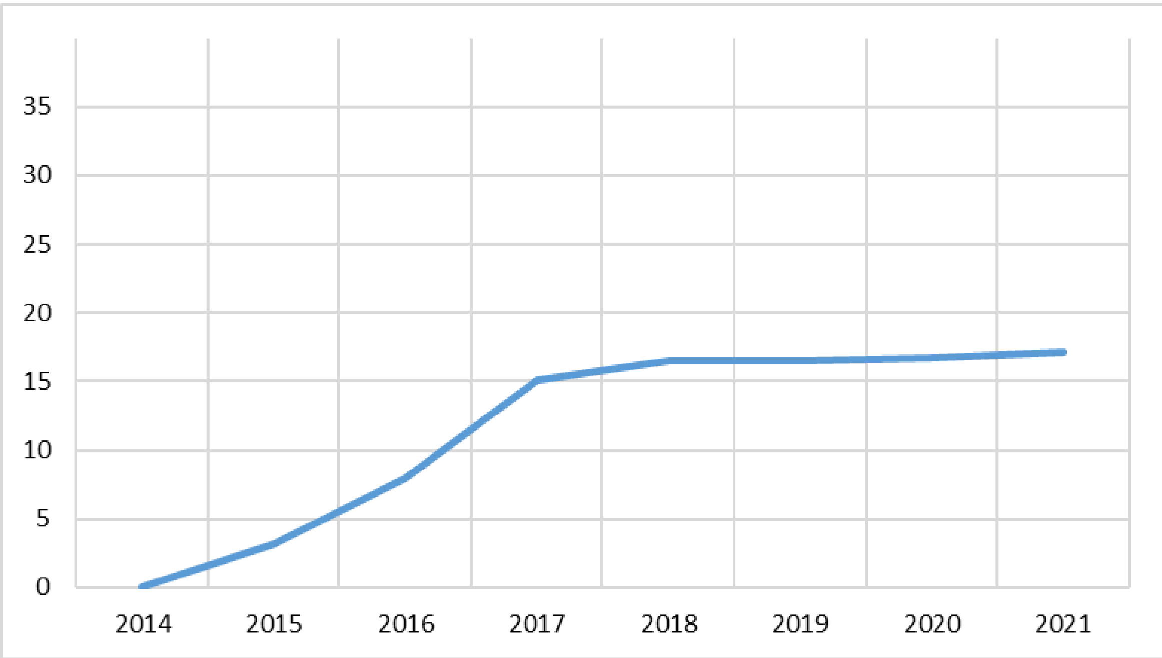

Figure 3.13. Percentage cumulative of yearly average NDVI values for 3 months (April-May- June)

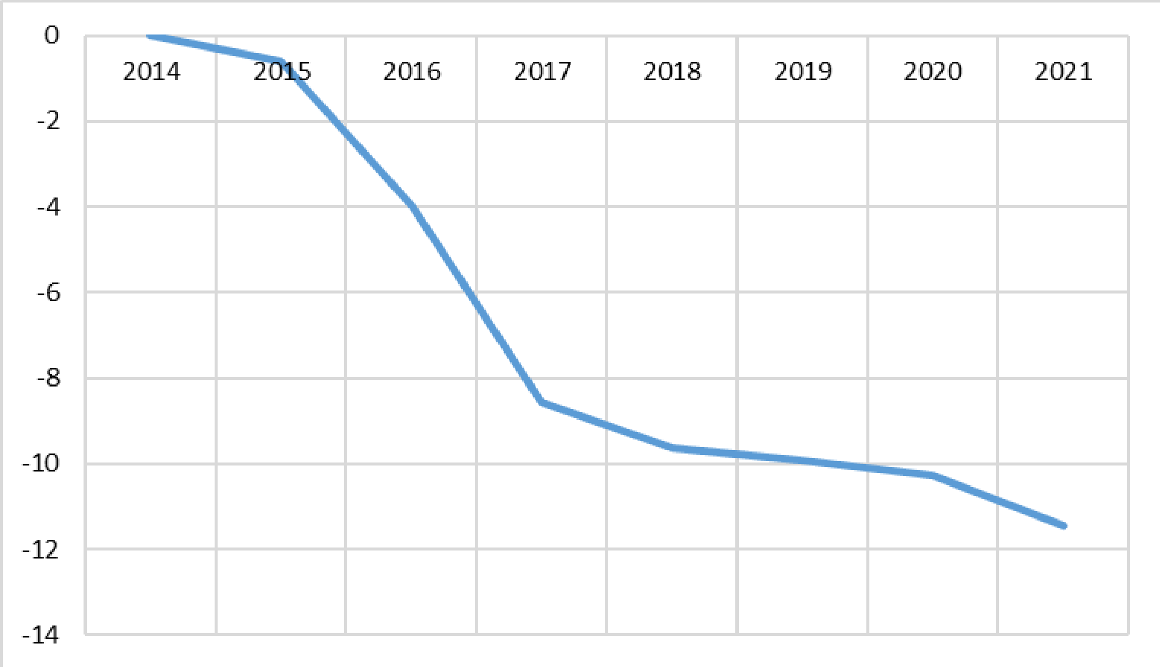

Figure 3.14. Percentage cumulative of yearly average BU values for all months

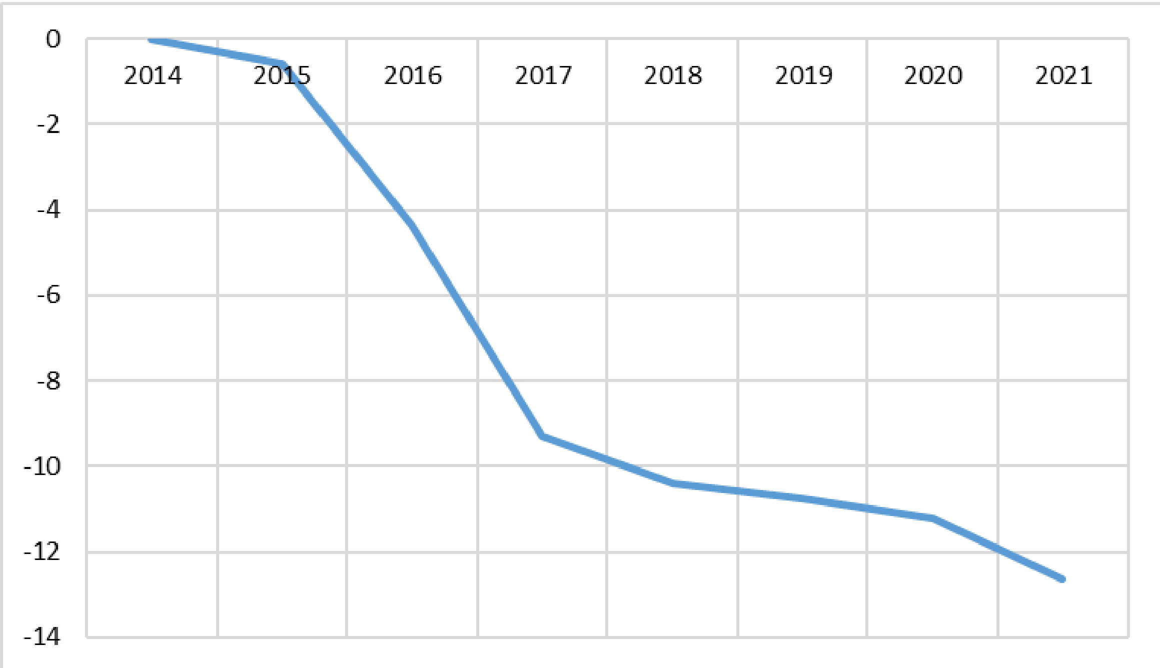

Figure 3.15. Percentage cumulative of yearly average BU values for 3 months (April- May-June)

In conclusion, the years of construction were determined for the buildings classified into three main categories of "residential buildings, commercial buildings, and industrial facilities" within the flood zone. In this way, the buildings in the study area and the construction threshold values for each of these structures were identified (Figure 3.16). This study has allowed the temporal calculation of flood risk.

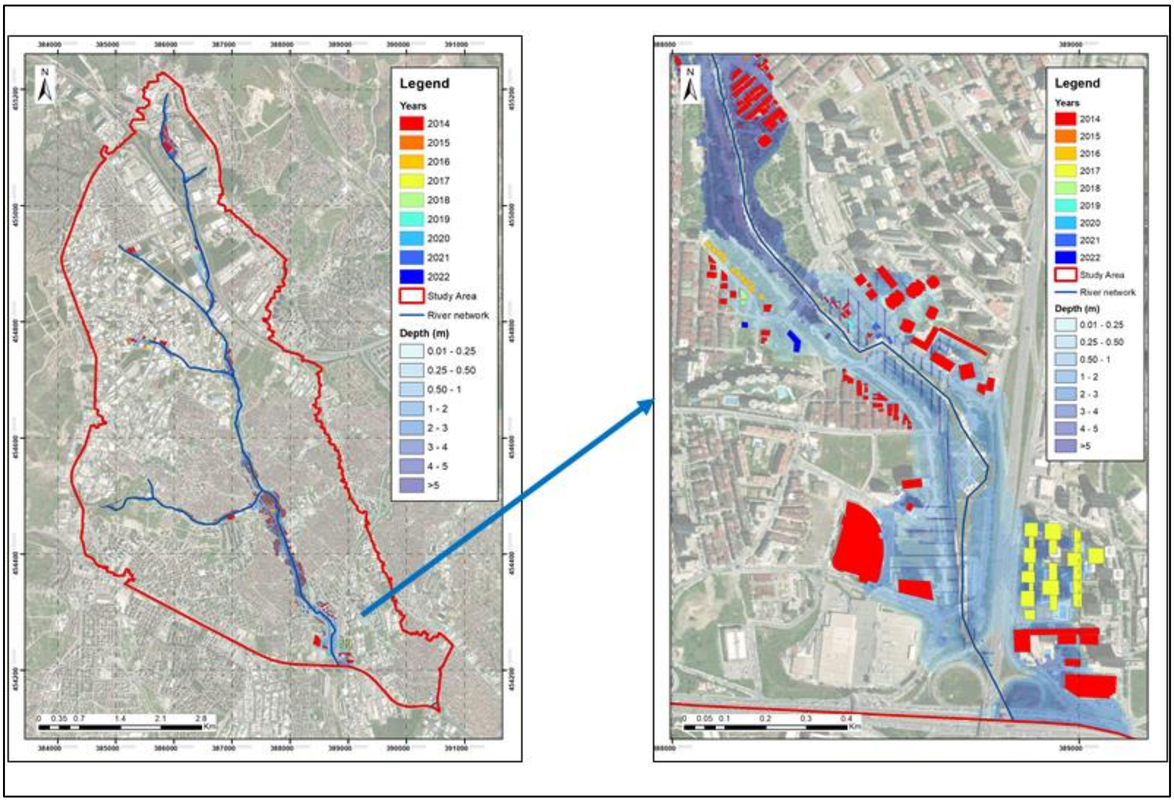

Figure 3.16. Construction years of the buildings

3.2.2. Flood risk methodology

In the literature, there are numerous methods used by both scholars and governments for calculating flood risk. These methods vary depending on the flood area, scale, data situation, and time period. In this study, the methodology applied in the Flood Management Plans by the General Directorate of Water Management, Republic of Turkey Ministry of Agriculture and Forestry was used for risk analyses. This methodology has been used by the Ministry in many flood management plans. These flood management plans where these methodologies have been applied are in the following basins: Northern Aegean Basin (2019), Eastern Mediterranean Basin (2019), Akarçay Basin (2019), Lake Van Basin (2020), Asi (2020), Eastern Black Sea Basin (2020). This methodology was applied in this thesis in a smaller basin and in more detail than the Flood Management Plans.

For flood risk, the flood inundated area and inundation depth were determined primarily under the scope of hazard analysis. To determine the flood areas, a flood modeling project carried out on the Haramidere Basin by İSKİ (Istanbul Water and Sewerage Administration General Directorate) in 2014 was used (İSKİ, 2014). Flood simulations were performed with 1 and 2-dimensional hydrodynamic models. In the study, MIKE 11 program was used for 1D in flood simulation, and MIKE FLOOD program was used for studies in which 1D and 2D were used integrated. Within the scope of this project, hydrological and hydrodynamic studies were conducted for 25, 100, and 500-year return periods. Q_{max} (maximum discharge) was calculated for each return period, these are: 218,53 m^3/s for Q_{25}, 376,91 m^3/s for Q_{100}, 535,28 m^3/s for Q_{500}. As a result of these studies, flood inundated areas and inundation depths were determined for each return period. The 100-year return period was used in this thesis because using the 100-year return period would give more realistic results in risk calculations.

For this thesis, the flood inundation area and depth corresponding to the 100-year return period in the project conducted in 2014 served as the basis. Rehabilitation work was carried out on the Haramidere River in the study area over time. However, to mitigate the impact of these rehabilitation works, the model results obtained in 2014 were utilized as the reference. It was assumed that there have been no structural interventions in the river network since 2014, and as a consequence, the flood areas and depths remained constant. For these reasons, historical risk assessments were examined from 2014 to 2020.

The inundated areas and inundation depth were then digitized for use in risk calculation. The digitized flood inundated areas (total 1,54 km^2) and depth, along with the flood-affected buildings, are shown in Map 3.5.

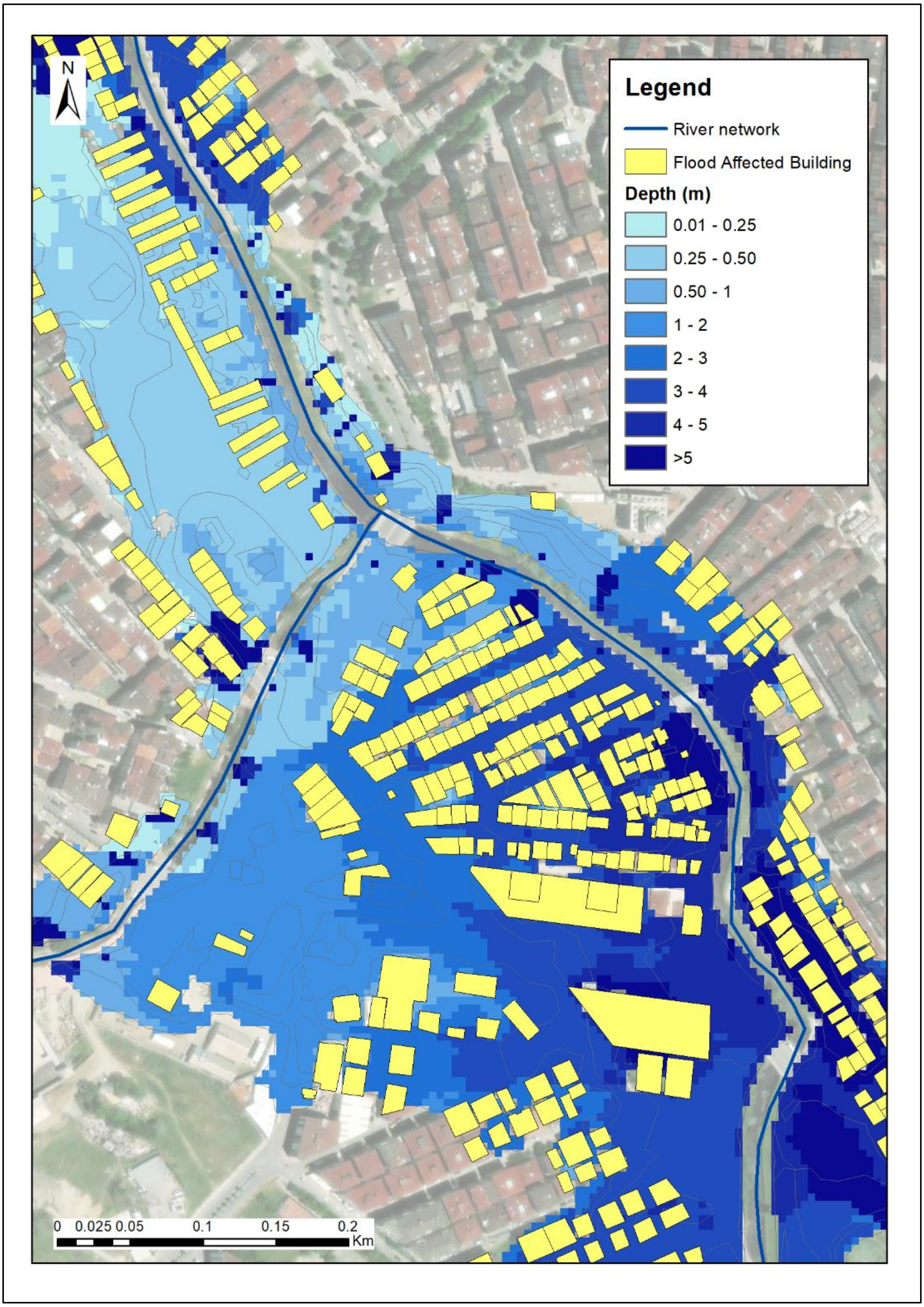

Map 3.5. Inundation depth (m) created with a 100-year return period and flood-affected buildings for 2022 (created by the author)

The depth measurement is in meters according to the digitized flood inundated areas and depth data. However, more detailed depth data is needed for flood risk analysis. For this reason, with the help of ArcGIS program, the depth of the flood was made in more detail depending on the river network by using the Height Above Nearest Drainage (HAND) method. This analysis was created using the digital elevation model of the study area and the river network. Height Above Nearest Drainage (HAND) is a topographical model that calculates the vertical distance from each part of a raster grid to the closest water course, like a river or stream. In simpler language, it figures out the elevation of any specific point on a landscape in relation to its closest water source. In this way, it was determined that the maximum level of the flood could be reached.

HAND modeling is crucial for predicting the course of water across a terrain, and it is particularly beneficial in assessing flood risk. By understanding the elevation of a location with respect to the nearest body of water, one can predict its susceptibility to flood during heavy rainfall. It offers a more precise and efficient way to forecast the boundaries and depths of potential floods. After examining the data in Map 3.5, the maximum water height was determined as 20 meters. Since the project in 2014 had a flood depth of over 10 meters, the HAND analysis was carried out to stay on the safe side by setting a limit of 20 meters. In addition, the sensitivity of the flood depth was reduced to the centimeter level. The flood areas identified in the flood modeling study conducted by İSKİ over the Haramidere Basin remained constant, and the measurement of the inundation depth was made more precise.

People affected by flood

Within the scope of the exposure analysis, affected people and buildings were identified. The affected building constitutes one of the two parts of the methodology and was discussed in detail under the heading of "Background analysis of buildings". Assumptions were made to determine the affected people due to exposure. One of the important assumptions is that everyone in the flood inundation area will be affected, regardless of the water depth. The household size of 3,43 people and the nighttime population were taken as a basis when calculating the affected population risk (URL-10). In Esenyurt district, the size of a residential apartment is assumed to be approximately 125 m^2. It was assumed that the average residential apartment has a net area ranging from 90 to 125 m^2, and to reach the gross area, an additional 15% was added, resulting in a total of 125 m^2. Accordingly, the number of people affected was calculated based on the number of residential floors and the floor area of building.

Economic damage

The damage assessment was carried out using vulnerability and exposure inputs together. In the methodology, it is emphasized that the economic damage has a linear relationship with the depth-damage. This approach has been accepted as the international standard approach in the literature, acknowledging a linear relationship between depth and damage. In this context, the economic damage calculations in the methodology and the standard approach in the literature are identical.

To determine the economic damage, the following formula was calculated separately for each building.

$$Z = DR \times A \times BF \times 0{,}6 \times 0{,}5 \times 1{,}18 \tag{3.4}$$

Z: Economic damage value (TL)
DR: Depth- damage function value
A: Floor area of building (m^2)
BF: Unit price of building (TL/m^2)

To calculate the flood risk in the applied formula, the depth-damage relationship should be determined first. Flood data (inundation depth) and economic damage data from past years are used to reveal the depth-damage relationship. However, due to the lack of sufficient data related to past floods in Turkey, depth-damage functions in the methodology named "Global flood depth-damage functions" published by the Joint Research Center (JRC) in 2017 were used (Huizinga et al., 2017). Depth-damage functions were created separately for each continent (Table 3.4).

According to the depth-damage functions in Table 3.4, the values produced for Europe were used within the scope of the methodology. The values used are given in Figure 3.17. Accordingly, the damage function value was determined for each building type and depth.

Table 3.4. Depth- damage functions (Huizinga et al., 2017)

Damage class	Flood depth, (m)	Damage function						
		EUROPE	North AMERICA	CentrandSouth AMERICA	ASIA	AFRICA	OCEANIA	GLOBAL
Residential buildings	0	0,00	0,20	0,00	0,00	0,00	0,00	-
	0,5	0,25	0,44	0,49	0,33	0,22	0,48	-
	1	0,40	0,58	0,71	0,49	0,38	0,64	-
	1,5	0,50	0,68	0,84	0,62	0,53	0,71	-
	2	0,60	0,78	0,95	0,72	0,64	0,79	-
	3	0,75	0,85	0,98	0,87	0,82	0,93	-
	4	0,85	0,92	1,00	0,93	0,90	0,97	-
	5	0,95	0,96	1,00	0,98	0,96	0,98	-
	6	1,00	1,00	1,00	1,00	1,00	1,00	-
Commercial buildings	0	0,00	0,02	0,00	0,00	-	0,00	0,00
	0,5	0,15	0,24	0,61	0,38	-	0,24	0,32
	1	0,30	0,37	0,84	0,54	-	0,48	0,51
	1,5	0,45	0,47	0,92	0,66	-	0,67	0,63
	2	0,55	0,55	0,99	0,76	-	0,86	0,74
	3	0,75	0,69	1,00	0,88	-	1,00	0,86
	4	0,90	0,82	1,00	0,94	-	1,00	0,93
	5	1,00	0,91	1,00	0,98	-	1,00	0,98
	6	1,00	1,00	1,00	1,00	-	1,00	1,00
Industrial buildings	0	0,00	0,03	0,00	0,00	0,00	-	0,00
	0,5	0,15	0,32	0,67	0,28	0,06	-	0,30
	1	0,27	0,51	0,89	0,48	0,25	-	0,48
	1,5	0,40	0,64	0,95	0,63	0,40	-	0,60
	2	0,52	0,74	1,00	0,72	0,49	-	0,69
	3	0,70	0,86	1,00	0,86	0,68	-	0,82
	4	0,85	0,94	1,00	0,91	0,92	-	0,92
	5	1,00	0,98	1,00	0,96	1,00	-	0,99
	6	1,00	1,00	1,00	1,00	1,00	-	1,00

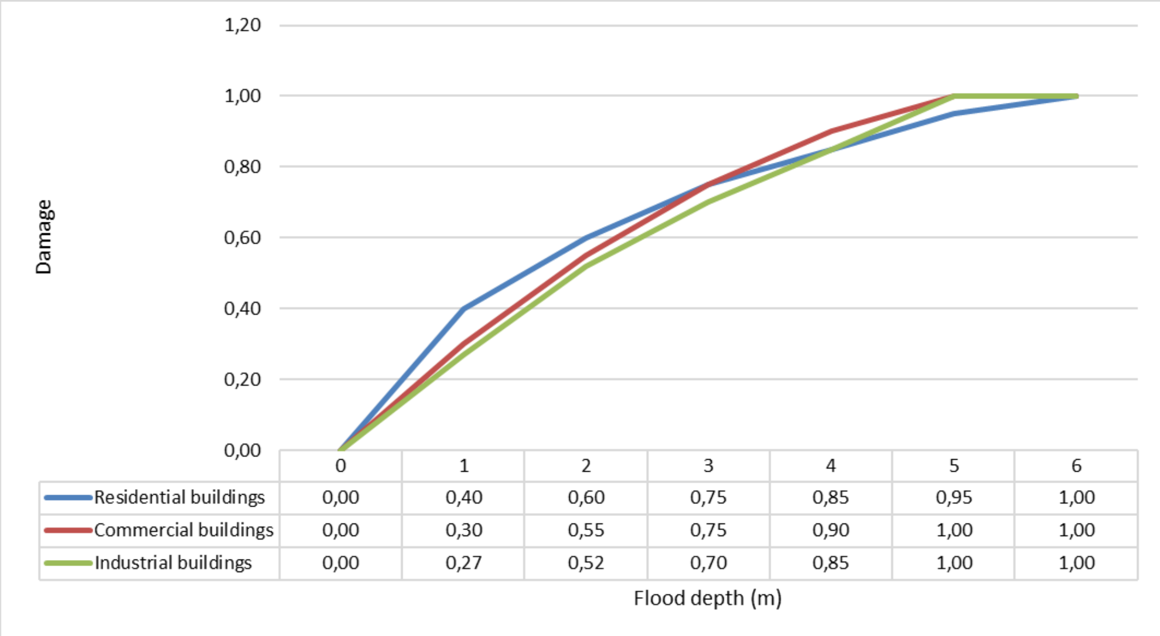

Figure 3.17. Depth-damage functions (Huizinga et al., 2017)

In the formula, the building unit cost indicated as "BF" is one of the significant contributors to determine economic loss. It indicates the economic value of one square meter of buildings. Building costs were obtained from the document titled "Announcement on Building Approximate Unit Costs to be Used in the Calculation of Architecture and Engineering Service Fees for the Year 2022/3" published by the Ministry of Environment, Urbanization and Climate Change, considering values specific to our country (URL-11). Using this document, the building cost that varies depending on the details such as the type of residential buildings, the number of floors, the height of the building; the number of floors of industrial buildings, and the type of production was obtained. For example, while the unit price of residences with a building height of less than 21,5 meters was 650 TL in 2014, it was 4 650 TL in 2022 (URL-12). The 2002 costs reached nearly 7 times the 2014 value. If the costs of each year were used in the risk analysis, extreme increases in economic damage would occur. Moreover, in this case, the risk change due to the buildings could not be detected because the unit price change would also affect the risk. For this reason, the values of 2022 are taken as constant for the cost of each year.

It is stated that the majority of the depth-damage curves asymptote at a value of 0,6 and regardless of the height of the water, 40% of it is not damaged by the flood at all, and this 40% part should not be used in maximum damage calculations (Huizinga et al., 2017: 55).

Therefore, the undamaged part of the buildings was considered in damage calculations and was reduced by 0,60.

It was suggested to use the depreciation factor in damage calculations based on the fact that the value of the buildings will decrease over time (Huizinga et al., 2017: 54). For this, different countries revised the maximum damage value that the buildings will suffer with coefficients varying between 0,50 and 0,63 in maximum damage calculations. In the methodology used, this value is taken as 0,50. Since the building approximate unit costs do not include VAT (value added tax), the calculated damage value was multiplied by 1,18.

The economic damage values mentioned above are only damage values belonging to the buildings and do not include contents damage. Contents damage was calculated as specified by Huizinga et al. (2017) between contents damage and building damage (Table 3.5). Contents damage was calculated by taking 50% of the building damage for residential areas, 100% of the building damage for commercial areas, and 150% of the building damage for industrial areas.

Table 3.5. Contents damage (as % of building damage) (Huizinga et al., 2017: 54)

Class of buildings	Contents damage (as % of building damage)
Residential	50
Commercial	100
Industrial	150

Final flood risk

According to the methodology, when calculating the final flood risk, economic damage and affected population values are used after normalization. The following formula was applied to normalize the data. As a result, economic damage and affected population values for each building were normalized to values between 0-1.

$$X_N = (X - X_{min}) / (X_{max} - X_{min}) \quad (3.5)$$

X_N: Normalized value

X : The value in the dataset

X_{min} : The minimum value in the dataset

X_{max} : The maximum value in the dataset

The total risk is calculated using the normalized economic damage and the affected population. The total risk value obtained is evaluated between 0-1.

$$\text{Total Risk} = 0{,}5 \times \text{Economic Risk (0-1)} + 0{,}5 \times \text{Population Risk (0-1)} \qquad (3.6)$$

As a result of the calculation, the final flood risk is reached for each building. The total risk calculation included economic and population values. As a result, the obtained risk outcomes provide a comprehensive result as they encompass not only physical damage but also the population.

3.3. Results of Urban Risk Analysis

Building-based risk analysis under high urbanization was carried out in two stages: background analysis of buildings from satellite images and risk analysis. Between the years 2014-2022, the buildings in the flood area determined by detecting the backgrounds of the buildings were used in the risk analysis. The applied methodology to reach the results of risk analysis incorporated both economic damage and affected population, consequently mapping the total flood risk. The number of buildings was 922 for the year 2014, and 1 051 for the year 2022 in flood inundated area (Table 3.6.). In 2014, there were 828 residential buildings (89,8%), 35 commercial buildings (3,8%), and 59 industrial buildings (6,4%). In 2022, there were 935 residential buildings (89%), 38 commercial buildings (3,6%), and 78 industrial buildings (7,4%). When the change from 2014 to 2022 is examined, the increases in the number of buildings are as follows:

- residential buildings 12,9%,
- commercial buildings 8,6%,
- industrial buildings 32,2%,
- total buildings 13,9%.

The economic risk was calculated depending on the physical features detected, such as the number of floors of the building, height, base area, and use. Likewise, the affected population was calculated depending on the number of floors and floor space of the building.

Table 3.6. Buildings in the flood inundated area by years

Years	Number of buildings						
	Residential		Commercial		Industrial		Total Building
	Building	%	Building	%	Building	%	
2022	935	89,0	78	7,4	38	3,6	1 051
2021	929	88,4	75	7,1	38	3,6	1 042
2020	929	88,4	71	6,8	38	3,6	1 038
2019	927	88,2	71	6,8	38	3,6	1 036
2018	927	88,2	70	6,7	38	3,6	1 035
2017	918	87,3	69	6,6	38	3,6	1 025
2016	867	82,5	65	6,2	36	3,4	968
2015	835	79,4	61	5,8	36	3,4	932
2014	828	78,8	59	5,6	35	3,3	922

Economic damage

Historical backgrounds of buildings in the flood inundated areas were determined as mentioned in the methodology for the calculation of flood risk. All of these buildings are given in Map 3.6.

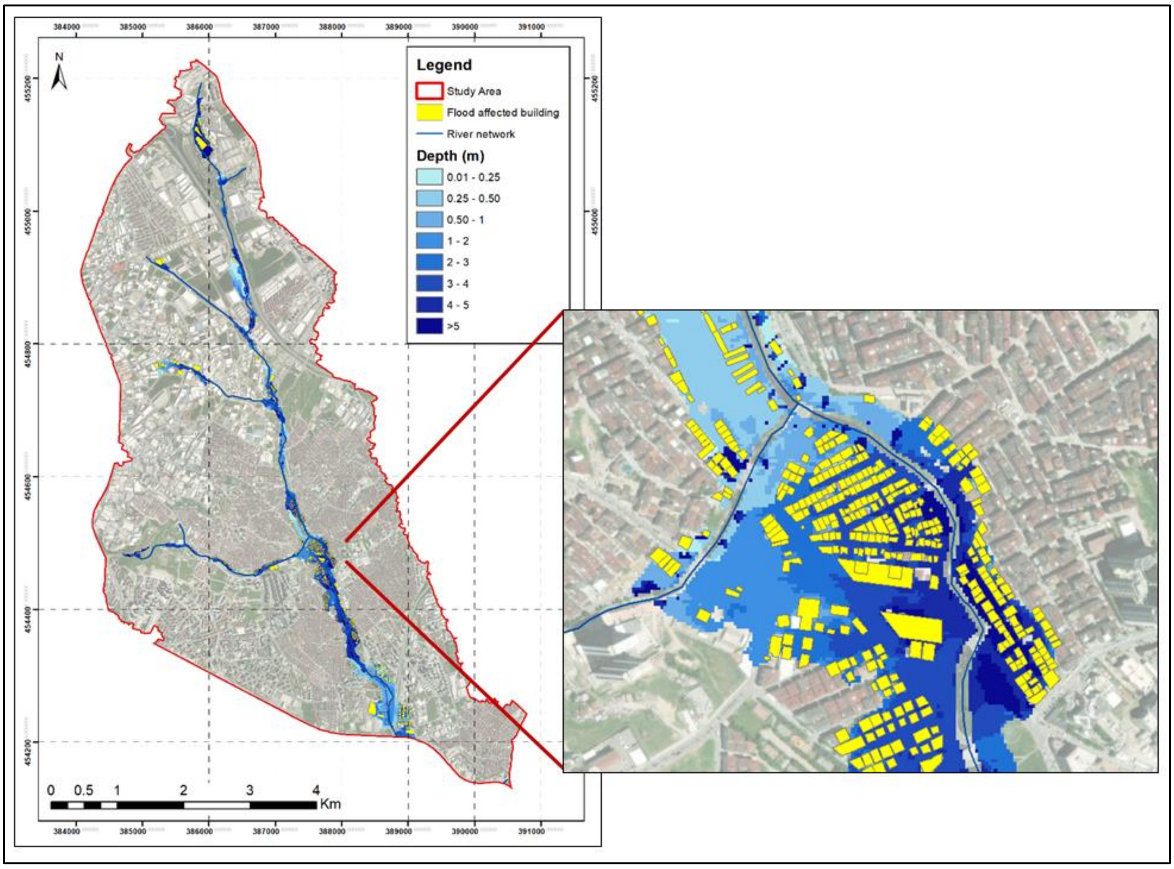

Map 3.6. Flood inundated area, inundation depth (m), and flood affected building in the study area (created by the author)

The path indicated in the methodology was followed to calculate the flood risk. Accordingly, the summary of the process followed to calculate economic damage is as follows.

1. Attributes were assigned to buildings as "residential, commercial, industrial" with the help of Google Earth and land use.
2. From the document titled "Announcement on Building Approximate Unit Costs to be Used in the Calculation of Architecture and Engineering Service Fees for the Year 2022/3", the unit cost was assigned to each building according to the number of floors, height, and usage (URL-11).
3. Then, the depth-damage functions were determined according to the flood depth where each building is located, as emphasized in the methodology.
4. The formula specified in the methodology was applied and economic damage was calculated. Contents damage was added to the economic damage. Contents damage was calculated by taking 50% of the building damage for residential buildings, 100% of the

building damage for commercial buildings, and 150% of the building damage for industrial areas.

At the end of the applied process, each building's economic damage was calculated as indicated in the methodology, considering the number of floors, building height, base area, and unit cost according to building use. These calculations made for all years are given in Table 3.7.

Table 3.7. Results of economic damage analysis

Years	Economic Damage (TL)						
	Residential		Commercial		Industrial		Total
	TL	%	TL	%	TL	%	
2022	434 488 988	55,6	202 981 662	26,0	144 573 498	18,5	782 044 148
2021	431 715 832	55,2	202 981 662	26,0	142 358 106	18,2	777 055 600
2020	431 715 832	55,2	202 981 662	26,0	140 802 139	18,0	775 499 633
2019	427 128 864	54,6	202 981 662	26,0	140 802 139	18,0	770 912 665
2018	427 128 864	54,6	202 981 662	26,0	140 288 118	17,9	770 398 644
2017	422 935 273	54,1	202 981 662	26,0	135 598 661	17,3	761 515 596
2016	370 137 872	47,3	182 956 149	23,4	133 669 714	17,1	686 763 735
2015	352 077 976	45,0	182 956 149	23,4	130 919 358	16,7	665 953 484
2014	343 124 144	43,9	170 183 638	21,8	126 089 445	16,1	639 397 227

According to the results obtained, the highest economic damage in all years was seen in residential buildings. Then, respectively, the highest economic damage is in commercial and industrial buildings. In 2022, there are 935 residential buildings, 38 commercial buildings, and 78 industrial buildings. When the relationship between the number of buildings and economic damage is examined, it is expected that the increase in buildings will cause an increase in the economic damage. The reason for this is the commercial centers with very large floor space. The average floor area of buildings is 307,5 m^2, and approximately 14% of the buildings in the flood inundated area are above the average size. When the floor area of buildings are arranged from largest to smallest, all of the top 10 buildings are composed of commercial structures (6 out of the top 10) and industrial facilities (4 out of the top 10). An example of this can be the shopping center named Anpa Gross Mega Avm, which has a building area of approximately 17 600 m^2. This structure constitutes 53 880 678 TL of economic damage.

From 2014 to 2022, the economic damage for residential buildings increased by about 90 million TL and its share in total damage increased by 11,6%. When commercial buildings are examined, the economic damage is about 30 million TL and its share in total damage increased by 4,2%. For industrial buildings, it increased by approximately 18 million TL, up by 2,4%.

When the total damage between 2014-2022 is examined, the total damage has increased by approximately 143 million TL. The economic damage in 2022 increased by 22,3% compared to 2014.

People affected by flood

When determining the affected population, every residential building where the flood had physical contact was taken into account. The population was determined based on the night population and thus only residential buildings were taken as a basis. While doing this calculation, the size of a residential flat was assumed to be approximately 125 m^2, and the number of residential flats was calculated depending on the floor area of the building. It was assumed that the average residential apartment has a net area ranging from 90 to 125 m^2, and to reach the gross area, an additional 15% was added, resulting in a total of 125 m^2. As previously stated in the methodology, the household size was assumed to be 3,43 people, and the affected population was determined along with the number of residential flats (Table 3.8).

Table 3.8. Number of affected people by flood

Years	People affected by flood	Population of Esenyurt district	The ratio of the population affected by the flood to the district population (%)
2022	50 407	983 571	5,1
2021	49 646	977 489	5,1
2020	49 646	957 398	5,2
2019	48 521	954 579	5,1
2018	48 521	891 120	5,4
2017	48 198	846 492	5,7
2016	40 282	795 010	5,1
2015	38 677	742 810	5,2
2014	37 936	686 968	5,5

According to the results obtained, the number of affected people in 2022 is 50 407. The number of people affected by the flood increased by 12 471 people, an increase of 32,9% compared to 2014. Although the number of people affected by the flood continued to increase until 2022, the rate decreased when compared to the population of the Esenyurt district. The reason for this is that the growth rate of the Esenyurt district population is much higher.

Total risk

While calculating the total risk of the study area according to the methodology, economic damage and affected population values are normalized and used. In this context, the flood risk for each building, consisting of both damage and population, was calculated on a building basis. Then, risk maps were created in the ArcGIS program at five risk levels (very low, low, moderate, high, and very high). These levels were classified by the natural break method. In this way, more understandable risk maps were created with the breaking points.

Since the analyses were based on buildings, the study area was divided into zones to observe the risk change. These zones were created considering building density and flood inundation areas, and flood risk maps for the five zones created were given separately for the nine years from 2014 to 2022. All the maps created were given according to zones (APPENDIX-3, APPENDIX-4, APPENDIX-5, APPENDIX-6, APPENDIX-7).

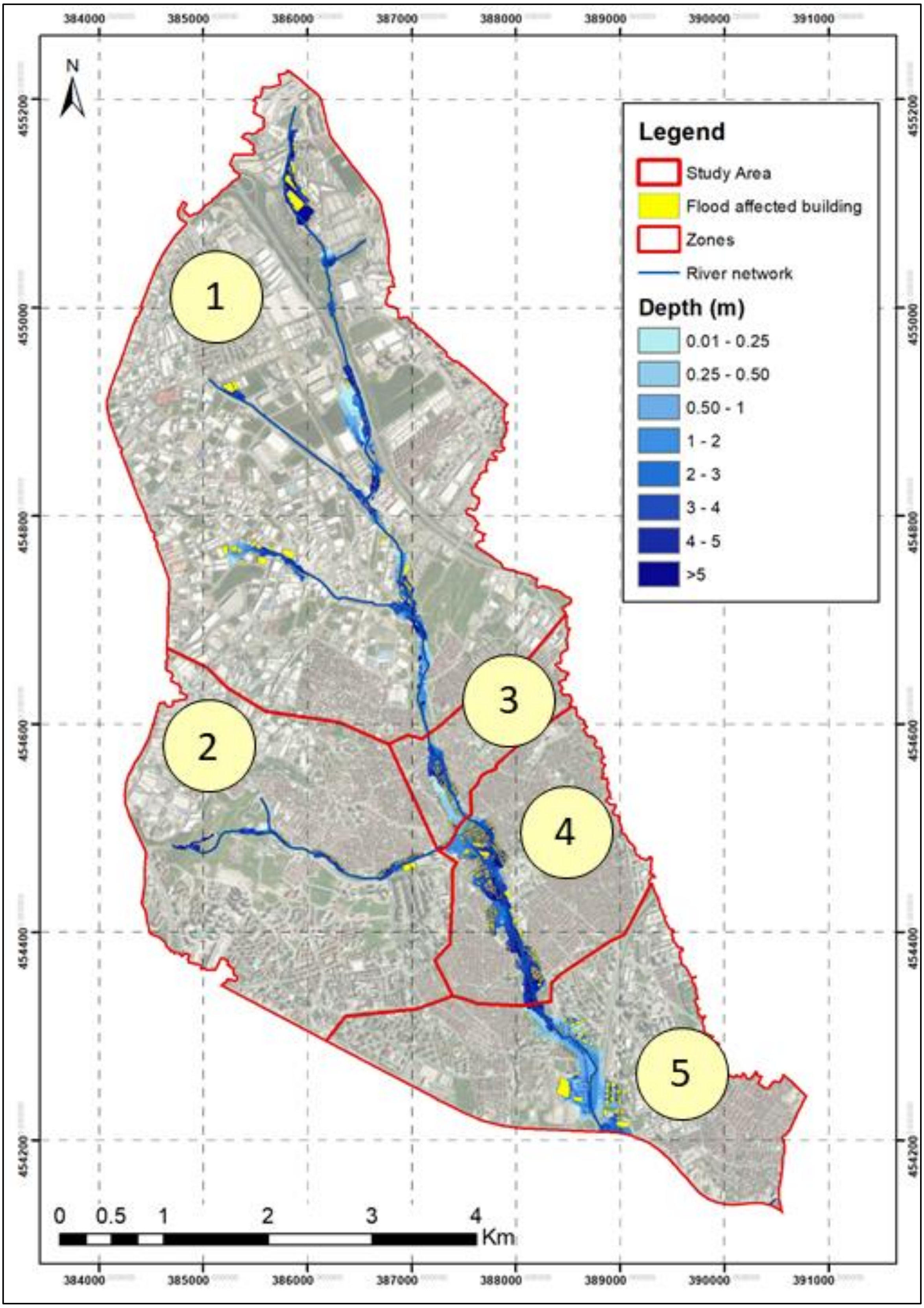

Map 3.7. Study area zones

Comparative examples from each zone were given for the risk analyses created, comparing the years 2014 and 2022, given in Map 3.8, Map 3.9 for Zone-2 and Map 3.10, Map 3.11 for Zone-4.

According to the given maps, in Zone-2 (Map 3.8 and Map 3.9), residential buildings were constructed approximately 20 meters away from the river after the year 2014 and it is classified in the "moderate" risk category. A similar situation occurred in Zone-4 given in Map 3.10 and Map 3.11. After 2014, residential buildings were constructed about 50 meters away from the river, and depending on the number of floors and the floor area of building, it was classified in the "very high" risk category.

In Map 3.8 and Map 3.9, there are 2 industrial buildings categorized as "high" risk, and both of them are single-story structures. All other buildings, except for the mentioned industrial facilities, are residential, and their risks are categorized as "low" and "very low". Therefore, depending on the depth in risk classes, the importance of floor area, number of floor and building use stands out in risk classification.

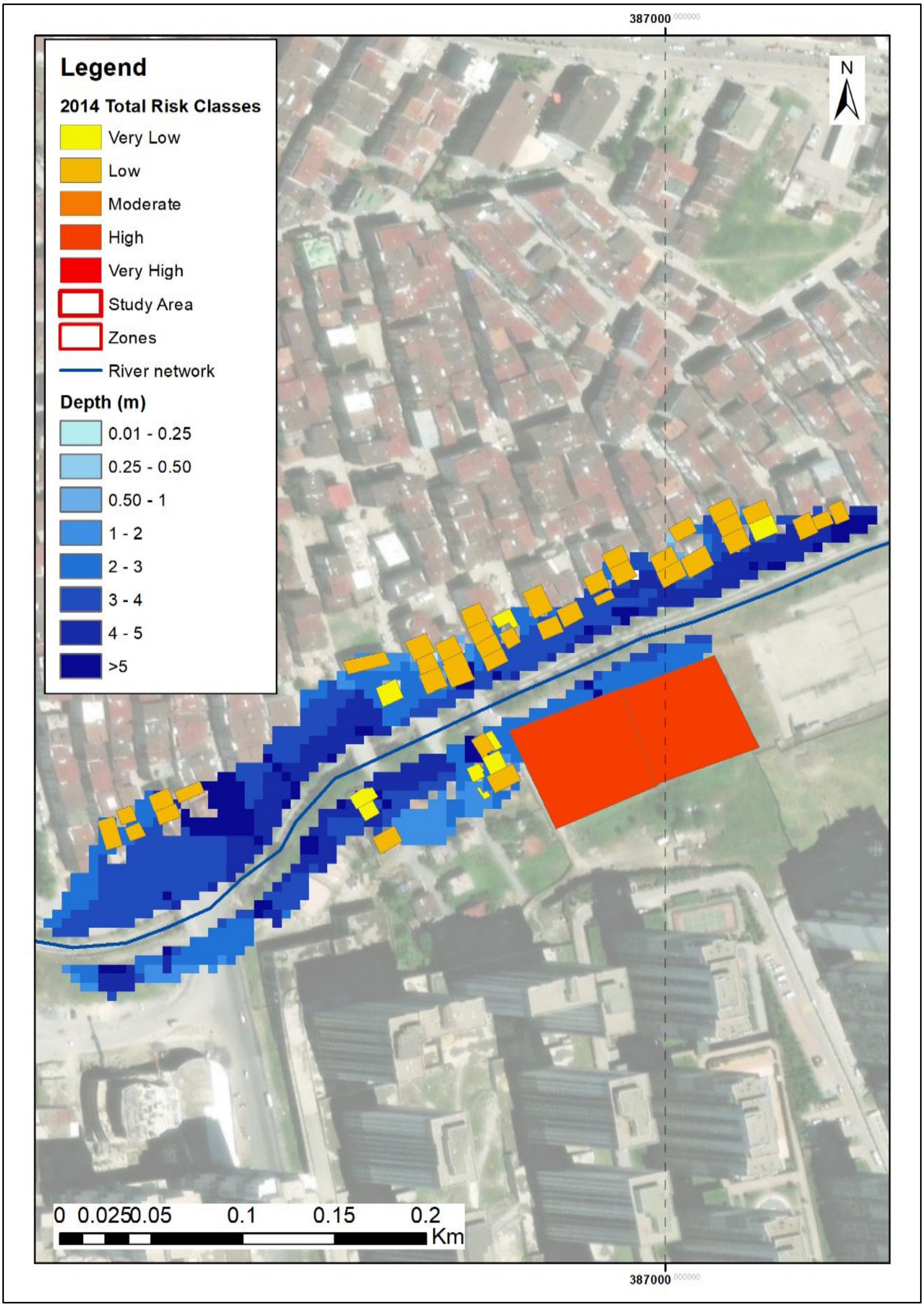

Map 3.8. Flood risk map for Zone-2, 2014

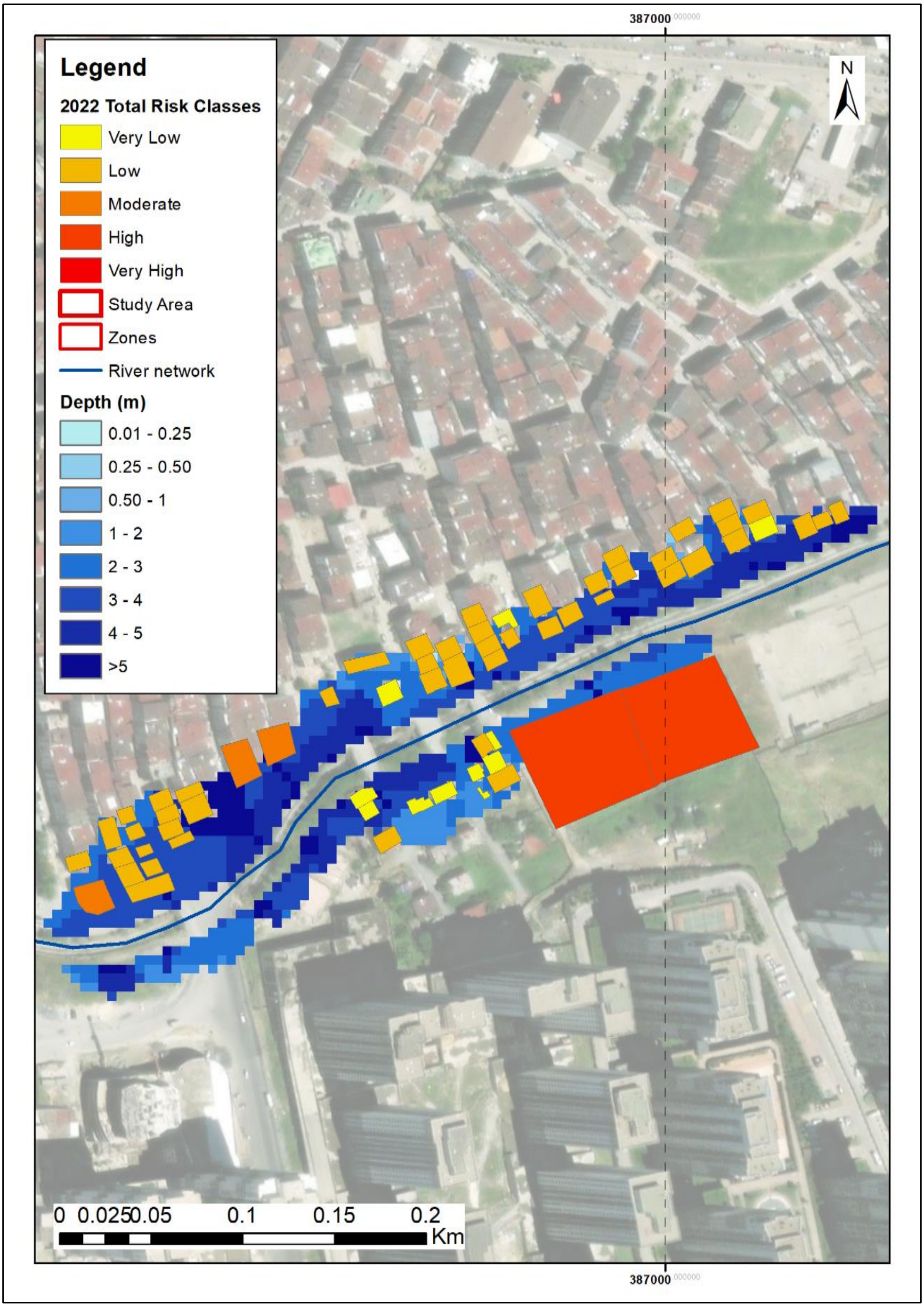

Map 3.9. Flood risk map for Zone-2, 2022

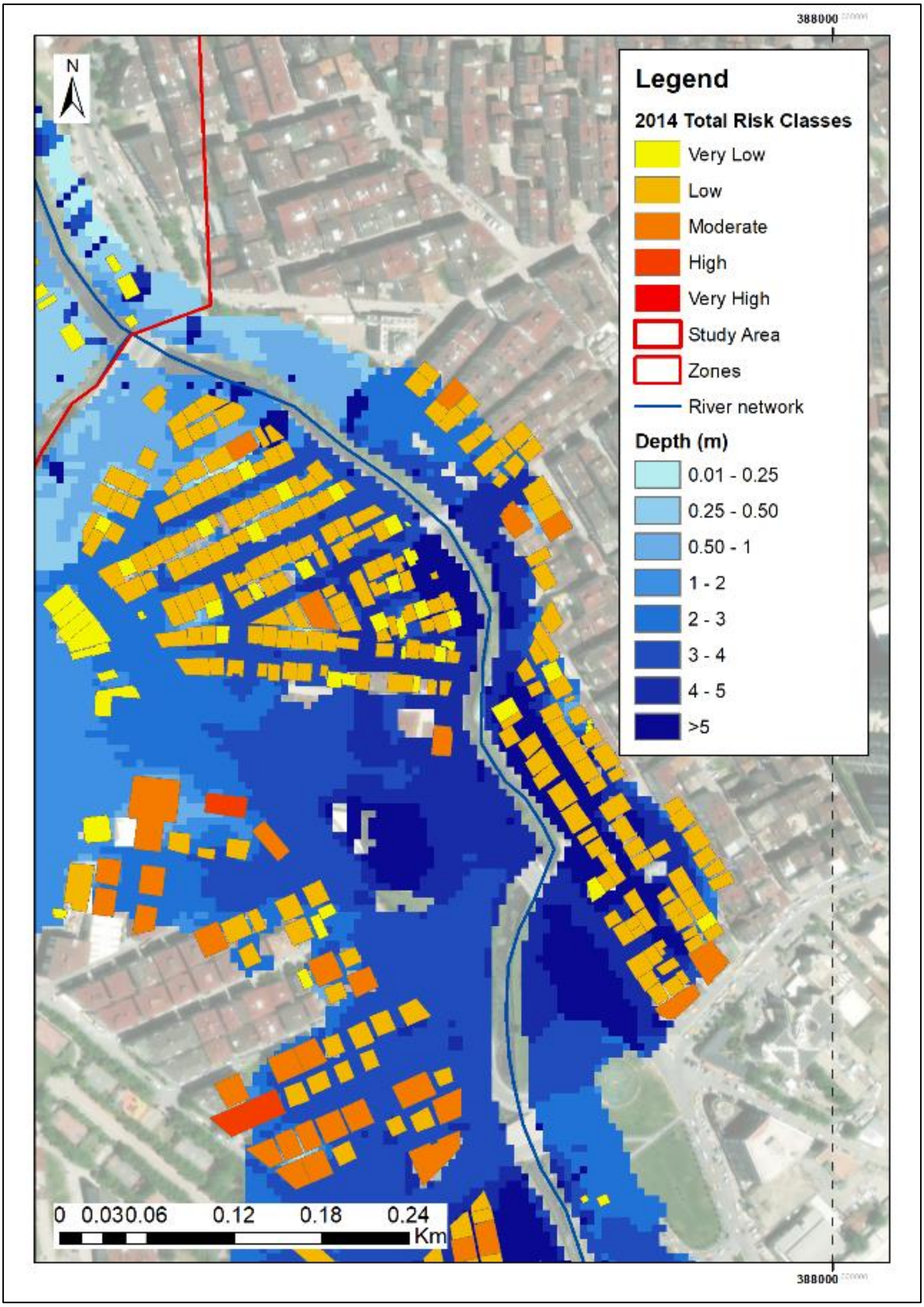

Map 3.10. Flood risk map for Zone-4, 2014

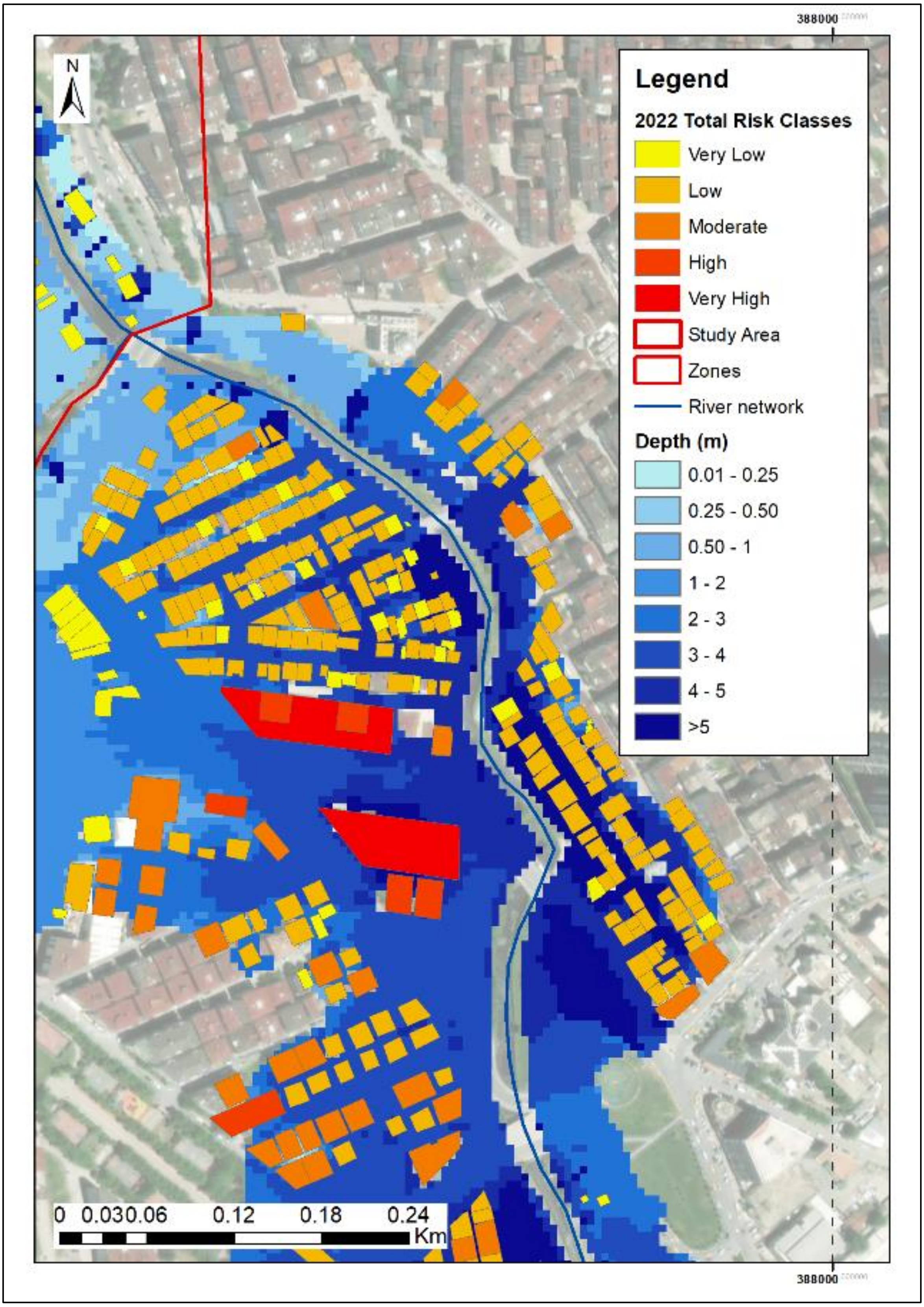

Map 3.11. Flood risk map for Zone-4, 2022

The results of the risk analysis at the building-specific level were examined. The average of these results was taken for the entire study area (Figure 3.18). Accordingly, the risk of residential buildings increased by 16,6%, the risk of commercial buildings increased by 9,9%, while the risk of industrial buildings decreased by 13,3% (Table 3.9). It has been determined that the reason for the decrease in the risk of industrial buildings is the reduce in the average floor area of the building towards 2022. When the entire study area was examined, it was concluded that the average total risk increased by 13,7% from 2014 to 2022.

Table 3.9. Risk averages of building use by years

Years	Residential Risk	Industrial Risk	Commercial Risk	Total Risk
2014	0,0314	0,0319	0,0728	0,0330
2015	0,0318	0,0321	0,0760	0,0335
2016	0,0319	0,0307	0,0760	0,0335
2017	0,0358	0,0293	0,0799	0,0370
2018	0,0357	0,0299	0,0799	0,0369
2019	0,0357	0,0296	0,0799	0,0369
2020	0,0364	0,0296	0,0799	0,0375
2021	0,0364	0,0283	0,0799	0,0374
2022	0,0366	0,0277	0,0799	0,0375

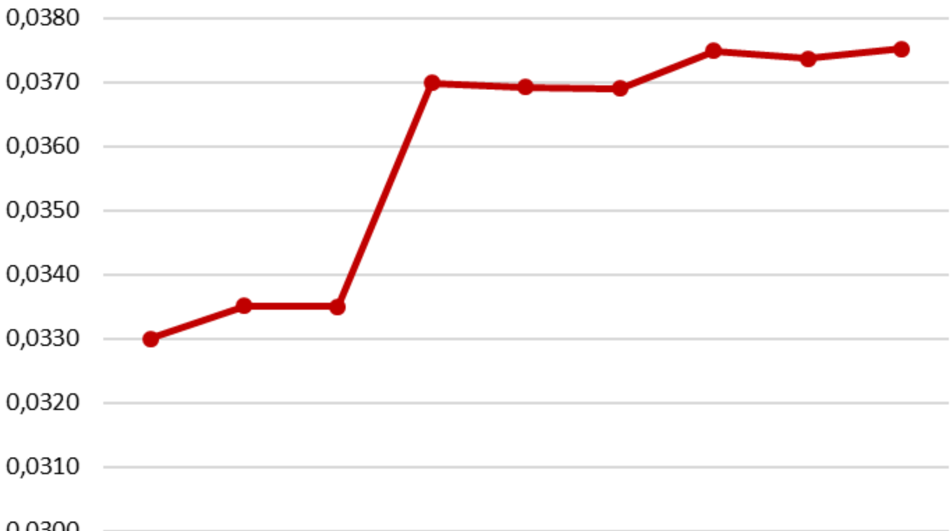

	2014	2015	2016	2017	2018	2019	2020	2021	2022
Total Risk	0,0330	0,0335	0,0335	0,0370	0,0369	0,0369	0,0375	0,0374	0,0375

Figure 3.18. Averages of total risk by years

The number of buildings and risk relationship were examined in Figure 3.19. It was concluded that risk change has a direct and strong relation with the number of buildings. It was observed that the increase in the number of buildings, especially in the year 2017, affected the total risk. However, it should not be overlooked that the inundation depth where buildings are located is the most significant factor in determining the risk.

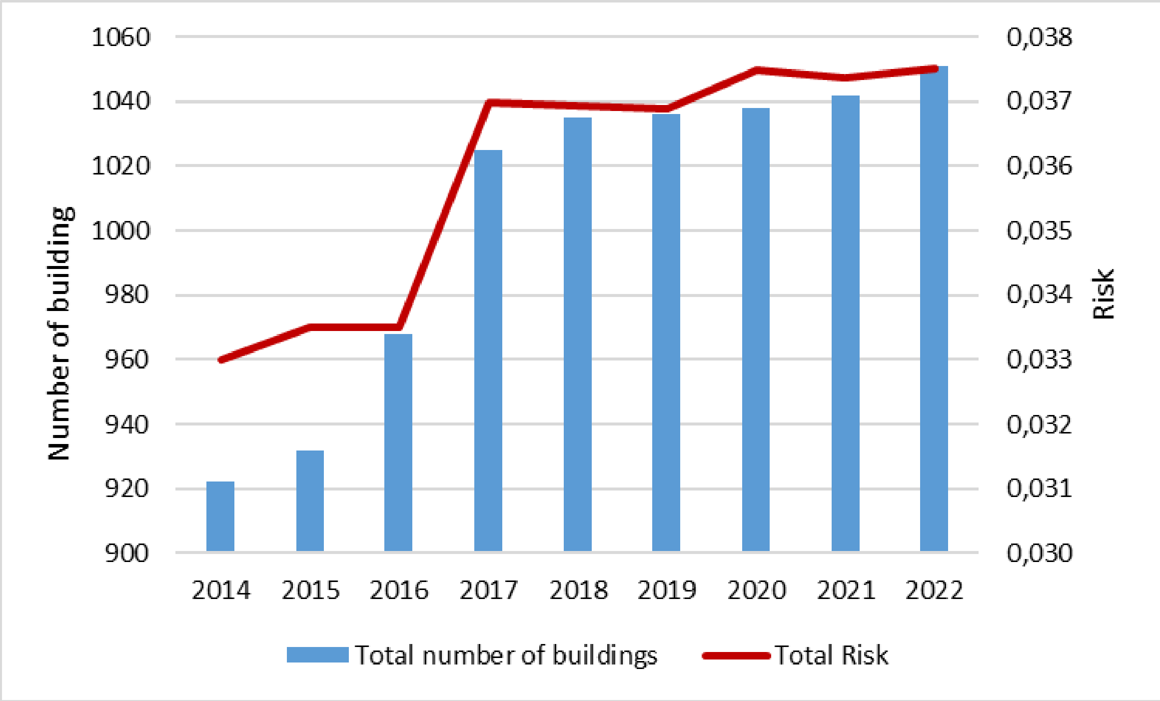

Figure 3.19. Relation between number of buildings and total risk

The relationship between the average floor of the building and the risk change was examined in Figure 3.20, and the relationship between the average floor area (m^2) of the building and the risk change in Figure 3.21. Accordingly, it was determined that the general trend of "number of floors" and "floor area of building" were compatible with the risk change.

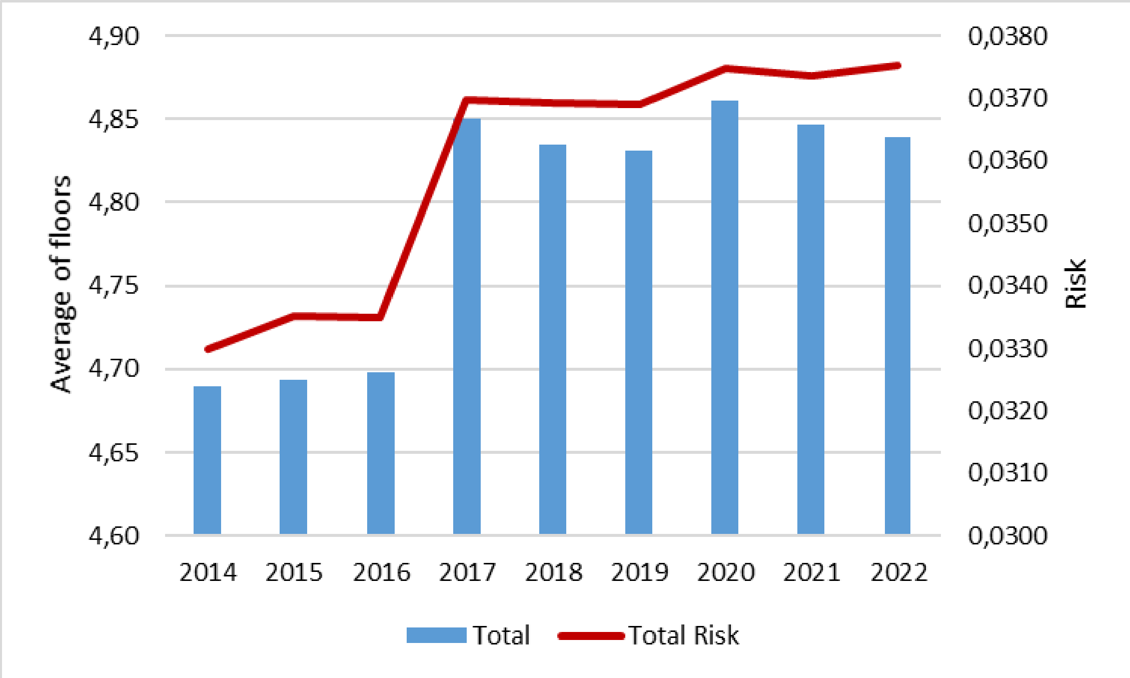

Figure 3.20. Relation between average of floors and total risk

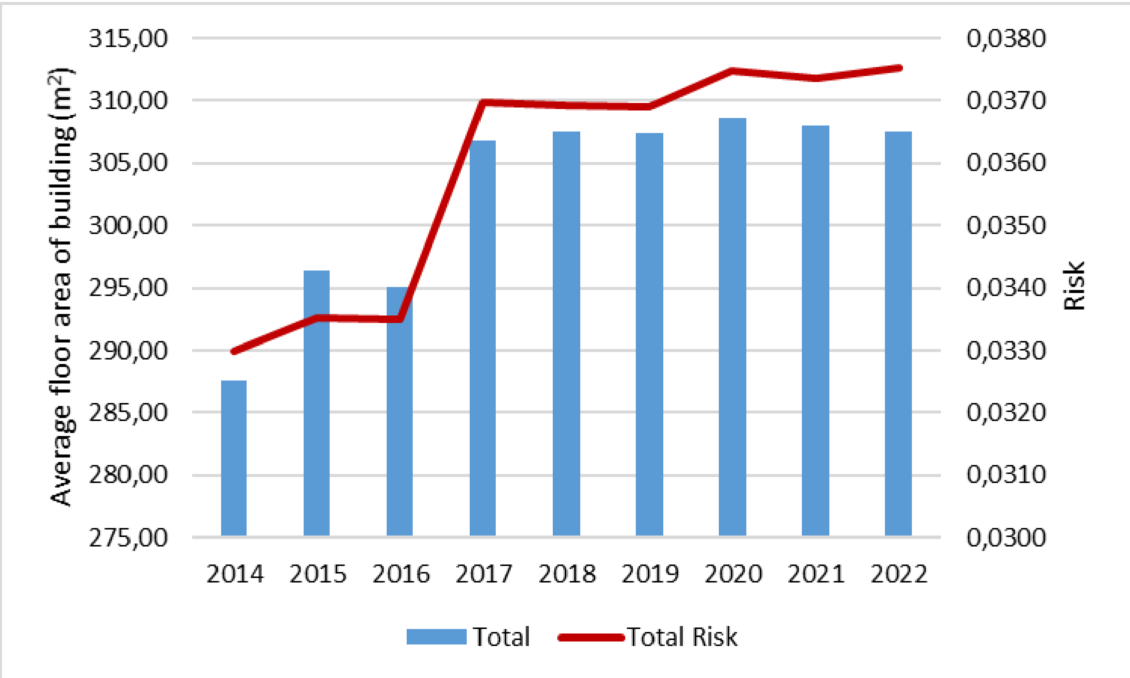

Figure 3.21. Relation between floor area of building (m^2) and total risk

4. FINDINGS AND DISCUSSION

Urbanization, which is shown as the cause of urban floods affecting the water cycle, is also affected by the flood risk. In the literature, the relationship between risk detection and urbanization has been established through the temporal and spatial changes of land use with the help of satellite images (Waghwala and Agnihotri,2019; Nirupama and Simonovic, 2007; Zope et al., 2016; Mustafa et al., 2018; Do et al., 2022). In addition to the detection of urban changes with satellite images, flood risk assessments also differ. As in this thesis, there are many studies that analyze it from the HVE framework (Nguyen et al., 2021; Li, Xiang, Tong and Wang, 2013; Yu et al., 2021; Aerts et al., 2018; Li et al., 2016). With these studies, it was seen that flood risk was discussed more comprehensively within the framework of HVE. In these studies conducted within the framework of HVE, different methodologies were applied. The methodology applied in this thesis is different from all of them because it is a methodology unique to Turkey. At this point, when the studies conducted in Turkey were examined, it was seen that the Analytical Hierarchy Method was generally used (Tokgözlü and Özkan, 2018; Taş, 2018; Ocak and Bahadır, 2020; Ünal, Çamcı, and Tonyaloğlu, 2022; Ekmekcioğlu, Koc and Özger, 2021). With the support of this methodology applied in Turkey with historical backgrounds of buildings, the original value of this study has emerged. Among the studies carried out in Turkey, it has made an important contribution to the literature both with the historical backgrounds of buildings with remote sensing technologies and with the historical flood risk analysis with the methodology applied.

Yu et al. (2021) conducted risk analysis on buildings that he called the smallest unit of urban space. While conducting this study, analyzes were made within the framework of HVE, taking into account building use. The temporal variation of hydrological factors considered in Singh and Singh (2011) and Hussein et al. (2020) was not considered in the study of Yu et al. (2021). In this thesis, the effects of the smallest unit of urban space change on the risk were examined by keeping the hydrological factors constant. In this sense, while the units (buildings) used for analysis are similar, this thesis is specific in terms of temporal detection of units by satellite images.

The results obtained from the analyses performed in the thesis are summarized in Table 4.1. According to the analysis results, the flood risk in the part of the Esenyurt district, which was determined as the study area and is located in the Haramidere Basin, was evaluated historically between the years 2014-2022. High urbanization has increased the people affected by flood by 32,9%, the economic damage in case of flood by 22,3% and the total flood risk by 13,6% from 2014 to 2022. This shows that flood risk has increased significantly in the last 9 years.

Table 4.1. Summary of the flood risk analysis results

Years	Number of buildings	Economic damage (TL)	People affected by flood	Total risk
2014	922	639 397 227	37 936	0,03300
2015	932	665 953 484	38 677	0,03351
2016	968	686 763 735	40 282	0,03350
2017	1 025	761 515 596	48 198	0,03698
2018	1 035	770 398 644	48 521	0,03693
2019	1 036	770 912 665	48 521	0,03690
2020	1 038	775 499 633	49 646	0,03749
2021	1 042	777 055 600	49 646	0,03737
2022	1 051	782 044 148	50 407	0,03752

In this thesis, according to the economic damage analysis created within the scope of the risk analysis, economic damage has increased from 2014 to 2022 in Esenyurt. This increase was 26,6% for residential buildings, 9,5% for commercial buildings, and 5,4% for industrial buildings. Despite the high number of industrial buildings, the economic damage they caused less than that of commercial buildings. The reasons for this are that industrial facilities are generally single-storey and the approximate unit cost is relatively less; commercial areas are more than one floor and the approximate unit cost is high. When the total economic damage is examined, it is 782 044 148 TL in 2022, while it was 639 397 227 TL in 2014. Accordingly, the risk today is 143 million TL higher than in 2014. This increase is approximately 22%. At the same time, the majority of the economic damage incurred occurs in residential buildings. The reasons for the damages occurring in residential buildings are as follows:

- The increase in urbanization and the establishment of settlements near river beds.
- The increase in the density of settlements in existing residential areas.

- The floor heights and therefore the approximate unit costs of the residential buildings constructed in recent years are high.

It was assumed that if residential buildings remain within the flood area, all the people in that building will be affected. According to the results obtained, the number of people who were affected by a possible flood in 2022 is 50 407. The number of people affected by the flood has increased by 12 471 people, or 32,9%, compared to 2014. At the same time, it was determined that there was an out-of-trend population increase in 2019, and accordingly, the residential risk and total risk increased in the following years. The most effective reasons for the increase in the number of affected people are "sudden population increases, the increase in urbanization and settlements near river beds, the increase in the density of settlements in existing residential areas, and the increase in the floor height of residential buildings built in recent years."

When flood risk maps were examined, it was seen that there was construction near the river bed and the density increased relatively. Esenyurt, the most populous district of Istanbul, has experienced an increase of approximately 14% in the number of buildings since 2014. This increase in 9 years increased the flood risk by 16,6%. In this case, 5,1% of the population of Esenyurt became vulnerable to the flood.

When determining the distance between the river and the buildings, the distance is measured horizontally from the right and left sides of the river. For example, when this distance is assumed to be 5 meters, a buffer area of 5 meters is created from the left and right sides of the river. This area is assumed to have flood hazard regardless of elevation. However, in areas where the elevation is high, it is not possible for the flood inundation water to reach the entire buffer area. For this reason, determining the risky areas according to the buffer regardless of elevation may not give accurate results according to the study area. In this study, elevation was taken into consideration when assessing buildings at risk of flood due to their proximity to the river. The HAND (Height Above Nearest Drainage) model, a topographic model that calculates the vertical distance of a point to the stream, was used.

The flood inundated areas where the Haramidere River can rise up to a maximum of 5 meters were identified (Figure 4.1). 525 (approximately 50%) of 1051 buildings for which flood risk analysis was conducted for 2022 are located in this area. Of the 525 buildings, 465 are residential buildings (88,5%), 47 are industrial buildings (9%), and 13 are commercial buildings (2,5%). In order to make comparisons, a buffer area of 5 meters was created to the right and left of the Haramidere River. Within this area, there are 5 buildings, 4 of which are industrial and 1 of which is residential. From these results, it was determined that important and vital boundaries such as the distance between buildings and the river should not be based on horizontal lengths because this length can be deceptive. For example, the flood depth may be close to zero in the area determined by the buffer. Similarly, risk may occur outside the buffer area depending on the flood depth. For these reasons, flood depths (vertical length) should be taken into account, not horizontal lengths, especially for determining the distances between the river and buildings.

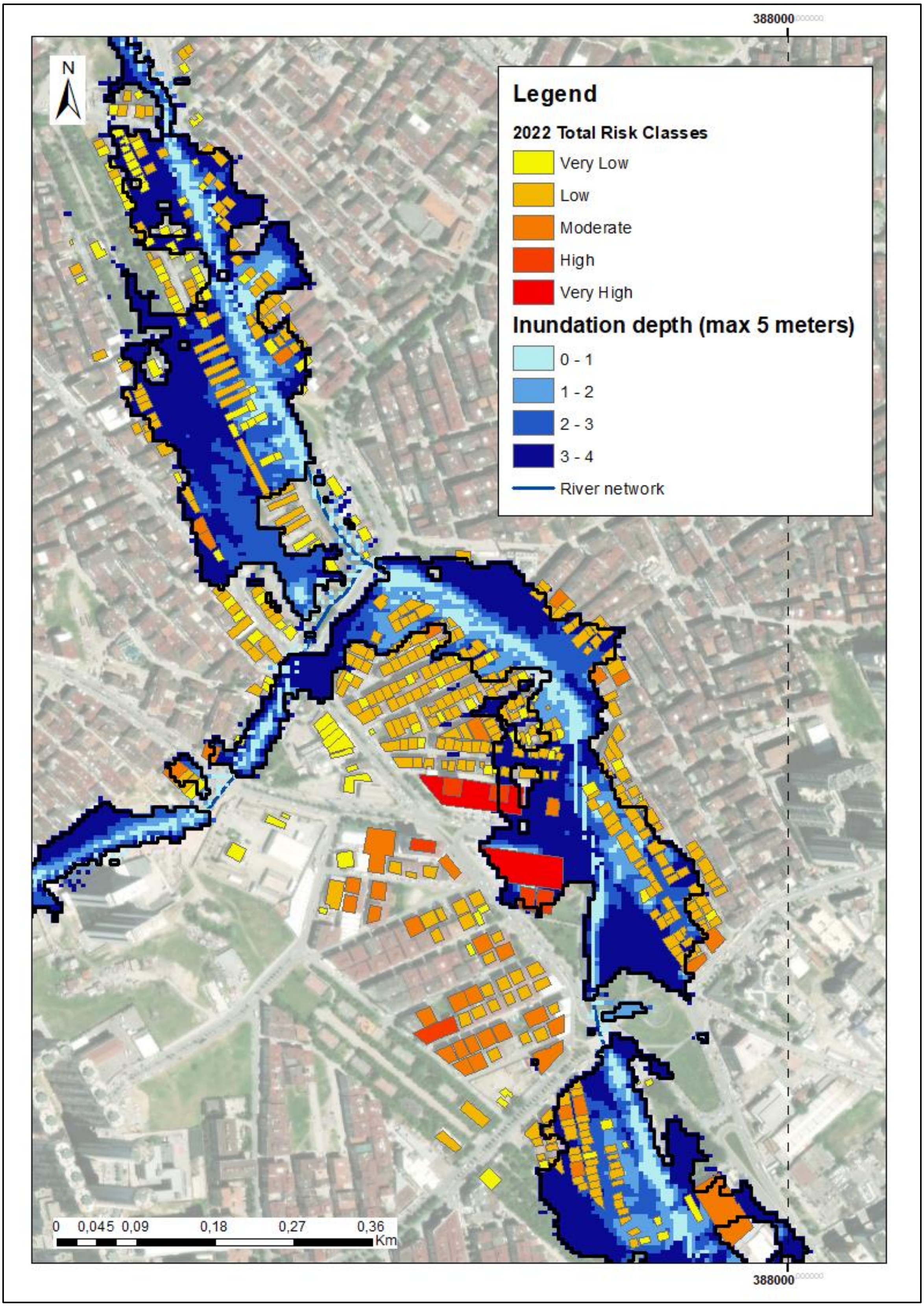

Figure 4.1. Flood inundation depth (max 5 meters)

In the area with a maximum inundation depth of 5 meters, there are 470 buildings in 2014 and 525 buildings in 2022. The number of buildings in this area increased by 11,7% from 2014 to 2022. If there were no buildings in the area with a maximum inundation depth of 5 meters and urbanization had not increased, the economic loss of 385 134 731 TL could have been prevented, and 19 873 people would have been spared from being affected by the flood in 2022. In this case, it is seen that inferences about urbanization are not made despite the history of damaging floods that cause loss of life in Esenyurt.

The most important tool in flood risk prevention is urban planning. Through urban planning, measures can be taken according to current and future flood risks. If possible, new settlements should not be built on the river bed and risky areas. Structural solutions, one of the flood prevention and risk reduction approaches, can be applied in existing settlements where this is not possible. Structural measures to be taken to reduce the risk of flood are intended to keep the flow away from the flood risk area at the time of flood. Examples include storage reservoirs to reduce the downstream flow of a canal, widening of the canal to increase the canal capacity, diversions to reduce the flow in the main channel, and embankments to protect areas close to the canal (de Andrade Cruz, de Andrade, Prestes, da Cruz Bezerra, and Polli, 2023). Istanbul Metropolitan Municipality started infrastructure works in the study area in 2020 and then rehabilitation works. Infrastructure strengthening works were carried out to separate rainwater and wastewater. The works continued with the widening of the stream cross-section, but these works have not yet been completed. While infrastructure and rehabilitation works continued, there were successive floods, especially in 2022.

In addition to structural measures, there are also non-structural and nature-based solutions for flood prevention and risk reduction (Conitz, Zingraff-Hamed, Lupp, and Pauleit, 2021). Non-structural measures aim to reduce flood risk, minimize flood damages and increase community resilience through non-physical interventions. Examples of these are:

- urban planning and its implementation,
- preparation of Flood Management and Mitigation Plans,
- development of floodplain zoning regulations to restrict development in high-risk areas,
- implementation of early warning systems about floods,

- public education on flood risks and preparedness measures.

Due to the lack of proper planning of urbanization and non-implementation of non-structural measures, the risk level increased over the years. Moreover, these changes occurring in flood risk areas increased potential losses in terms of human life and property (Şenol Balaban, 2016). In addition to the economic damages calculated in this study, structural measures frequently applied in Turkey to prevent floods also bring additional costs. The embankments created, rehabilitations, and other structural measurements may prove insufficient against many parameters such as the frequency, speed, and depth of the flood (Bruwier et al., 2015).

In this case, model-based approaches such as Green Infrastructures (rain gardens, green roofs, permeable pavement, bioswales, constructed wetlands, rainwater harvesting etc.), Sustainable Urban Drainage Systems (SUDS), Low Impact Development (LID), Sponge Cities and Nature-based Solutions (NbS) become effective (Qi et al., 2021). Although the effects of these approaches on the hydrological cycle are labelled differently in the literature, they have fundamentally similar objectives and solutions (Buurman and Padawangi, 2018; Ferreira, Potočki, Kapović-Solomun, and Kalantari, 2021). These differences in terminology stem from the region where each approach originated (Huang et al., 2020).

Among these approaches, nature-based solutions is a concept defined as actions inspired, supported or copied from nature and used as a reference for diverse alternative terminologies around the world (Cohen-Shacham, Walters, Janzen, and Maginnis, 2016; Huang et al., 2020). This approach intends to collaborate with the natural surroundings to mitigate the risks of flood, improve the capacity to retain water, and promote the holistic well-being of ecosystems. Green infrastructures are implemented to ensure these contributions and green infrastructures support the NbS through the integration of green and blue spaces in urban areas (Ferreira et al., 2021). Examples of NbS components established for urban flood risk management are as follows (Huang et al., 2020; Shaver, 2000):

- rainwater harvesting to slow runoff processes and mitigate drought impacts,
- green roofs to slow runoff processes,
- rain barrels for rainwater collection
- permeable pavements to increase permeability,

- infiltration trenches to increase permeability,
- bioswales to increase permeability, use water efficiently and provide ecological benefits,
- retention ponds to mitigate surface runoff.

It has the effects of recycling and efficient use of water, reducing impervious surfaces (reducing the amount and velocity of runoff), being more economical than structural solutions and reducing urban flood in the long term. NbS are widely considered to be particularly effective measures against urban flood risks (Kabisch et al., 2016). The effectiveness of NbS for flood risk mitigation has been addressed by several prior studies, mainly focusing on the reduction in peak flow (Jackisch and Weiler, 2017), runoff (Dreelin, Fowler, and Carroll, 2006), flood volume (Mei et al., 2018), flood inundated area and flood inundation depth (Costa et al., 2021). Nature-based solutions can create significant changes in these characteristics of flood that are critical for flood risk. These differences depend on NbS surface area, location, type and local conditions (Costa et al., 2021; Ferreira et al., 2021). For this reason, the importance of spatial planning emerges especially in the implementation phase. Urban planning gains importance especially in the design of impervious surfaces and green spaces, which are two important factors.

The applicability of nature-based, multiple-benefit solutions should be investigated on a site-specific basis and implemented by local authorities with a strong knowledge of site characteristics. In Esenyurt, combining nature-based solutions with urban planning is a recommended approach to mitigate flood risk. As it offers flexible and adaptable solutions, it increases urban resilience and makes a significant difference in reducing flood risk. In this case, considering the loss of both life and property, it is concluded that urban planning and model-based approaches such as NbS instead of structural solutions for flood resilient cities should be given more consideration.

5. CONCLUSION

Floods are one of the most frequent natural induced disasters in the world. The economic losses and loss of life caused by floods are considerable. These losses are directly related to the rapid population growth and consequently increasing urbanization. In order to determine this relationship, flood risk has to be evaluated in the context of urbanization.

Flood risk is a multidimensional issue that can be evaluated from many perspectives and analyzed by more than one method. Along with this study, the flood risk and its causes caused by Haramidere River, known to frequently experience floods, in the Esenyurt district were revealed. The reasons for selecting Esenyurt as the study area are as follows: being the most populous district of Istanbul with a population of 1 million, experiencing rapid population growth when examined over the past years, having high building density due to the coexistence of industrial and residential areas, and experiencing flood with loss of life in Esenyurt in 2020.

The most important feature of the study is that it reaches the flood risk by considering urbanization in the historical process together with hydrodynamic features. The methodology applied in Flood Management Plans in Turkey has been applied to the study area. This methodology was applied in this thesis in a smaller basin and in more detail than the Flood Management Plans. In the methodology, the background analysis of the building was determined using satellite imagery and utilized in flood risk analysis. The continuity of the data was ensured by using satellite images to determine the backgrounds of the building. As a result, the unique value of the methodology is to address the urbanization in the historical process with the help of remote sensing and GIS, together with hydrodynamic features, and reach the flood risk.

The research has significantly contributed to the scientific field, particularly in the use of remote sensing and GIS technologies for flood risk assessment and management. By utilizing remote sensing data, such as high-resolution satellite imagery, valuable insights were obtained regarding background analysis of buildings and its temporal evolution over time. This data facilitated a detailed analysis of how rapid urbanization impacts flood risk. Furthermore, the integration of GIS technology in the research enabled spatial analysis and visualization of flood risk data. GIS-based flood risk maps were created, displaying the spatial distribution of flood hazards, vulnerabilities, and exposed elements in the study area. These maps played a critical role in identifying high-risk zones, evaluating potential flood impacts on the population, and informing urban planning decisions. In summary, the research has advanced the application of remote sensing and GIS in flood risk assessment, providing a comprehensive and data-driven approach to understanding the intricate interactions between urbanization and flood risks.

This thesis has made several significant contributions to the field of urban flood risk assessment. Firstly, it introduced and applied the HVE (Hazard, Vulnerability, Exposure) framework as a comprehensive approach to understanding and addressing flood-related issues in urban planning. This framework allowed for a holistic assessment of flood risks by considering multiple dimensions, such as flood hazards, vulnerabilities of exposed elements, and the presence and value of assets within flood-prone areas. It was determined that the flood risk increased over the years, and this increase was particularly caused by urbanization in risk areas along with rapid population increases. It was concluded that population and risk increases show parallelism on a yearly basis.

Secondly, the research offered valuable insights into the relationship between urbanization and flood risk. The identification of high-risk areas allows for minimizing economic losses, and reducing the number of affected populations. By identifying the hotspots of flood risk where hazards, vulnerabilities, and exposures converge, the research provided essential information for targeting risk reduction and adaptation measures effectively. In addition to these, the suggestions made as a result of the study in terms of urban planning are also important. The first of these suggestions relates to the fact that analysing flood risk areas determined by river proximity with buffer areas (horizontal distances) is misleading. It was concluded that determining the distance between the river and buildings by considering the elevation gives more accurate results. As a result, the HAND method for determining the distance between the river and buildings can be applied in the followings:

- in assessing the flood hazard depending on the distance to the river,
- flood management and mitigation plans, master plans,
- directing urban development.

Thus, this crucial boundary for flood risk, the distance between the river and buildings, is determined in a more realistic manner, taking into account flood depth.

Second suggestion is the implementation of urban planning and model-based flood prevention and mitigation strategies such as nature-based solutions by investigating the basin in detail, as well as the structural measures taken by the municipality. While determining nature-based solutions, Esenyurt's high population and dense urbanization should be taken into consideration. In addition to these characteristics, morphological, hydrological, meteorological, geological, hydrogeological and slope characteristics of the area should also be examined and sustainable methods suitable for socio-economic investment should be applied. Due to dense urbanization, it is not possible to implement nature-based solutions that require large areas. However, if small-scale solutions are offered, it is necessary to implement them in a large number of areas in order to reduce flood risk. This situation is not considered appropriate considering the socio-economic structure of Esenyurt. Another situation is related to the climate; the district is classified as arid to semi-humid, but it has the possibility of becoming semi-arid due to the decrease in precipitation in recent years. Therefore, it is concluded that offering green infrastructures under nature-based solutions such as plant-based green corridors, green roofs, bioswales, etc. for the region will not be suitable for climatic conditions when considered in terms of sustainability. For the reasons stated above, it is recommended to "basically retain the rainfall before turning to runoff" in order to reduce the flood risk. Firstly, the ongoing and planning infrastructure and rehabilitation works (structural measures) in Esenyurt should be completed. Then, considering these characteristics of the area, NbS applications can be proposed in two different approaches. One of them is rainwater harvesting, which can both reduce flood risk and provide multiple benefits against the possibility of drought in Istanbul. Another one is the creation of permeable areas to reduce surface runoff. Permeable areas can be created with permeable pavements, infiltration trenches, retention ponds by analysing the area characteristics in detail. As a result of these analyses, adaptive designs for rainwater harvesting and the creation of permeable surfaces are identified that can adapt to climatic conditions and urban growth. The location, size and type of these designs are determined on a site-specific basis. By creating green infrastructure with the applications made as a result of the designs, many benefits are provided in addition to reducing floods such as reducing drought effects, reducing the urban heat island effect and creating recreational areas.

It is thought that the flood risk will be reduced as a result of the implementation of these suggestions by analysing them for Esenyurt. GIS is of great importance in making the necessary analyses for the application, as in the determination of flood risk. It allows simulation of different scenarios for planning factors such as the location, size and type of NbS applications. In addition, it supports urban planning by identifying the effects of climate changes and urban growth in the long term, and ensures the continuity of sustainability by increasing the capacity to adapt to changing conditions. GIS is also used before and after NbS applications to ensure sustainability. Thus, it helps to evaluate the potential results of various flood mitigation strategies before implementation. After implementation, GIS helps to monitor the performance of green infrastructure and NbS elements. Regular data collection and analysis helps to ensure that these features continue to work effectively in reducing flood risk. In summary, GIS provides a robust framework for the analysis, visualization and management of complex spatial data associated with the planning of nature-based solutions to enhance flood resilience. It facilitates informed decision making, the optimisation of flood risk reduction strategies and the creation of urban areas that are both resilient and sustainable.

This thesis made a significant contribution to solving the serious problem of understanding and managing flood risks in rapidly urbanizing in Istanbul-Esenyurt. By conducting historical flood risk analyses from 2014 to 2022, the study identified the areas at risk and quantified the economic losses and population affected associated with floods. It suggests that the flood risk, which is directly affected by urbanization and population growth, should be solved by urban planning. Results and suggestions of the thesis are crucial for urban planners and policymakers in Esenyurt to prioritize flood risk reduction measures, improve urban planning decisions. Furthermore, the research will guide local governments to develop urban planning policies for sustainable and resilient cities by emphasizing the importance of considering the interaction between urbanization and flood risk.

REFERENCES

Acedo, F. J., Barroso, C., Casanueva, C., and Galán, J. L. (2006). Co-authorship in management and organizational studies: An empirical and network analysis. *Journal of Management Studies*, 43(5), 957-983.

Aerts, J. C., Botzen, W. J., Clarke, K. C., Cutter, S. L., Hall, J. W., Merz, B., and Kunreuther, H. (2018). Integrating human behaviour dynamics into flood disaster risk assessment. *Nature Climate Change*, 8(3), 193-199.

Anderson, D. G. (1970). *Effects of urban development on floods in northern Virginia*. Washington, DC, USA: US Government Printing Office, 22.

Anim, D. O., Kabo-bah, A. T., Nkrumah, P. N., & Murava, R. T. (2013). Evaluation of NDVI using Spot-5 satellite data for Northern Ghana. *Environmental Management and Sustainable Development*, *2*(1), 167.

Apel, H., Aronica, G. T., Kreibich, H., and Thieken, A. H. (2009). Flood risk analyses-how detailed do we need to be?, *Natural Hazards*, 49, 79–98.

Apel, H., Merz, B., and Thieken, A. H. (2008). Quantification of uncertainties in flood risk assessments. *International Journal of River Basin Management*, 6(2), 149-162.

Ayhan, F. (2019). Esenyurt ilçesinde nüfusun gelişimi ve bu gelişimde rol oynayan etmenler. *Kent Akademisi*, 12(37), 67-81.

Bae, S., and Chang, H. (2019). Urbanization and floods in the Seoul Metropolitan area of South Korea: What old maps tell us. *International Journal of Disaster Risk Reduction*, 37, 101186.

Bahrawi, J., Ewea, H., Kamis, A., and Elhag, M. (2020). Potential flood risk due to urbanization expansion in arid environments, Saudi Arabia. *Natural Hazards*, 104, 795-809.

Beshir, A. A., and Song, J. (2021). Urbanization and its impact on flood hazard: the case of Addis Ababa, Ethiopia. *Natural Hazards*, 109(1), 1167-1190.

Bruwier, M., Erpicum, S., Pirotton, M., Archambeau, P., Dewals, B.J. (2015). Assessing the operation rules of a reservoir system based on a detailed modelling chain. *Natural Hazards and Earth System Sciences*, 15, 365–379.

Buurman, J., and Padawangi, R. (2018). Bringing people closer to water: integrating water management and urban infrastructure. *Journal of Environmental Planning and Management*, 61(14), 2531-2548.

Bürgler, M., Vetsch, D. F., Boes, R. M., and Vanzo, D. (2023). Systematic comparison of 1D and 2D hydrodynamic models for the assessment of hydropeaking alterations. *River Research and Applications*, 39(3), 460-477.

Cançado, V., Brasil, L., Nascimento, N., and Guerra, A. (2008). *Flood risk assessment in an urban area: Measuring hazard and vulnerability*. In 11th International Conference on Urban Drainage, Edinburgh, Scotland, UK, 1-10.

Chen, Y., Xie, W., and Xu, X. (2019). Changes of population, built-up land, and cropland exposure to natural hazards in China from 1995 to 2015. *International Journal of Disaster Risk Science*, 10, 557-572.

Chen, Y.R., Yeh, C.H., and Yu, B. (2011). Integrated application of the analytic hierarchy process and the geographic information system for flood risk assessment and flood plain management in Taiwan. *Natural Hazards*, 59(3), 1261–1276.

Chinh, D. T., Dung, N. V., Gain, A. K., and Kreibich, H. (2017). Flood loss models and risk analysis for private households in Can Tho City, Vietnam. *Water*, 9(5), 313.

Citeau, J.-M. (2003). *A new control concept in the Oise Catchment area: Definition and assessment of flood compatible agricultural activities*, FIG (Fédération Internationale des géométres) Working Week, Paris, France, 1-19.

Cohen-Shacham, E., Walters, G., Janzen, C., and Maginnis, S. (2016). Nature-based solutions to address global societal challenges. *IUCN: Gland, Switzerland*, 97, 2016-2036.

Conitz, F., Zingraff-Hamed, A., Lupp, G., and Pauleit, S. (2021). Non-Structural flood management in European rural mountain areas—are scientists supporting ımplementation?. *Hydrology*, 8(4), 167.

Costa, S., Peters, R., Martins, R., Postmes, L., Keizer, J. J., & Roebeling, P. (2021). Effectiveness of nature-based solutions on pluvial flood hazard mitigation: The case study of the city of Eindhoven (The Netherlands). *Resources*, 10(3), 24.

Dams, J., Dujardin, J., Reggers, R., Bashir, I., Canters, F., and Batelaan, O. (2013). Mapping impervious surface change from remote sensing for hydrological modeling. *Journal of Hydrology*, 485, 84-95.

De Andrade Cruz, L. G., De Andrade, F. O., Prestes, M. F., da Cruz Bezerra, S. M., and Polli, S. A. (2023). Hydrologic and hydraulic modeling to assess the efficiency of structural flood control measures: Case study of Audi-União District in the city of Curitiba, Brazil. *Revista Ambiente & Água*, 18, 1-17.

Diaconu, D. C., Costache, R., and Popa, M. C. (2021). An overview of flood risk analysis methods. *Water*, 13(4), 474.

Díez-Herrero, A., and Garrote, J. (2020). Flood risk analysis and assessment, applications and uncertainties: A bibliometric review. *Water 2020*, 12, 2050.

Ding, W., Wu, J., Tang, R., Chen, X., and Xu, Y. (2022). A Review of flood risk in China during 1950–2019: Urbanization, socioeconomic ımpact trends and flood risk management. *Water*, 14(20), 3246.

Do, T. A. T., Do, A. N. T., and Tran, H. D. (2022). Quantifying the spatial pattern of urban expansion trends in the period 1987–2022 and identifying areas at risk of flooding due to the impact of urbanization in Lao Cai city. *Ecological Informatics*, 72, 101912.

Donthu, N., Kumar, S., Mukherjee, D., Pandey, N., and Lim, W. M. (2021). How to conduct a bibliometric analysis: An overview and guidelines. *Journal of Business Research*, 133, 285-296.

Dreelin, E. A., Fowler, L., and Carroll, C. R. (2006). A test of porous pavement effectiveness on clay soils during natural storm events. *Water Research*, 40(4), 799-805.

Du, J., Qian, L., Rui, H., Zuo, T., Zheng, D., Xu, Y., and Xu, C. Y. (2012). Assessing the effects of urbanization on annual runoff and flood events using an integrated hydrological modeling system for Qinhuai River basin, China. *Journal of Hydrology*, 464, 127-139.

Ekmekcioğlu, Ö., Koc, K., and Özger, M. (2021). District based flood risk assessment in Istanbul using fuzzy analytical hierarchy process. *Stochastic Environmental Research and Risk Assessment*, 35, 617-637.

Environmental Master Plan. (2009). 1/100 000 Scale Environmental Master Plan Report. *İstanbul Water and Sewerage Administration, City Planning Directorate*. İstanbul.

European Commission, Directorate-General for Research and Innovation, (2015). Towards an EU research and innovation policy agenda for Nature-Based Solutions & Re-Naturing Cities. Final Report of the Horizon 2020 Expert Group on Nature-Based Solutions and Re-Naturing Cities. *Directorate General for Research and Innovation–Climate Action, Environment, Resource Efficiency and Raw Materials.* European Commission, Brussels, Belgium.

European Council. (2007). EU Directive of the European Parliament and of the European Council on the estimation and management of flood risks (2007/60/EU). *Official Journal of the European Union.*

FEMA. (2013). Multi-hazard loss estimation methodology, flood model, HAZUS, technical manual. *FEMA.*Washington DC.

Ferreira, C. S. S., Potočki, K., Kapović-Solomun, M., and Kalantari, Z. (2021). Nature-based solutions for flood mitigation and resilience in urban areas. *Handbook of Environmental Chemistry*, 107, 59–78.

Gharbi, M., Soualmia, A., Dartus, D., and Masbernat, L. (2016). Comparison of 1D and 2D hydraulic models for floods simulation on the Medjerda Riverin Tunisia. *Journal of Materials and Environmental Science*, 7(8), 3017-3026.

Gigović, L., Pamučar, D., Bajić, Z., and Drobnjak, S. (2017). Application of GIS-ınterval rough AHP methodology for flood hazard mapping in urban areas. *Water*, 9(6), 360.

Guerriero, L., Focareta, M., Fusco, G., Rabuano, R., Guadagno, F. M., and Revellino, P. (2018). Flood hazard of major river segments, Benevento Province, Southern Italy. *Journal of Maps*, 14(2), 597-606.

Guo, Y. M., Huang, Z. L., Guo, J., Li, H., Guo, X. R., and Nkeli, M. J. (2019). Bibliometric analysis on smart cities research. *Sustainability*, 11(13), 3606.

Hallegatte, S., Green, C., Nicholls, R. J., and Corfee-Morlot, J. (2013). Future flood losses in major coastal cities. *Nature Climate Change*, 3(9), 802-806.

Handayani, W., Chigbu, U. E., Rudiarto, I., and Putri, I. H. S. (2020). Urbanization and Increasing flood risk in the Northern Coast of Central Java—Indonesia: An assessment towards better land use policy and flood management. *Land*, 9(10), 343.

Haque, C. E., Mahmud, K. H., and Walker, D. (2022). Understanding flood risk and vulnerability of a place: Estimating prospective loss and damage using the HAZUS Model. *Geographies*, 2(3), 453-475.

Holben, B. N. (1986). Characteristics of maximum-value composite images from temporal AVHRR data. *International Journal of Remote Sensing*, 7, 1417-1434.

Hollis, G. E. (1975). The effect of urbanization on floods of different recurrence interval. *Water Resources Research*, 11(3), 431-435.

Huang, G. (2019). A revisit to impact of urbanization on flooding. *Urban Planning and Water-Related Disaster Management*, 43-56.

Huang, Y., Tian, Z., Ke, Q., Liu, J., Irannezhad, M., Fan, D., ... and Sun, L. (2020). Nature-based solutions for urban pluvial flood risk management. *Wiley Interdisciplinary Reviews: Water*, 7(3), e1421.

Huizinga, J., De Moel, H. and Szewczyk, W. (2017). Global flood depth-damage functions: Methodology and the database with guidelines. *Joint Research Centre (JRC).* Luxembourg, 1-114.

Internet: The World Bank. (2023). Urban Development. URL-1: https://www.worldbank.org/en/topic/urbandevelopment/overview#:~:text=Today%2C%20some%2056%25%20of%20the,billion%20inhabitants%20%E2%80%93%20live%20in%20cities. Last Access Date: 23.04.2023.

Internet: TÜİK. (2023a). Address Based Population Registration System Results. URL-2: https://biruni.tuik.gov.tr/medas/?kn=95andlocale=tr. Last Access Date: 23.04.2023.

Internet: EM-DAT. (2022). The International Disaster Database. URL-3: https://www.emdat.be/. Last Access Date: 23.04.2023.

Internet: UN. (1979). Office of the United Nations Disaster Relief Coordinator. Natural Disasters and Vulnerability Analysis. URL-4: https://digitallibrary.un.org/record/95986. Last Access Date: 23.04.2023.

Internet: TÜİK. (2023b). General Population Census. URL-5: https://biruni.tuik.gov.tr/medas/?kn=95andlocale=tr. Last Access Date: 18.06.2023.

Internet: Land use. (2023). İstanbul Büyükşehir Belediyesi, Şehir Planlama Müdürlüğü. URL-6: https://sehirplanlama.ibb.istanbul/esenyurt-ilcesi/#arazi. Last Access Date: 16.07.2023.

Internet: Classification Algorithms and Methods. (2023). URL-7: https://seos-project.eu/classification/classification-c01-p05.html. Last Access Date: 25.07.2023.

Internet: SAPTALDA (2023). Vegetation Indices. URL-8: https://satpalda.co/vegetation-indices. Last Access Date: 25.07.2023.

Internet: Weier, J., and Herring, D. (2000). Measuring vegetation (NDVI & EVI). *NASA, Eatrh Observatory*. URL-9: https://earthobservatory.nasa.gov/features/MeasuringVegetation/measuring_vegetation_2.php. Last Access Date: 30.04.2023.

Internet: Household size. (2023). Istanbul Metropolitan Municipality, Open Data Portal. URL-10: https://data.ibb.gov.tr/en/dataset/ilce-bazli-ortalama-hane-halki-buyuklugu. Last Access Date: 18.07.2023.

Internet: Building Approximate Unit Costs. (2022/3). Mimarlık ve Mühendislik Hizmet Bedellerinin Hesabında Kullanılacak 2022/3 Yılı Yapı Yaklaşık Birim Maliyetleri Hakkında Tebliğ. Republic of Türkiye Ministry Of Environment Urbanisation And Climate Change. URL-11: https://www.resmigazete.gov.tr/eskiler/2022/09/20220913-4.htm. Last Access Date: 21.07.2023.

Internet: Building Approximate Unit Costs. (2014). Mimarlık ve Mühendislik Hizmet Bedellerinin Hesabında Kullanılacak 2014 Yılı Yapı Yaklaşık Birim Maliyetleri Hakkında Tebliğ. Republic of Türkiye Ministry of Environment, Urbanisation and Climate Change. URL-12: https://www.resmigazete.gov.tr/eskiler/2014/05/20140506-5.htm. Access Date: 21.07.2023.

Internet: Esenyurt Municipality. (2023). Esenyurt Sokaklarında Dönüşüm Devam Ediyor. URL-13: https://www.esenyurt.bel.tr/home/IcerikDetay?haberdetay?projedetay=Esenyurt_Soklar%C4%B1nda_D%C3%B6n%C3%BC%C5%9F%C3%BCm_Devam_Ediyor&&id=3086. Last Access Date: 14.06.2023.

Internet: Esenyurt. (2023). Esenyurt. URL-14: https://tr.wikipedia.org/wiki/Esenyurt. Last Access Date: 14.06.2023.

IPCC. (2012). Field, C.B., Barros, V., Stocker, T.F., Dahe, Q., Dokken, D.J. (Eds.). *Managing the Risks of Extreme Events and Disasters to Advance Climate Change Adaptation: Special Report of the Intergovernmental Panel on Climate Change*. Cambridge, UK: Cambridge University Press, (2)1, 101.

İSKİ. (2014). Haramidere Taşkın Risk Haritası Çalışması Hidrolik Model Raporu. *İstanbul Water and Sewerage Administration.* İstanbul.

Jackisch, N., & Weiler, M. (2017). The hydrologic outcome of a Low Impact Development (LID) site including superposition with streamflow peaks. *Urban Water Journal*, 14(2), 143-159.

Jha, A., Lamond, J., Bloch, R., Bhattacharya, N., Lopez, A., Papachristodoulou, N., Bird, A., Proverbs, D., Davies, J., and Barker, R. (2011). Five feet high and rising: cities and flooding in the 21st century. *Policy Research Working Paper*, 1-174.

Johnson, S.L. and Sayre, D.M. (1973). Effects of urbanization on floods in the Houston, Texas metropolitan area. *United States Geological Survey Water Resources Inventory*, 50, 3-73.

Jongman, B., Kreibich, H., Apel, H., Barredo, J. I., Bates, P. D., Feyen, L., and Ward, P. J. (2012). Comparative flood damage model assessment: towards a European approach. *Natural Hazards and Earth System Sciences*, 12(12), 3733-3752.

Kabisch, N., Frantzeskaki, N., Pauleit, S., Naumann, S., Davis, M., Artmann, M., and Bonn, A. (2016). Nature-based solutions to climate change mitigation and adaptation in urban areas: perspectives on indicators, knowledge gaps, barriers, and opportunities for action. *Ecology and society*, 21(2).

Karanam, H. K., & Neela, V. B. (2017). Study of normalized difference built-up (NDBI) index in automatically mapping urban areas from Landsat TN imagery. *International Journal of Engineering, Science andMathematics*, 6(8), 239-248.

Klijn, F., Baan, P. J. A., De Bruijn, K. M., and Kwadijk, J. (2007). *Overstromingsrisico's in Nederland in een veranderend klimaat.* WL delft hydraulics. Delft, 165.

Kok, M., Huizinga, H. J., Vrouwenfelder, A. C. W. M., and Barendregt, A. (2004). Standard Method 2004. Damage and casualties caused by flooding. *Highway and Hydraulic Engineering Department*, 66.

Kong, D. C., and Wu, F. P. (2012). Study on the evaluation models of direct economic losses in urban flood disasters. *Advanced Materials Research*, 433, 4878-4882.

Kreibich, H., Seifert, I., Merz, B., and Thieken, A. H. (2010). Development of FLEMOcs – A new model for the estimation of flood losses in the commercial sector. *Hydrological Sciences Journal*, 55, 1302–1314.

Kron, W. (2005). Flood risk= hazard values vulnerability. *Water International*, 30(1), 58-68.

Kshetri, T. (2018). NDVI, NDBI & NDWI calculation using Landsat. *GeoWorld*, 2, 32-34.

Kuddus, M. A., Tynan, E., and McBryde, E. (2020). Urbanization: A problem for the rich and the poor?. *Public Health Reviews*, 41, 1-4.

Leopold, L.B. (1968). *Hydrology for urban land planning – a guidebook on the hydrologic effects of urban land use, geological survey circular*. Washington, DC: United States Department of the Interior Publication, 1-18.

Li, C., Cheng, X., Li, N., Du, X., Yu, Q., and Kan, G. (2016). A framework for flood risk analysis and benefit assessment of flood control measures in urban areas. *International Journal of Environmental Research and Public Health*, 13(8), 787.

Li, C., Sun, N., Lu, Y., Guo, B., Wang, Y., Sun, X., and Yao, Y. (2022). Review on urban flood risk assessment. *Sustainability*, 15(1), 765.

Li, G. F., Xiang, X. Y., Tong, Y. Y., and Wang, H. M. (2013). Impact assessment of urbanization on flood risk in the Yangtze River Delta. *Stochastic Environmental Research and Risk Assessment*, 27, 1683-1693.

Li, Y., Ahuja, A., and Padgett, J. E. (2012). Review of methods to assess, design for, and mitigate multiple hazards. *Journal of Performance of Constructed Facilities*, 26(1), 104-117.

Li, Y., and Wang, C. (2009). Impacts of urbanization on surface runoff of the Dardenne Creek watershed, St. Charles County, Missouri. *Physical Geography*, 30(6), 556-573.

Lin, B., Wicks, J. M., Falconer, R. A., and Adams, K. (2006). Integrating 1D and 2D hydrodynamic models for flood simulation. *Proceedings of the Institution of Civil Engineers-Water Management,* 159(1), 19-25.

Liselotte, J. (2022). *Understanding loss and damage: Addressing the unavoidable impacts of climate change.* EPRS: European Parliamentary Research Service. Belgium, 1-8.

Liu, Y., Huang, X., and Yang, H. (2022). An integrated approach to investigate the coupling coordination between urbanization and flood disasters in China. *Journal of Cleaner Production*, 375, 134191.

Lu, K., and Wolfram, D. (2012). Measuring author research relatedness: A comparison of word-based, topic-based, and author cocitation approaches. *Journal of the American Society for Information Science and Technology*, 63(10), 1973-1986.

Luino, F., Turconi, L., Petrea, C., and Nigrelli, G. (2012). Uncorrected land-use planning highlighted by flooding: The Alba case study (Piedmont, Italy). *Natural Hazards and Earth System Sciences*, 12(7), 2329-2346.

Marsalek, J., Cisneros, B. J., Karamouz, M., Malmquist, P. A., Goldenfum, J. A., and Chocat, B. (2008). *Urban water cycle processes and interactions: Urban water series-UNESCO-IHP.* (1st edition). London: CRC Press, 1-152.

McGrane, S. J. (2016). Impacts of urbanisation on hydrological and water quality dynamics, and urban water management: A review. *Hydrological Sciences Journal*, 61(13), 2295-2311.

Meals, D. W., Dressing, S. A., and Davenport, T. E. (2010). Lag time in water quality response to best management practices: A review. *Journal of Environmental Quality*, 39(1), 85-96.

Mei, C., Liu, J., Wang, H., Yang, Z., Ding, X., and Shao, W. (2018). Integrated assessments of green infrastructure for flood mitigation to support robust decision-making for sponge city construction in an urbanized watershed. *Science of the Total Environment*, 639, 1394-1407.

Merz, B., Kreibich, H., Thieken, A., and Schmidtke, R. (2004). Estimation uncertainty of direct monetary flood damage to buildings. *Natural Hazards and Earth System Sciences*, 4(1), 153-163.

Meyer, V., Becker, N., Markantonis, V., Schwarze, R., van den Bergh, J. C., Bouwer, L. M., and Viavattene, C. (2013). Assessing the costs of natural hazards–state of the art and knowledge gaps. *Natural Hazards and Earth System Sciences*, 13(5), 1351-1373.

Meyer, V., Haase, D., and Scheuer, S. (2009). Flood risk assessment in European river basins—concept, methods, and challenges exemplified at the Mulde River. *Integrated Environmental Assessment and Management*, 5(1), 17-26.

Miller, J. D., Kim, H., Kjeldsen, T. R., Packman, J., Grebby, S., and Dearden, R. (2014). Assessing the impact of urbanization on storm runoff in a peri-urban catchment using historical change in impervious cover. *Journal of Hydrology*, 515, 59-70.

Mustafa, A., Bruwier, M., Archambeau, P., Erpicum, S., Pirotton, M., Dewals, B., and Teller, J. (2018). Effects of spatial planning on future flood risks in urban environments. *Journal of Environmental Management*, 225, 193-204.

Nguyen, H. D., Fox, D., Dang, D. K., Pham, L. T., Viet Du, Q. V., Nguyen, T. H. T., and Petrisor, A. I. (2021). Predicting future urban flood risk using land change and hydraulic modeling in a river watershed in the central Province of Vietnam. *Remote Sensing*, 13(2), 262.

Nigussie, T. A., and Altunkaynak, A. (2019). Modeling the effect of urbanization on flood risk in Ayamama Watershed, Istanbul, Turkey, using the MIKE 21 FM model. *Natural Hazards*, 99, 1031-1047.

Nirupama, N., and Simonovic, S. P. (2007). Increase of flood risk due to urbanisation: A Canadian example. *Natural Hazards*, 40, 25-41.

Ocak, F., and Bahadır, M. (2020). Örnek taşkın risk modeli oluşturulması ve Ünye şehrindeki derelere ait taşkın risk analizleri. *Journal of Academic Social Science Studies*, 13(80).

Penning-Rowsell, E., Johnson, C., Tunstall, S., Tapsell, S., Morris, J., Chatterton, J.B., and Green, C. (2005). *The benefits of flood and coastal risk management: A manual of assessment techniques*. UK: Middlesex University Press, 38.

Pistrika, A. (2010). Flood damage estimation based on flood simulation scenarios and a GIS platform. *European Water*, 30, 3-11.

Pistrika, A. K., and Jonkman, S. N. (2009). Damage to residential buildings due to flooding of New Orleans after hurricane Katrina. *Natural Hazards*, 54, 413-434.

Pistrika, A., and Tsakiris, G. (2007). *Flood risk assessment: A methodological framework*. Water Resources Management: New Approaches and Technologies, European Water Resources Association, Greece, 1-10.

Polat, Z. A., Alkan, M., Paulsson, J., Paasch, J. M., and Kalogianni, E. (2022). Global scientific production on LADM-based research: A Bibliometric Analysis from 2012 to 2020. *Land Use Policy*, 112, 105847.

Qi, W., Ma, C., Xu, H., Chen, Z., Zhao, K., and Han, H. (2021). A review on applications of urban flood models in flood mitigation strategies. *Natural Hazards*, 108, 31-62.

Quan, R.S. (2012). *Research on risk assessment of rainstorm waterlogging disaster in typical coastal cities*. Shanghai, China: East China Normal University, 1-12.

Rincón, D., Khan, U., and Armenakis, C. (2018). Flood risk mapping using GIS and Multi-Criteria Analysis: A Greater Toronto Area Case Study. *Geosciences*, 8(8), 275.

Saaty, T. L. (1980). *The analytic hierarchy process: Planning, priority setting, resource allocation*. New York: McGraw-Hill, 287.

Salman, A. M. and Li, Y. (2018). Flood risk assessment, future trend modeling, and risk communication: A review of ongoing research. *Natural Hazards Review*, 19(3), 1-21.

Salvadore, E., Bronders, J., and Batelaan, O. (2015). Hydrological modelling of urbanized catchments: A review and future directions. *Journal of Hydrology*, 529, 62-81.

Shaver, E. (2000). Low Impact Design manual for the Auckland Region. *Auckland Regional Council*. Auckland, New Zealand, 1-25.

Sheng, J., and Wilson, J. P. (2009). Watershed urbanization and changing flood behavior across the Los Angeles metropolitan region. *Natural Hazards*, 48, 41-57.

Shi, P., and Kasperson, R. (2015). *World atlas of natural disaster risk*. Heidelberg: Springer.

Smith, D. I. (1994). Flood damage estimation-A review of urban stage-damage curves and loss functions. *Water SA*, 20(3), 231-238.

Smith, K. and Ward, R. (1998). *Floods: Physical processes and human impacts*. Chichester, UK: John Wiley and Sons, 337.

SYGM. (2017). Taşkın Yönetimi. *Republic of Türkiye Ministry of Agriculture and Forestry, General Directorate of Water Management.* Ankara, 24- 26.

SYGM. (2019). Eastern Mediterranean Basin Flood Management Plan. *Republic of Turkey Ministry of Agriculture and Forestry, General Directorate of Water Management.*

SYGM. (2020). Van Lake Basin Flood Management Plan. *Republic of Turkey Ministry of Agriculture and Forestry, General Directorate of Water Management.*

Şenol Balaban, M. (2016). An assessment of flood risk factors ın riverine cities of turkey: lessons for resilience and urban planning. *METU Journal of The Faculty of Architecture*, 33, 45–71.

Tarboton, D. G. (2003). *Rainfall runoff processes*. Utah: Civil and Environmental Engineering Faculty Publications of Utah State University, 1-159.

Taş, E. (2018). Coğrafi Bilgi Sistemleri teknikleri kullanılarak taşkın risk potansiyelinin değerlendirilmesi: Afyonkarahisar Çay Deresi Havzası. *İklim Değişikliği ve Çevre,* 3(1), 68-74.

Thieken, A. H., Olschewski, A., Kreibich, H., Kobsch, S., and Merz, B. (2008). Development and evaluation of FLEMOps – a new Flood Loss Estimation Model for the private sector, Proverbs, D., Brebbia, C. A., and Penning-Rowsell, E. (Eds.) *Flood Recovery, Innovation and Response I*, London, UK: WIT Press, 315–324.

Thieken, A.H., Muller, M., Kreibich, H., Merz, B. (2005). Flood damage and influencing factors: New insights from the August 2002 flood in Germany. *Water Resources Research*, 41(12), 1-16.

Tokgözlü, A., and Özkan, E. (2018). Taşkın risk haritalarında AHP yönteminin uygulanması: Aksu Çayı Havzası örneği. *Süleyman Demirel Üniversitesi Fen-Edebiyat Fakültesi Sosyal Bilimler Dergisi*, (44), 151-176.

UN. (1992). Internationally agreed glossary of basic terms related to disaster management. *UN DHA (United Nations Department of Humanitarian Affairs)*. Geneva, Switzerland, 1-81.

USACE. (1996). Risk-based analysis for flood damage reduction studies. *US Army Corps of Engineers.* Washington DC, 1-236.

Ünal, A., Çamcı, K. G., and Tonyaloğlu, E. E. (2022). Çok Kriterli Karar Analizi ile doğal afetlerde haritalama: Aydın ili sel-taşkın riski örneği. *Ulisa: Uluslararası Çalışmalar Dergisi*, 6(2), 136-150.

Van Eck, N. and Waltman, L. (2010). Software survey: VOSviewer, a computer program for bibliometric mapping. *Scientometrics*, 84(2), 523-538.

Van Steenbergen, N., Ronsyn, J., and Willems, P. (2012). A non-parametric data-based approach for probabilistic flood forecasting in support of uncertainty communication. *Environmental Modelling and Software*, 33, 92-105.

Vanneuville, W., Maddens, R., Collard, C., Bogaert, P., de Maeyer, P., and Antrop, M. (2006). Impact op mens en economie t.g.v. overstromingen bekeken in het licht van wijzigende hydraulische condities, omgevingsfactoren en klimatologische omstandigheden. *Vakgroep Geografie*, Universiteit Gent, Gent, Belgium, MIRA/2006/02.

Verbeiren, B., Van de Voorde, T., Canters, F., Binard, M., Cornet, Y., and Batelaan, O. (2013). Assessing urbanisation effects on rainfall-runoff using a remote sensing supported modelling strategy. *International Journal of Applied Earth Observation and Geoinformation*, 21, 92-102.

Waghwala, R. K., and Agnihotri, P. G. (2019). Flood risk assessment and resilience strategies for flood risk management: A case study of Surat City. *International Journal of Disaster Risk Reduction*, 40, 101155.

Walsh, C. J., Roy, A. H., Feminella, J. W., Cottingham, P. D., Groffman, P. M., and Morgan, R. P. (2005). The urban stream syndrome: current knowledge and the search for a cure. *Journal of the North American Benthological Society*, 24(3), 706-723.

Wang, H., and Yang, Y. (2019). Neighbourhood walkability: A review and Bibliometric Analysis. *Cities*, 93, 43-61.

Ward, A. D, and Trimble, S. W. (2003). *Environmental Hydrology, Second Edition. Boca Raton*, London, New York, Washington, D.C: Lewis Publishers, 1-493.

Yu, I., Park, K., and Lee, E. H. (2021). Flood risk analysis by building use in urban planning for disaster risk reduction and climate change adaptation. *Sustainability*, 13(23), 1-16.

Zhou, Q., Leng, G., Su, J. and Ren, Y. (2019). Comparison of urbanization and climate change impacts on urban flood volumes: Importance of urban planning and drainage adaptation. *Science of the Total Environment*, 658, 24–33.

Zope, P. E., Eldho, T. I., and Jothiprakash, V. (2016). Impacts of land use–land cover change and urbanization on flooding: A case study of Oshiwara River Basin in Mumbai, India. *Catena*, 145, 142-154.

Zupic, I., and Čater, T. (2015). Bibliometric methods in management and organization. *Organizational Research Methods*, 18(3), 429-472.

APPENDIX

APPENDIX-1. News about historical floods in Esenyurt

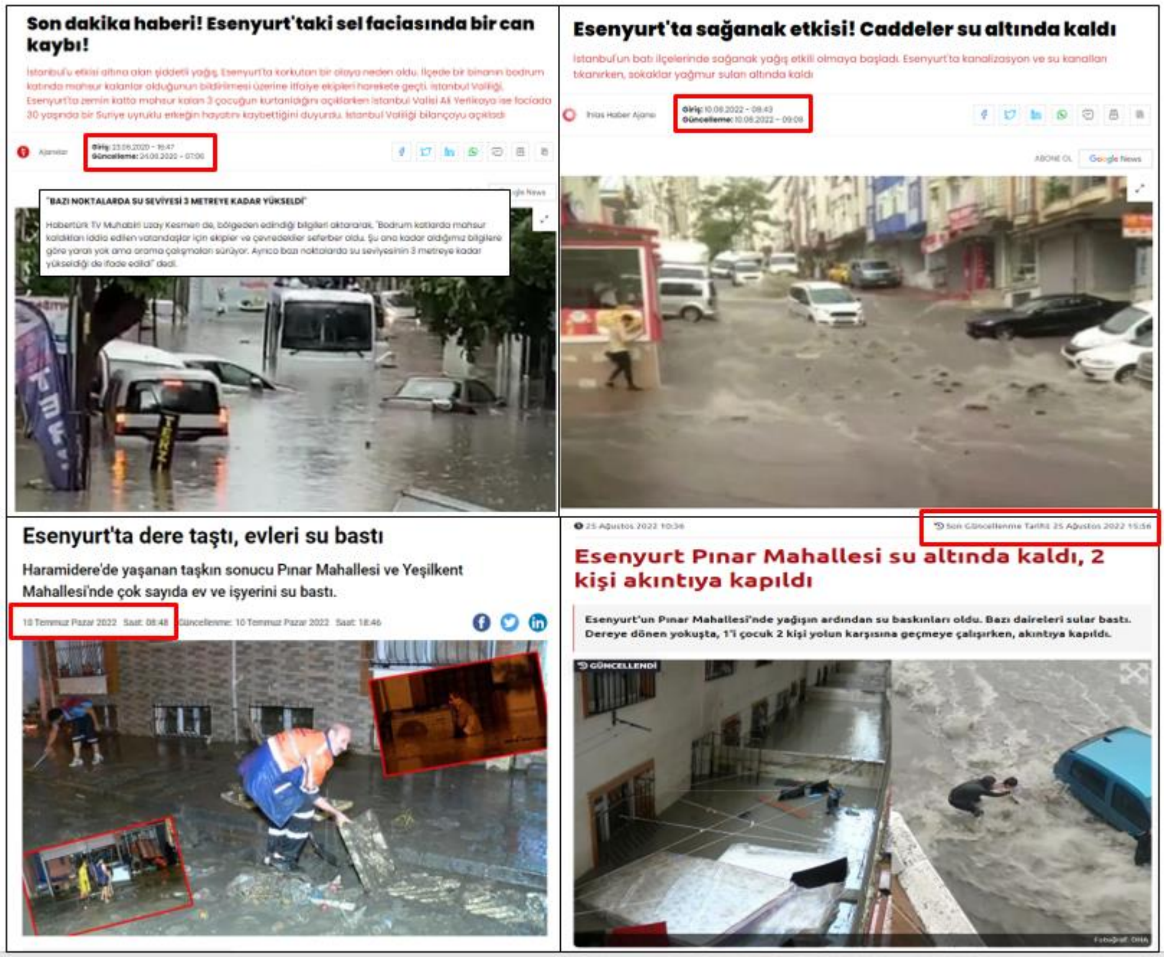

Figure 1.1. News on the historic floods of Haramidere River

APPENDIX-2. Study area photographs

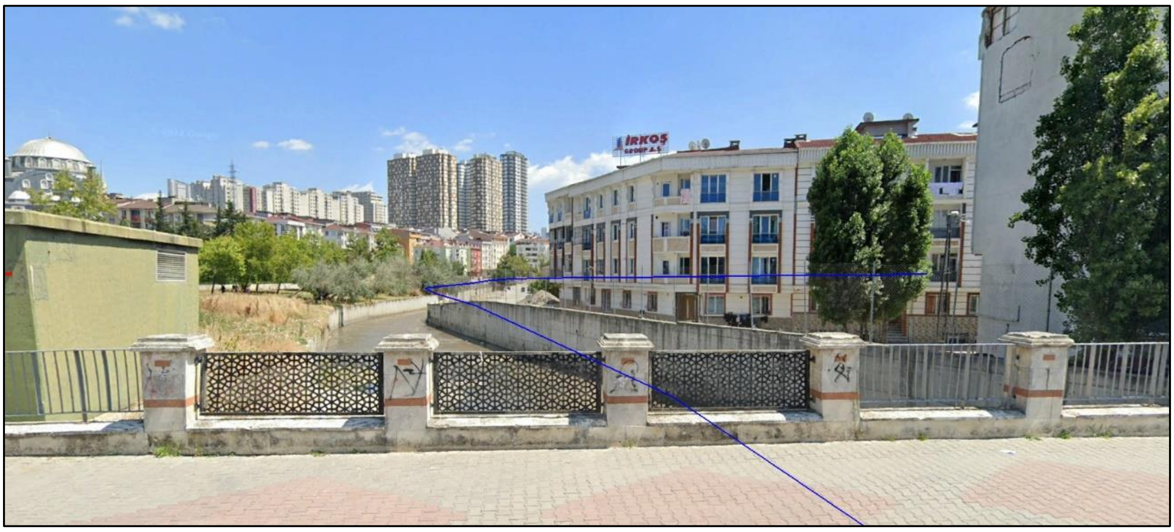

Figure 2.1. Haramidere River in Esenyurt (Google Earth)

Figure 2.2. A street in Esenyurt (URL-13)

APPENDIX-2. (continued) Zone-2 urban flood risk maps

Figure 2.3. Haramidere River in Esenyurt (URL-14)

Figure 2.4. Haramidere River in Esenyurt (taken by the author on 15.05.2023)

APPENDIX-2. (continued) Zone-2 urban flood risk maps

Figure 2.5. Haramidere River in Esenyurt (taken by the author on 15.05.2023)

APPENDIX-3. Zone-1 urban flood risk maps

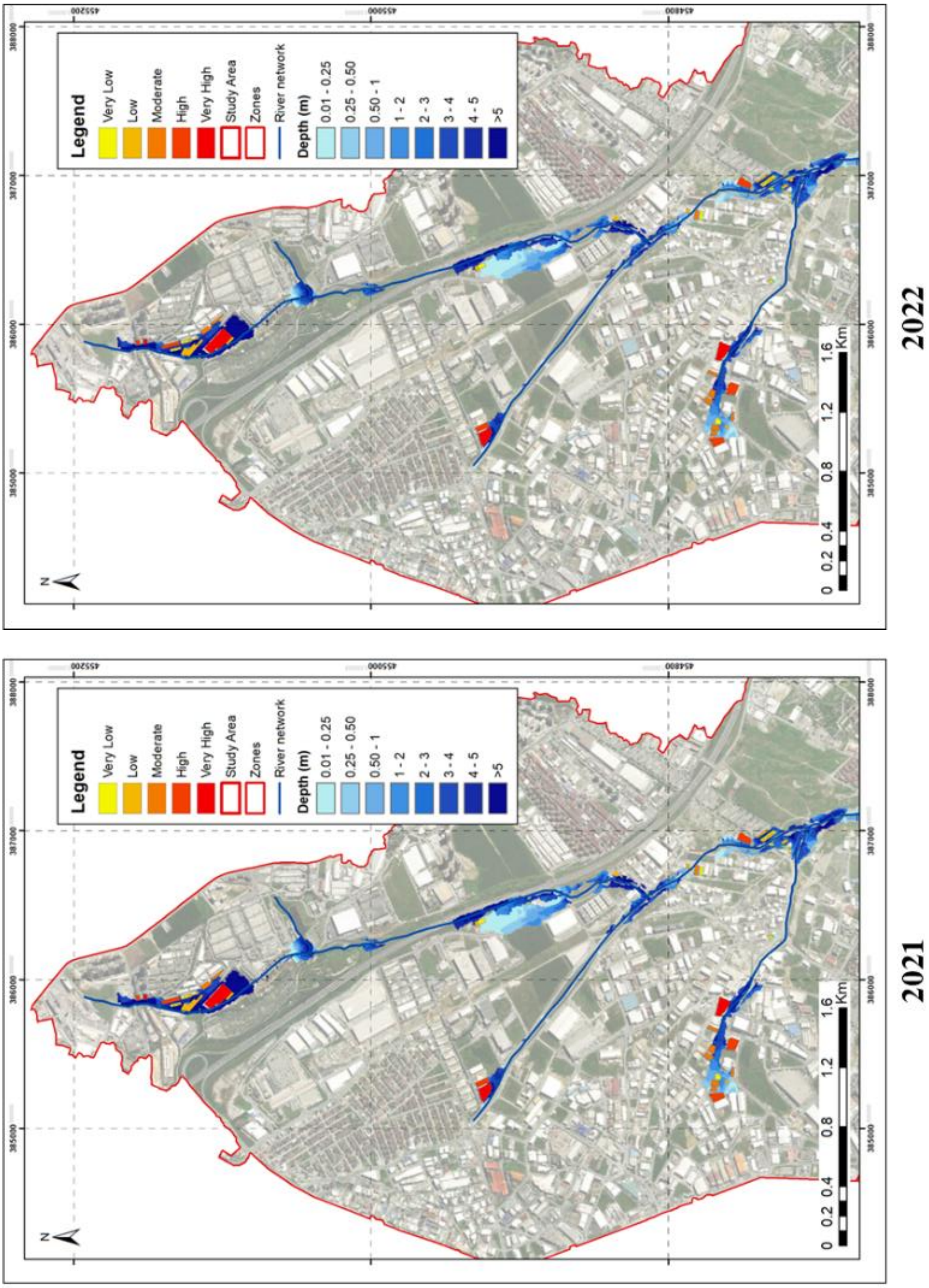

Figure 3.1. Zone-1 urban flood risk maps (2022-2021)

APPENDIX-3. (continued) Zone-1 urban flood risk maps

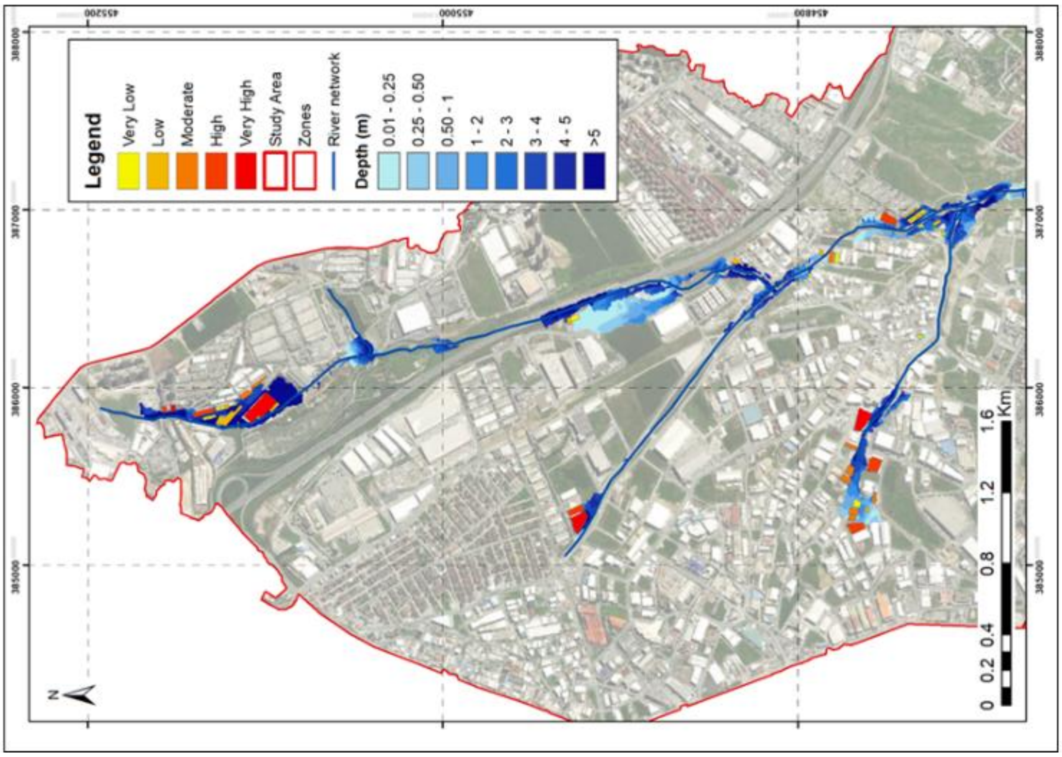

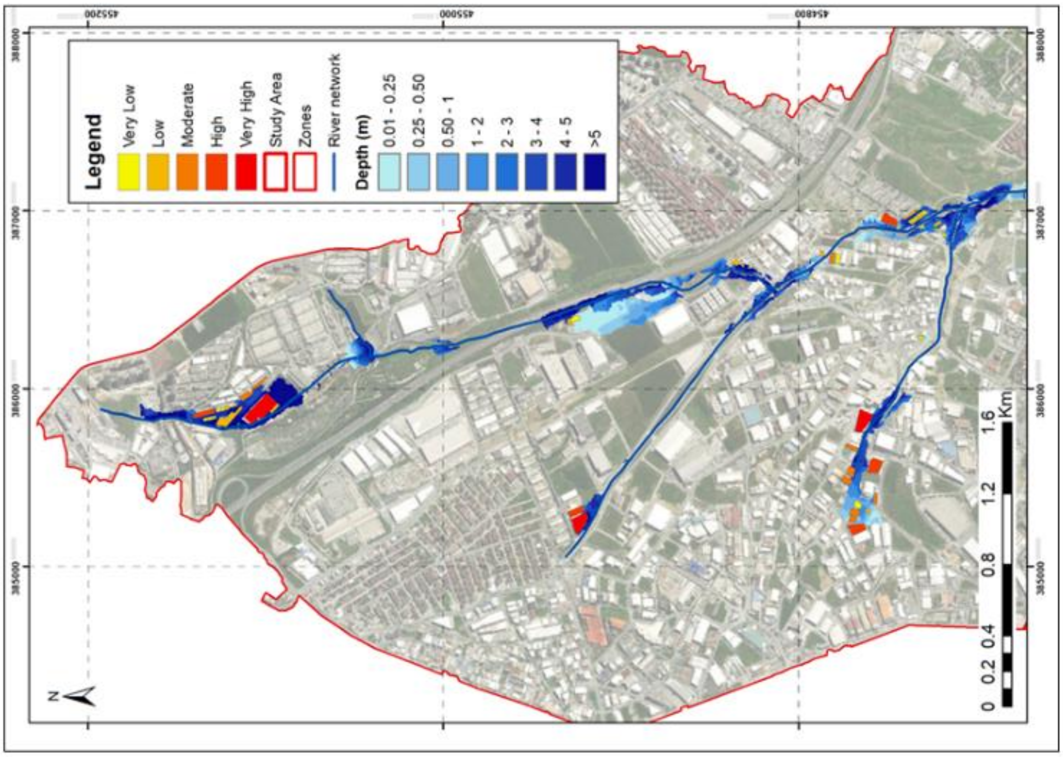

Figure 3.2. Zone-1 urban flood risk maps (2020-2019)

APPENDIX-3. (continued) Zone-1 urban flood risk maps

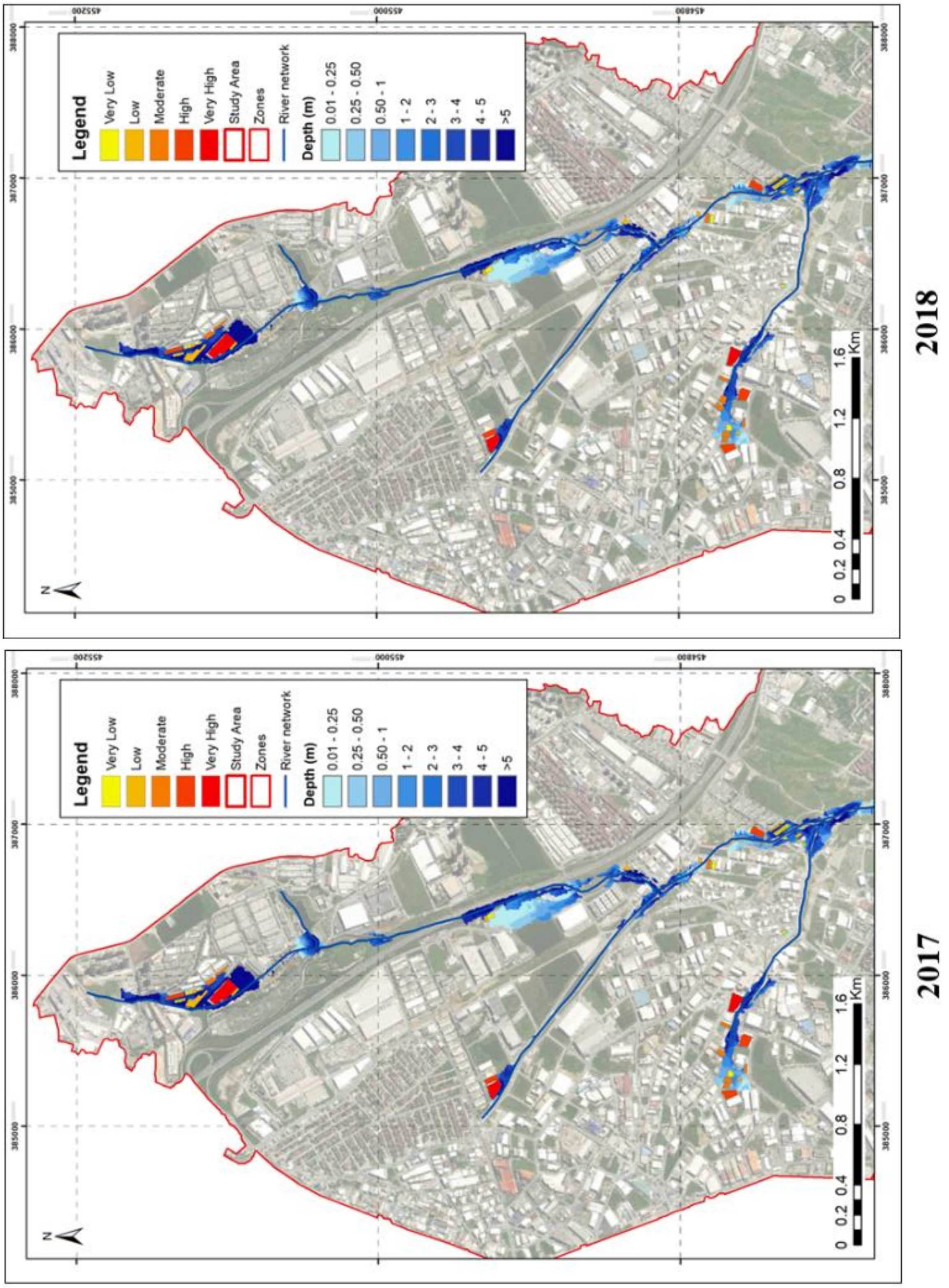

Figure 3.3 Zone-1 urban flood risk maps (2018-2017)

APPENDIX-3. (continued) Zone-1 urban flood risk maps

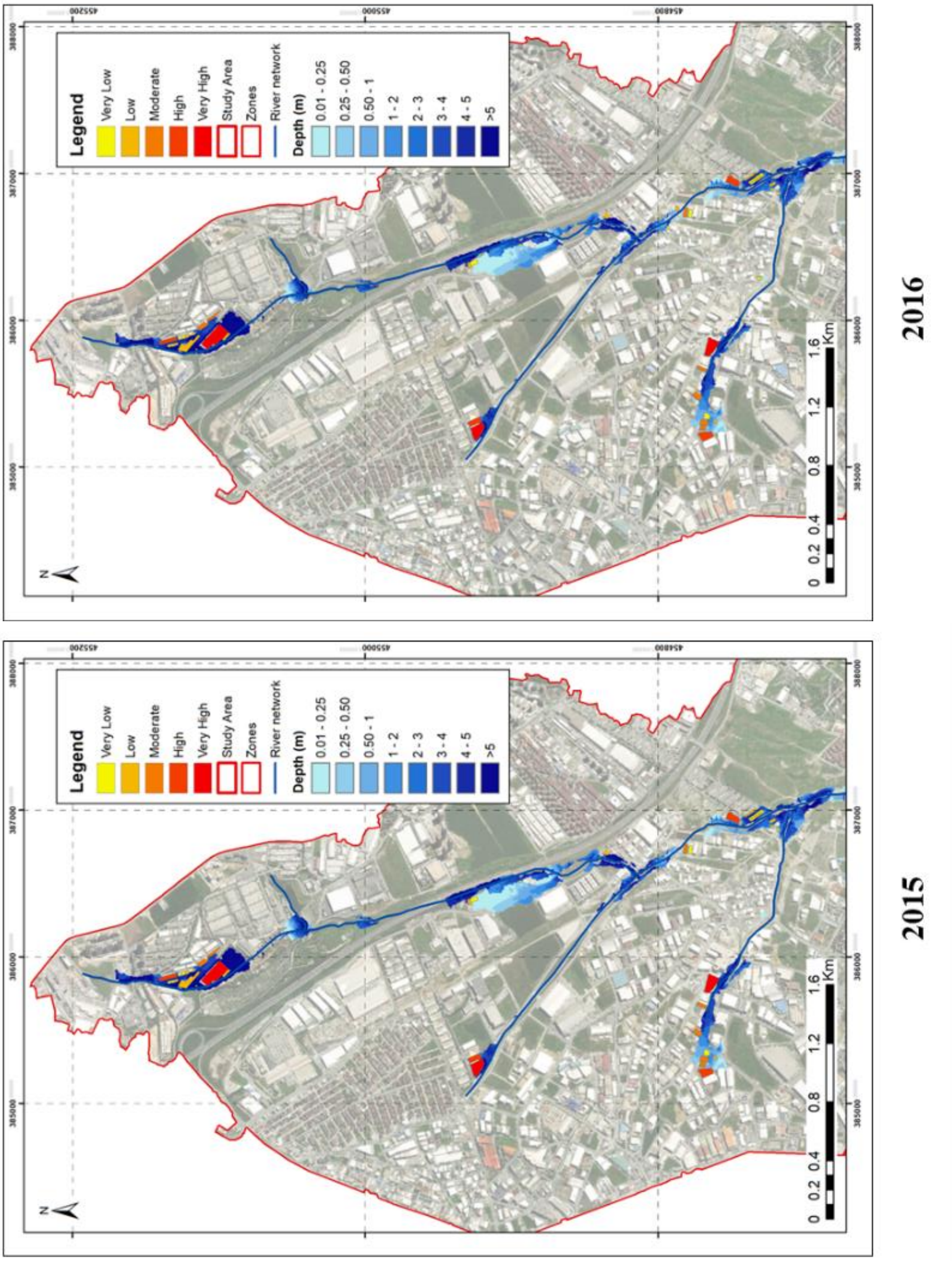

Figure 3.4. Zone-1 urban flood risk maps (2016-2015)

APPENDIX-3. (continued) Zone-1 urban flood risk maps

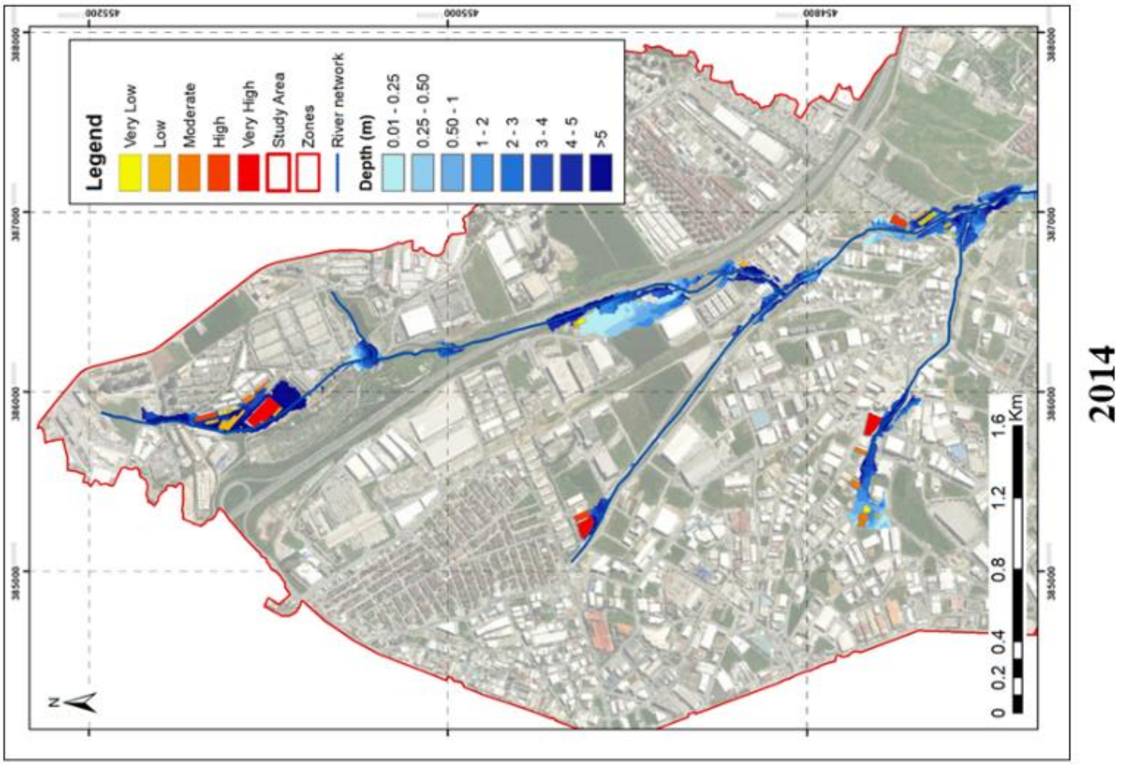

Figure 3.5. Zone-1 urban flood risk maps (2014)

APPENDIX-4. Zone-2 urban flood risk maps

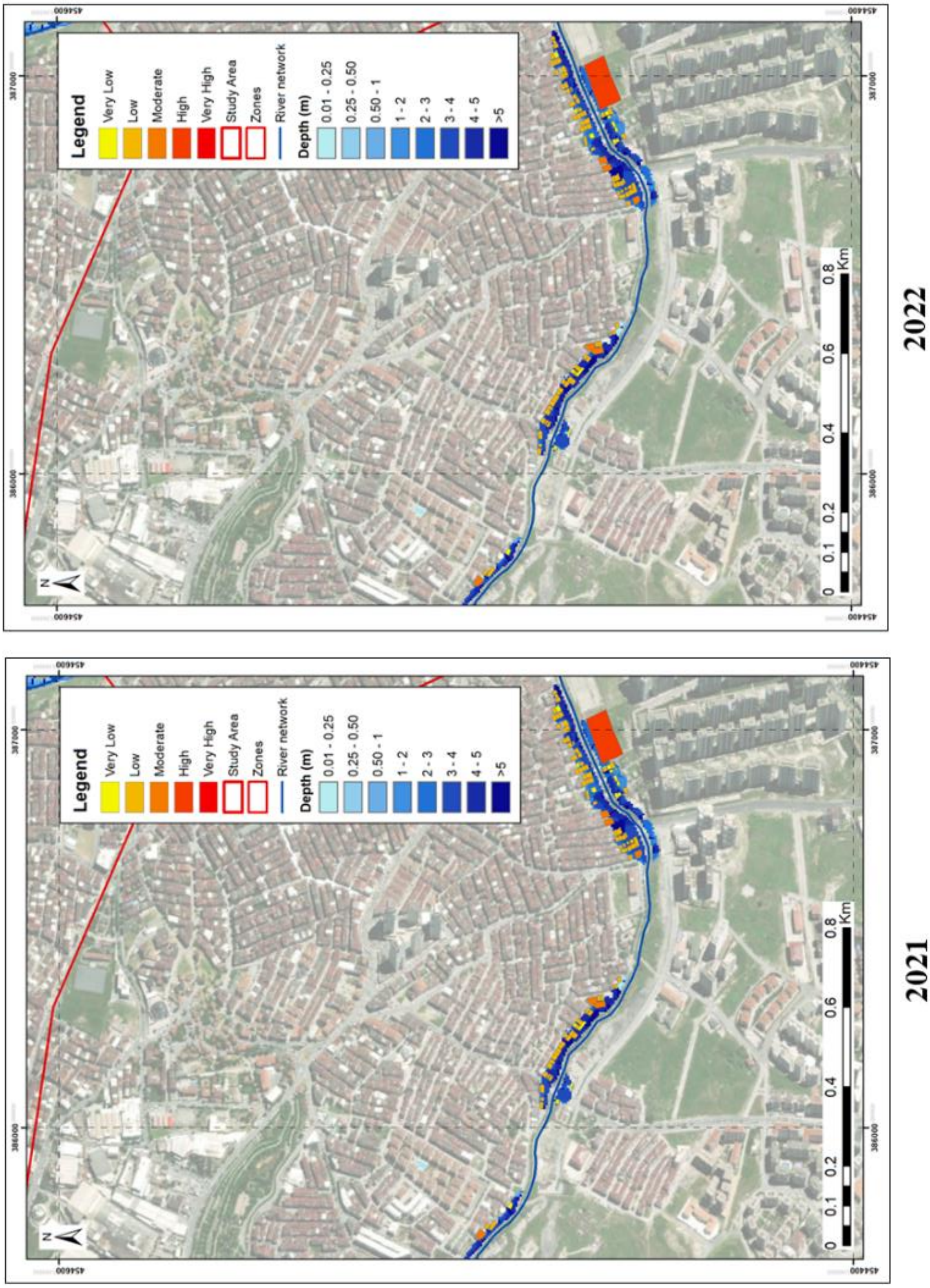

Figure 4.1. Zone-2 urban flood risk maps (2022-2021)

APPENDIX-4. (continued) Zone-2 urban flood risk maps

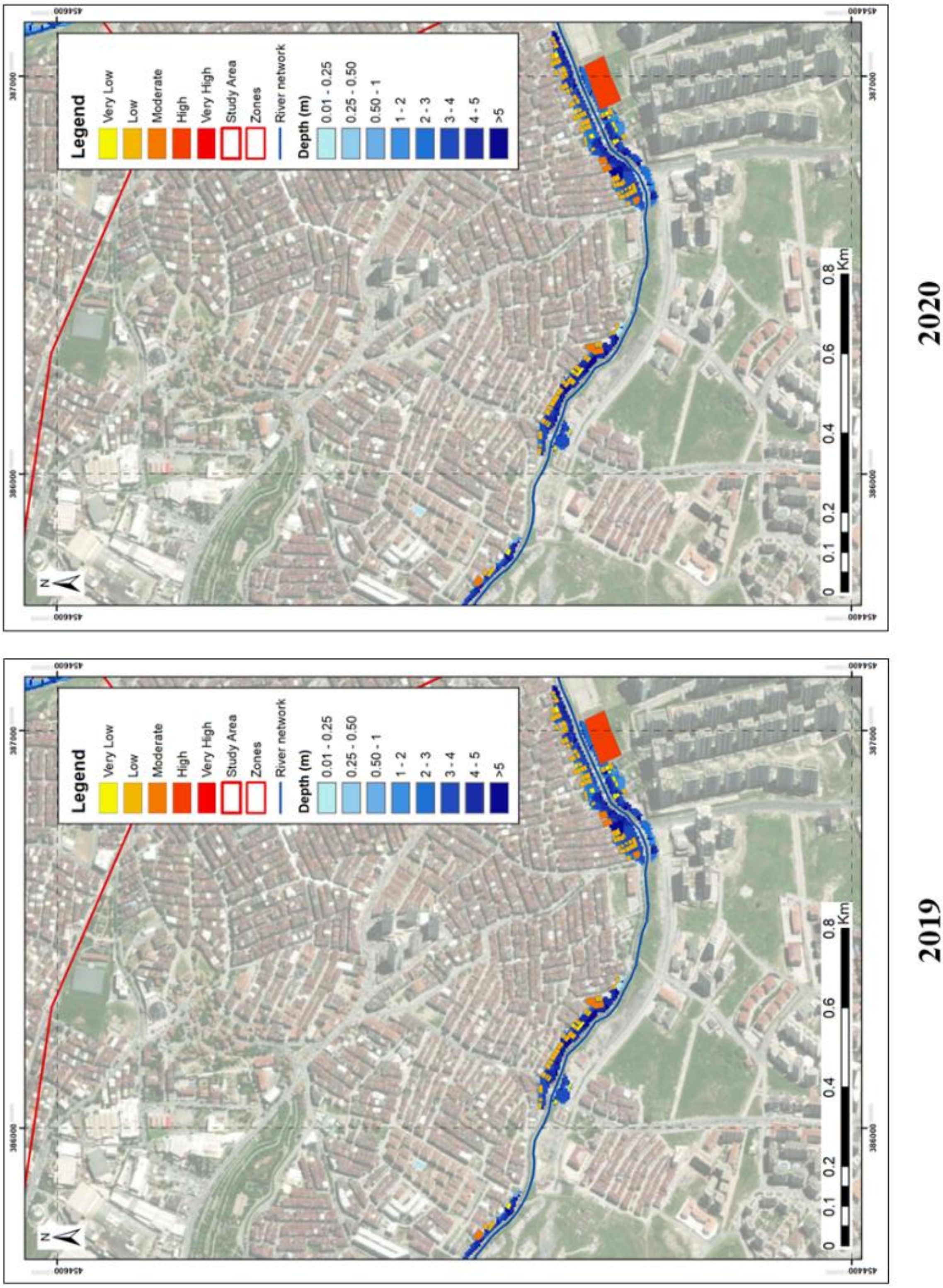

Figure 4.2. Zone-2 urban flood risk maps (2020-2019)

APPENDIX-4. (continued) Zone-2 urban flood risk maps

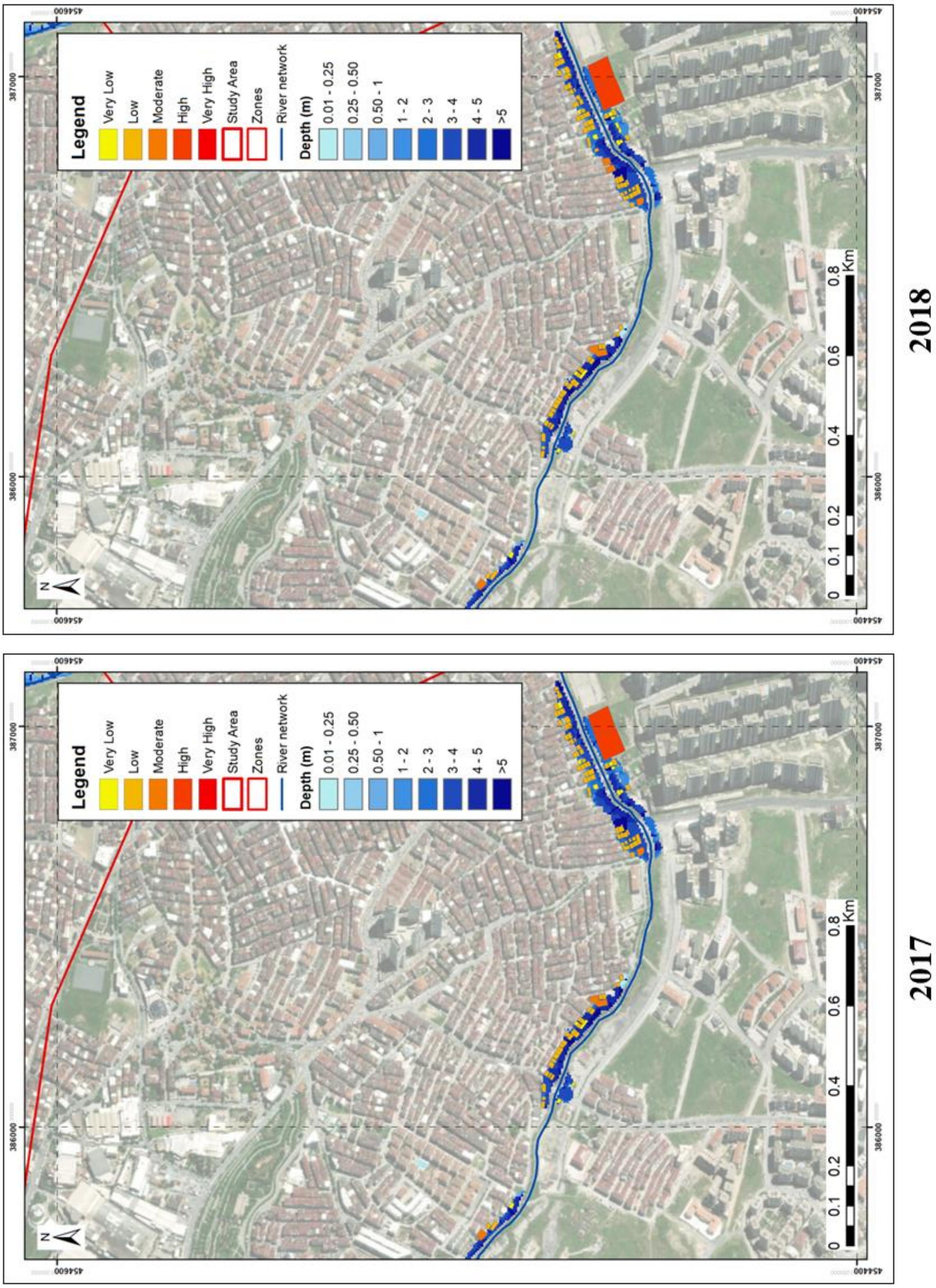

Figure 4.3. Zone-2 urban flood risk maps (2018-2017)

APPENDIX-4. (continued) Zone-2 urban flood risk maps

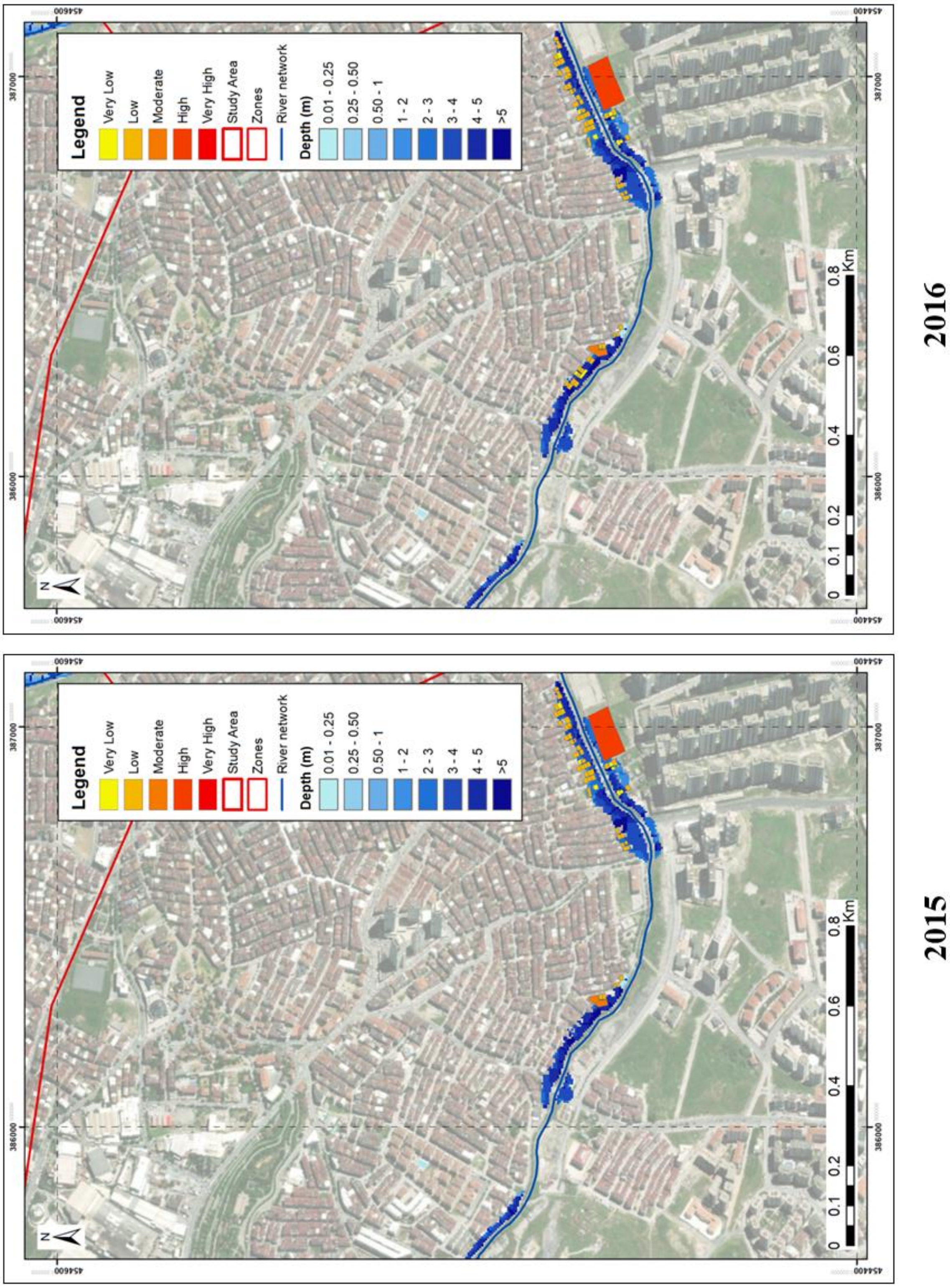

Figure 4.4. Zone-2 urban flood risk maps (2016-2015)

APPENDIX-4. (continued) Zone-2 urban flood risk maps

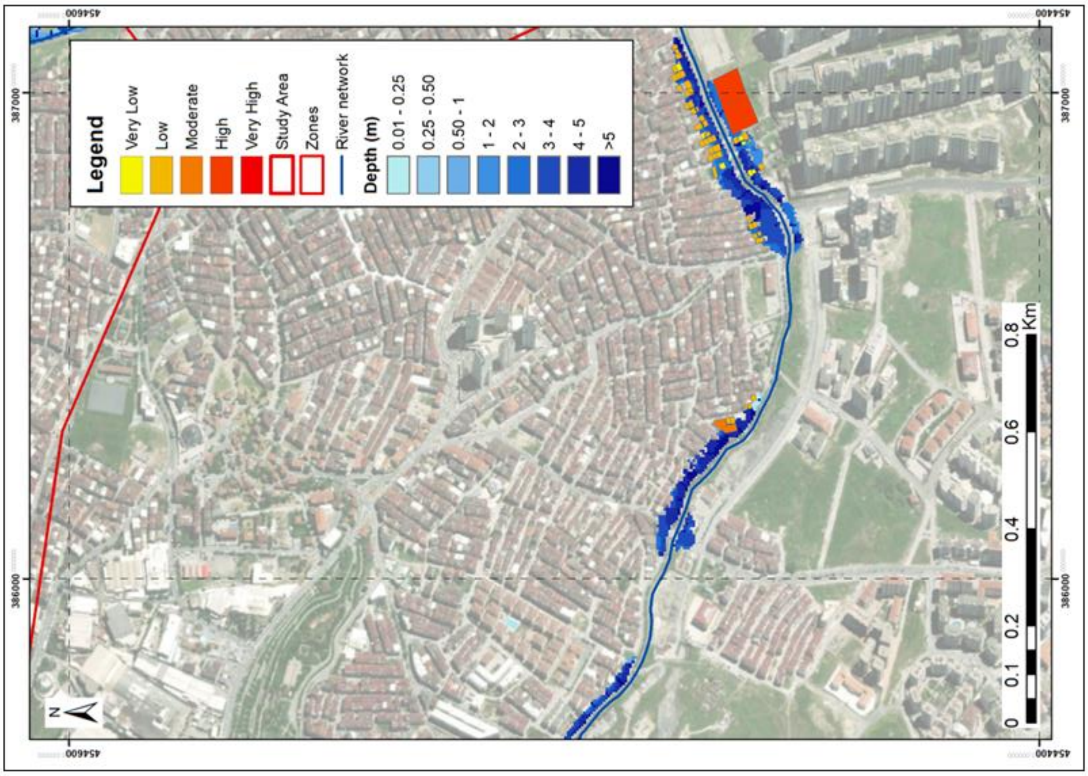

2014

Figure 4.5. Zone-2 urban flood risk maps (2014)

APPENDIX-5. Zone-3 urban flood risk maps

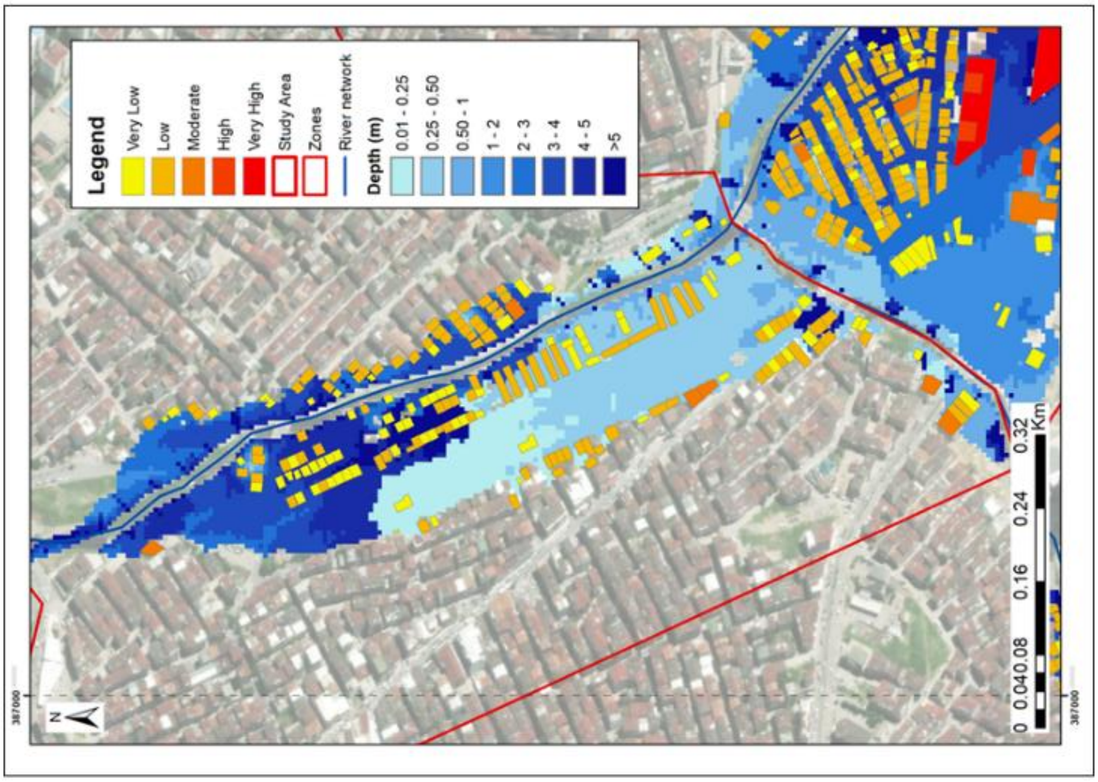

2022

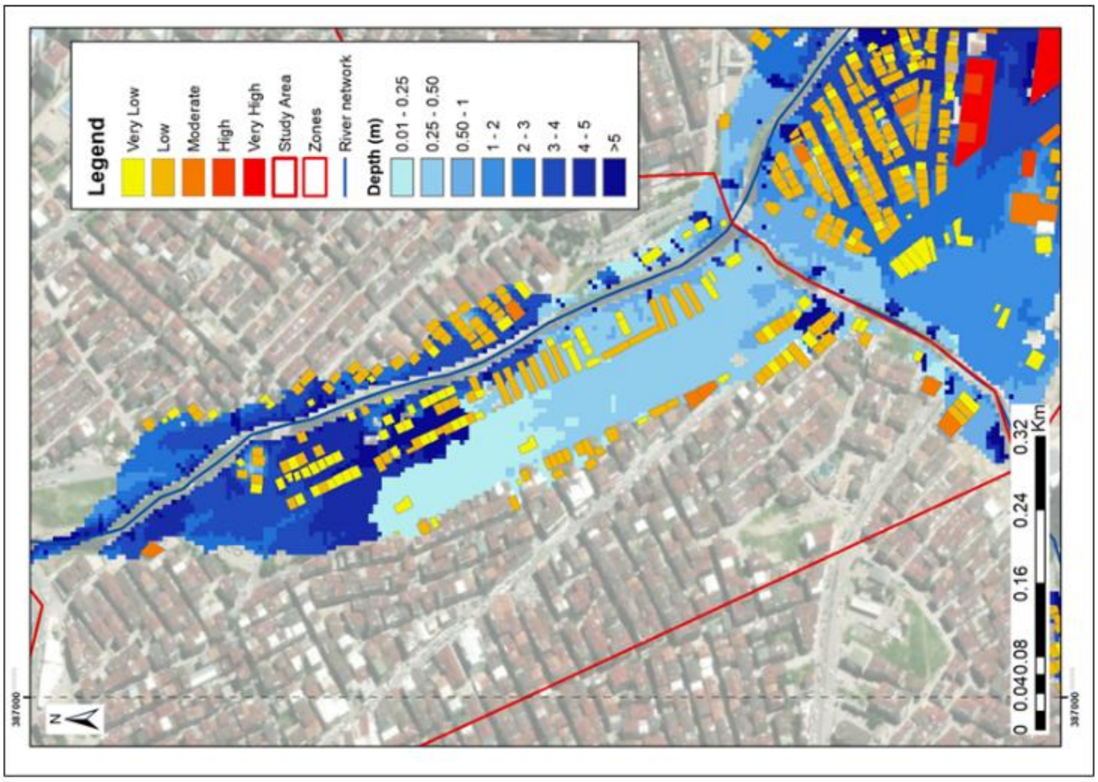

2021

Figure 5.1. Zone-3 urban flood risk maps (2022-2021)

APPENDIX-5. (continued) Zone-3 urban flood risk maps

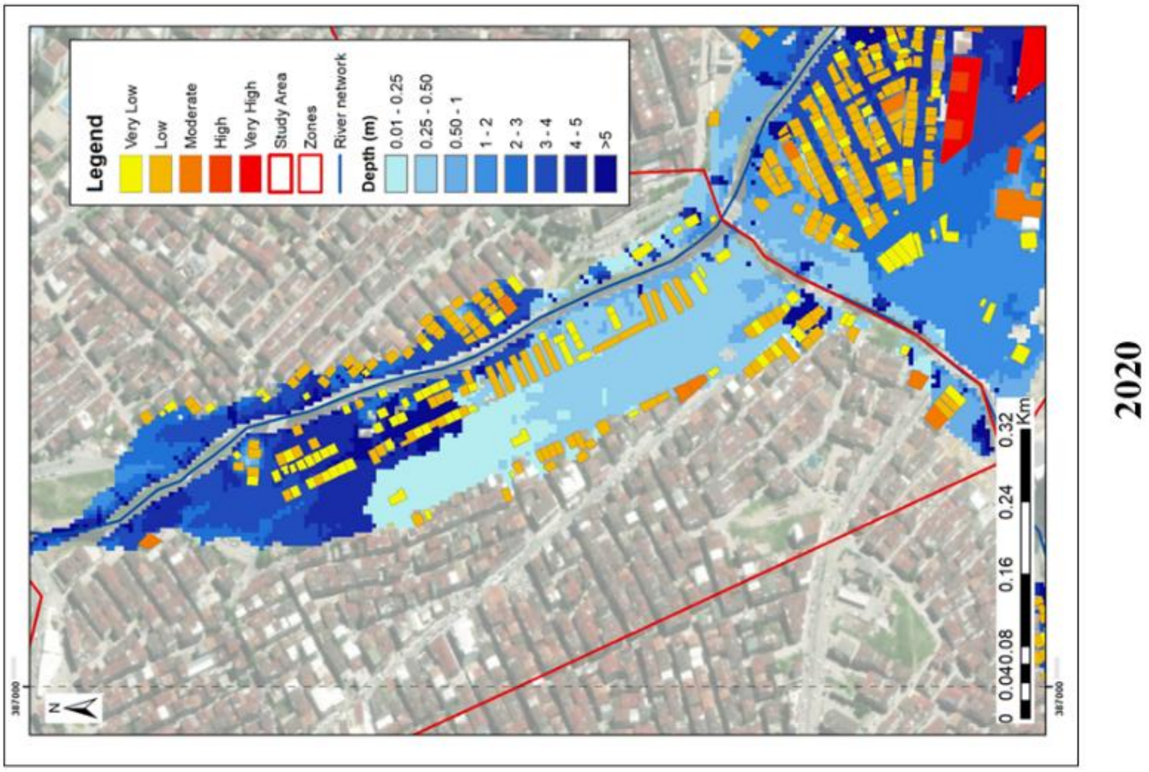

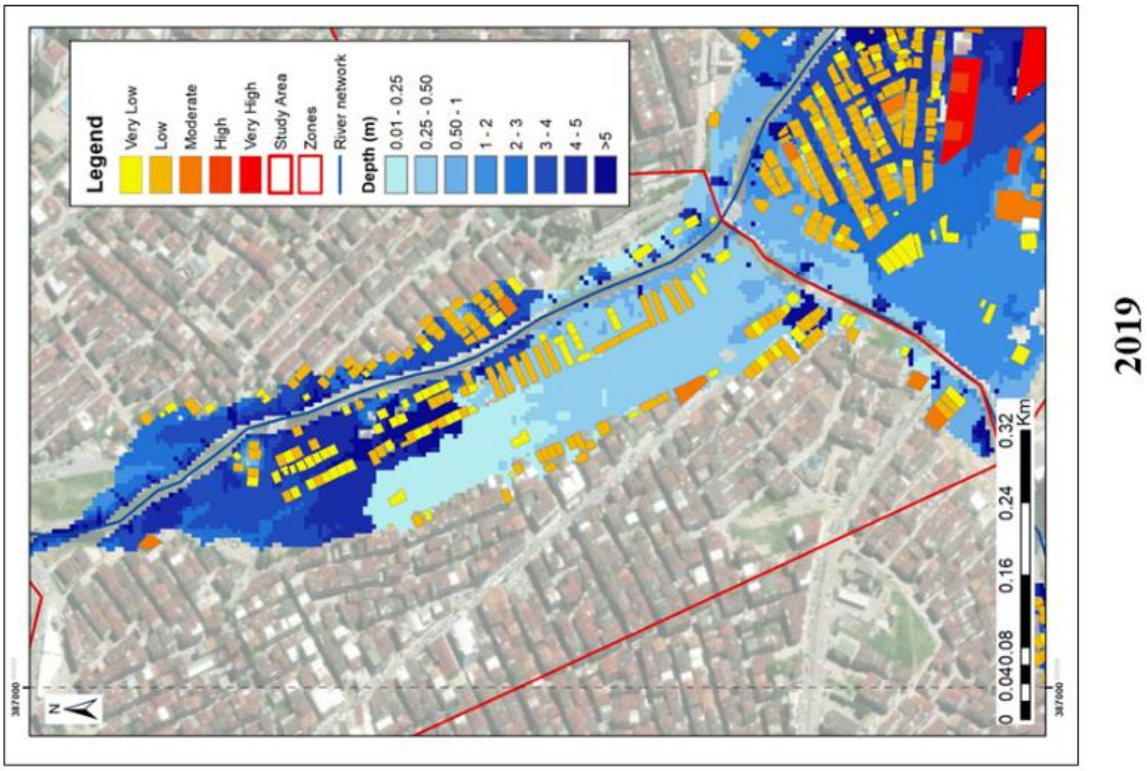

Figure 5.2. Zone-3 urban flood risk maps (2020-2019)

APPENDIX-5. (continued) Zone-3 urban flood risk maps

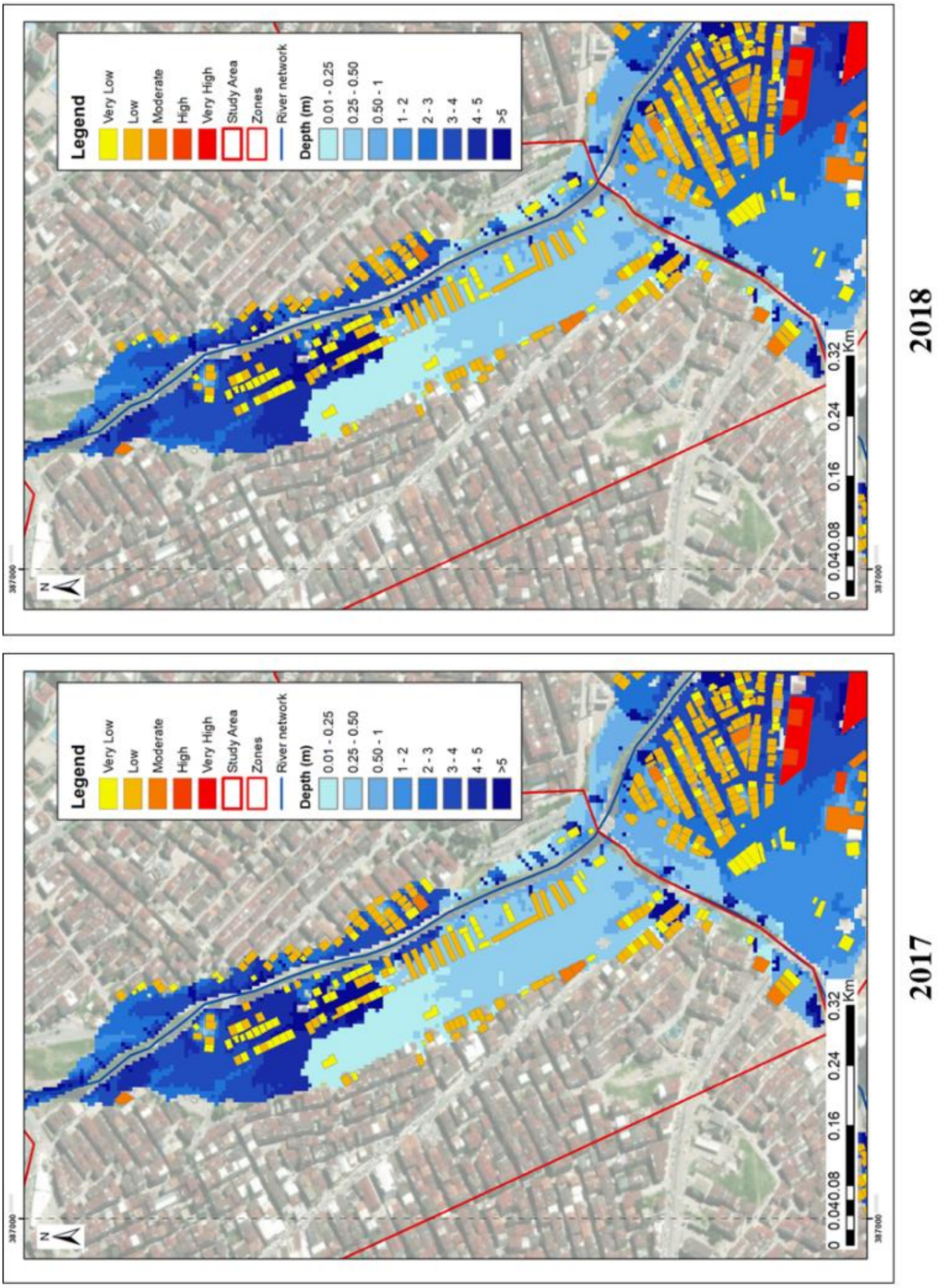

Figure 5.3. Zone-3 urban flood risk maps (2018-2017)

APPENDIX-5. (continued) Zone-3 urban flood risk maps

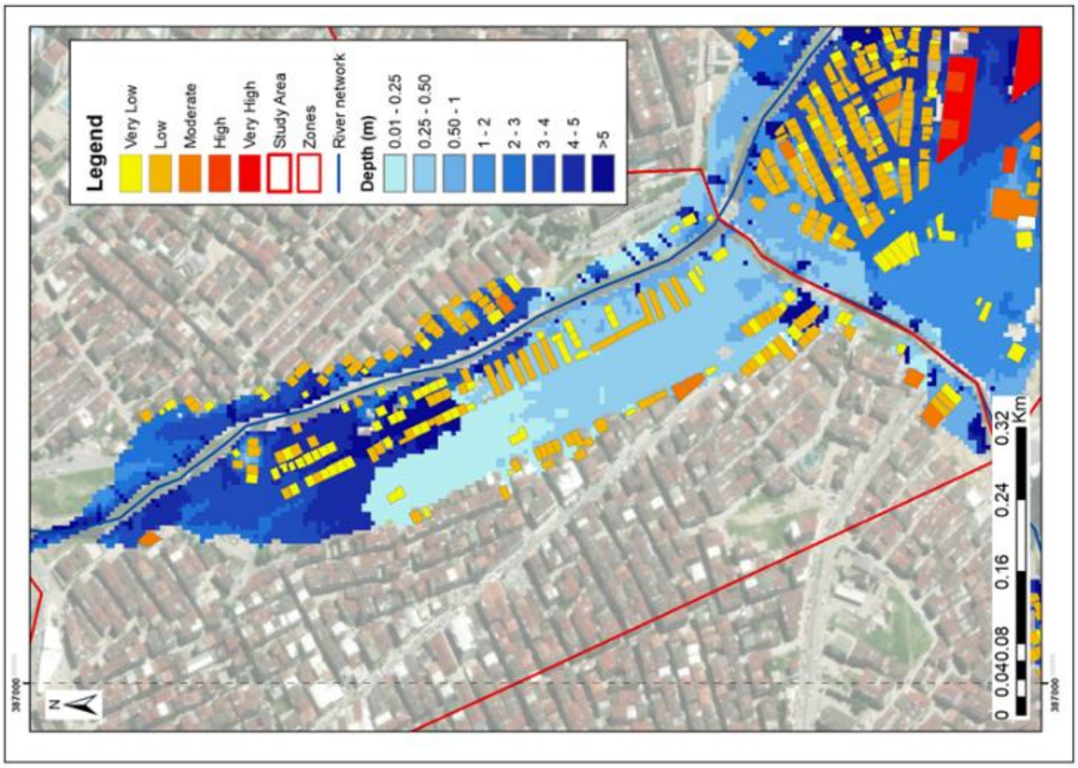

2016

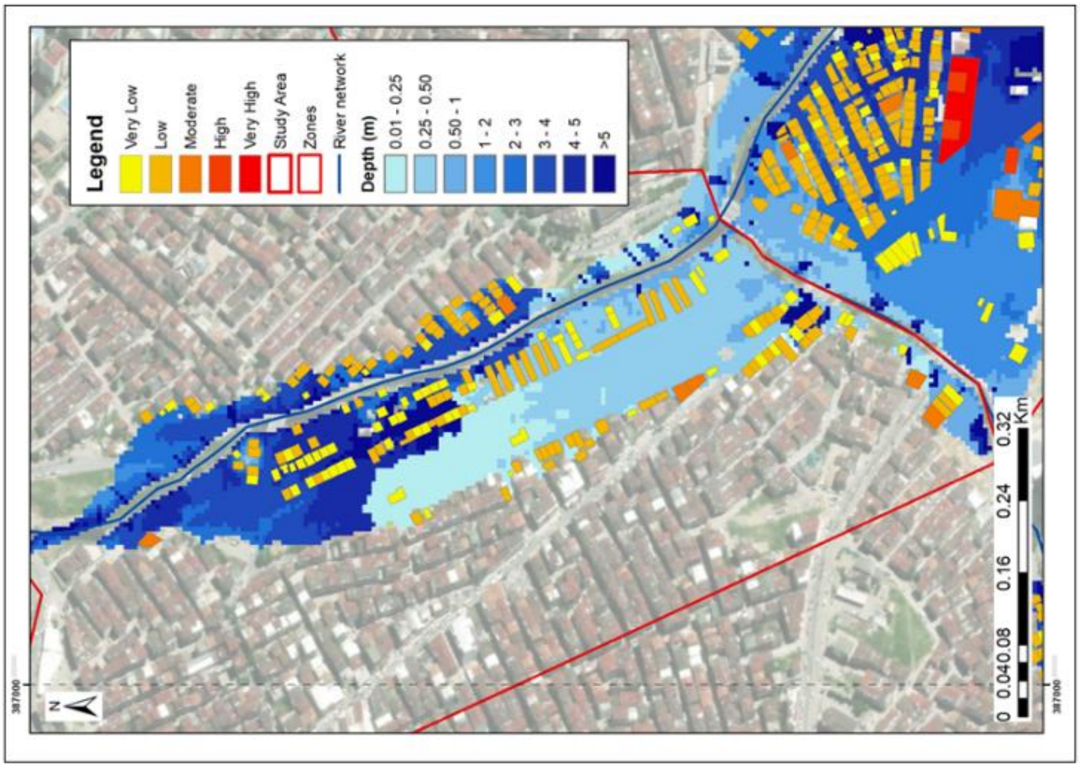

2015

Figure 5.4. Zone-3 urban flood risk maps (2016-2015)

APPENDIX-5. (continued) Zone-3 urban flood risk maps

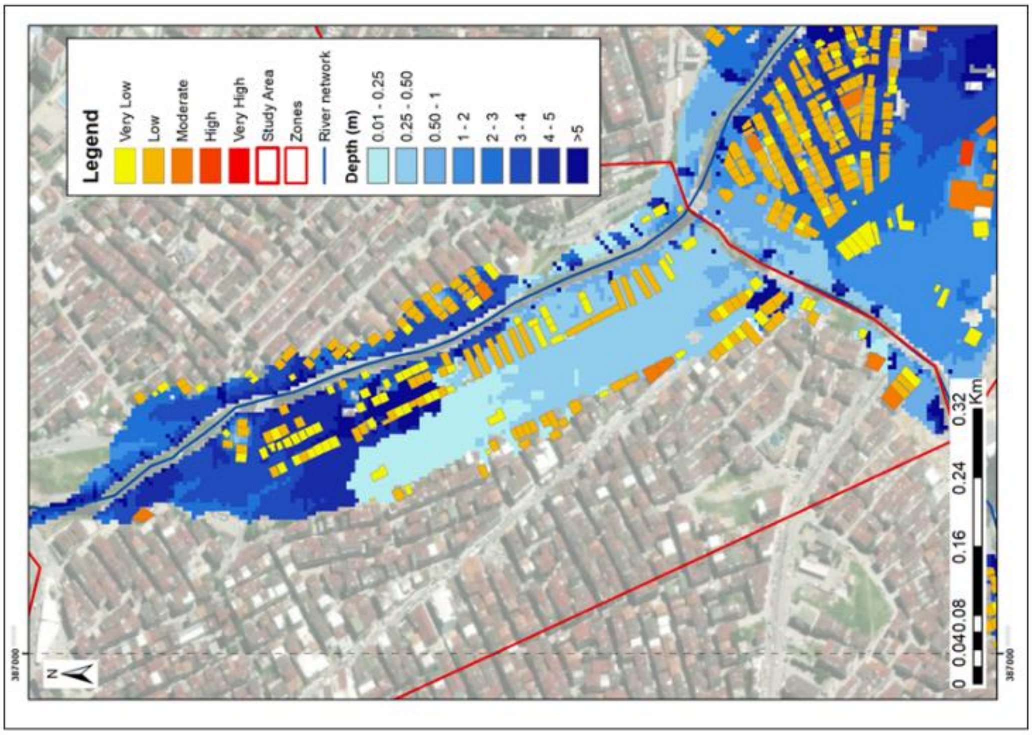

2014

Figure 5.5. Zone-3 urban flood risk maps (2014)

APPENDIX-6. Zone-4 urban flood risk maps

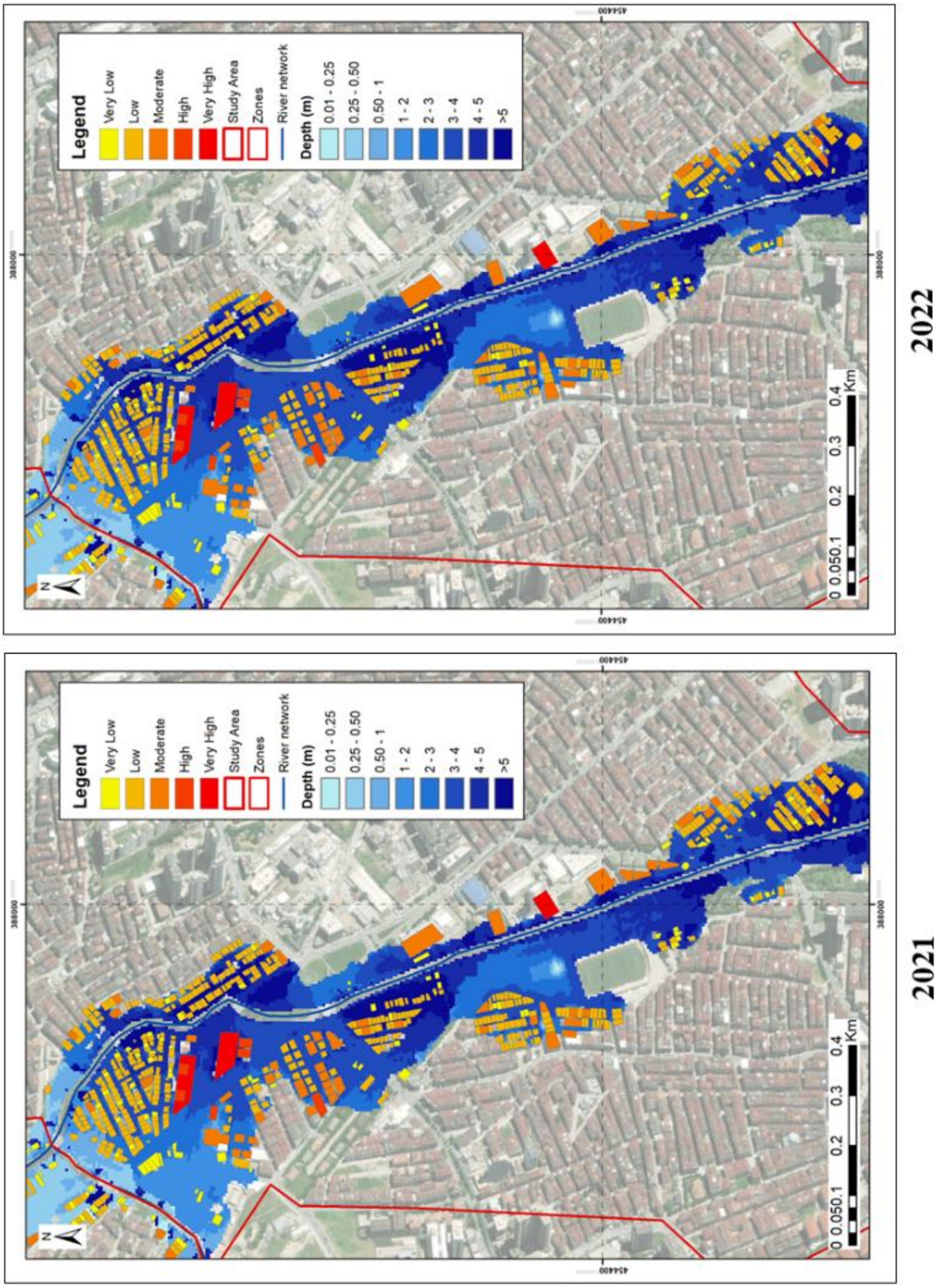

Figure 6.1. Zone-4 urban flood risk maps (2022- 2021)

APPENDIX-6. (continued) Zone-4 urban flood risk maps

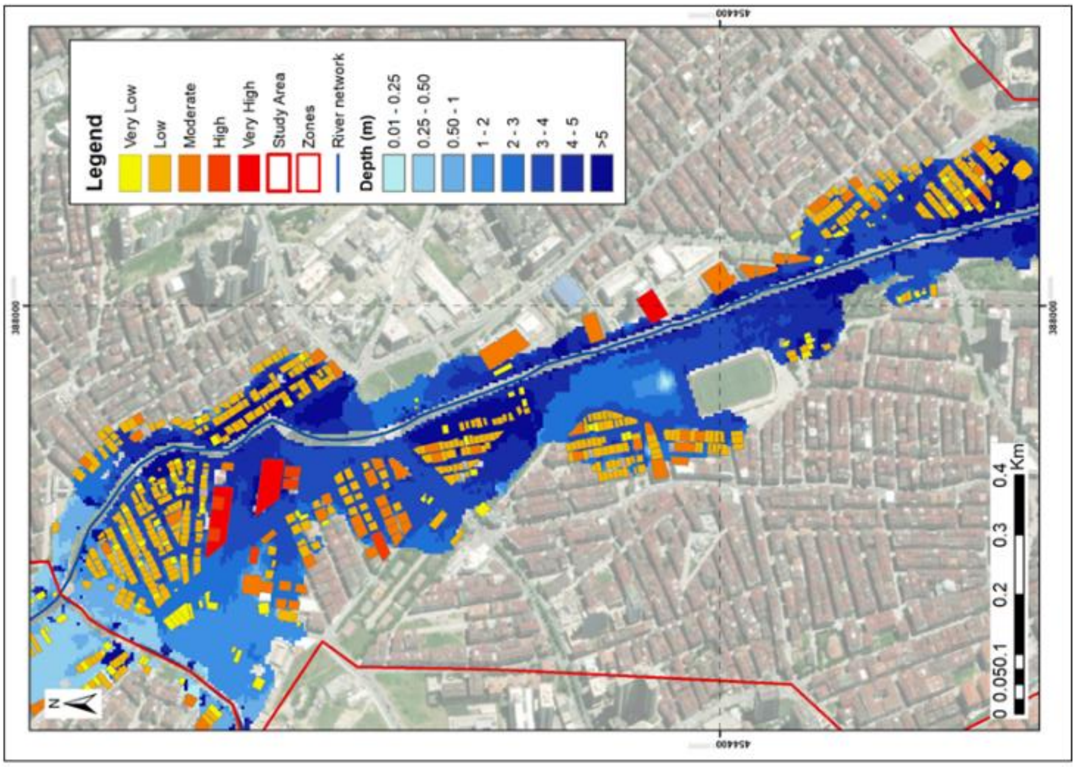

2020

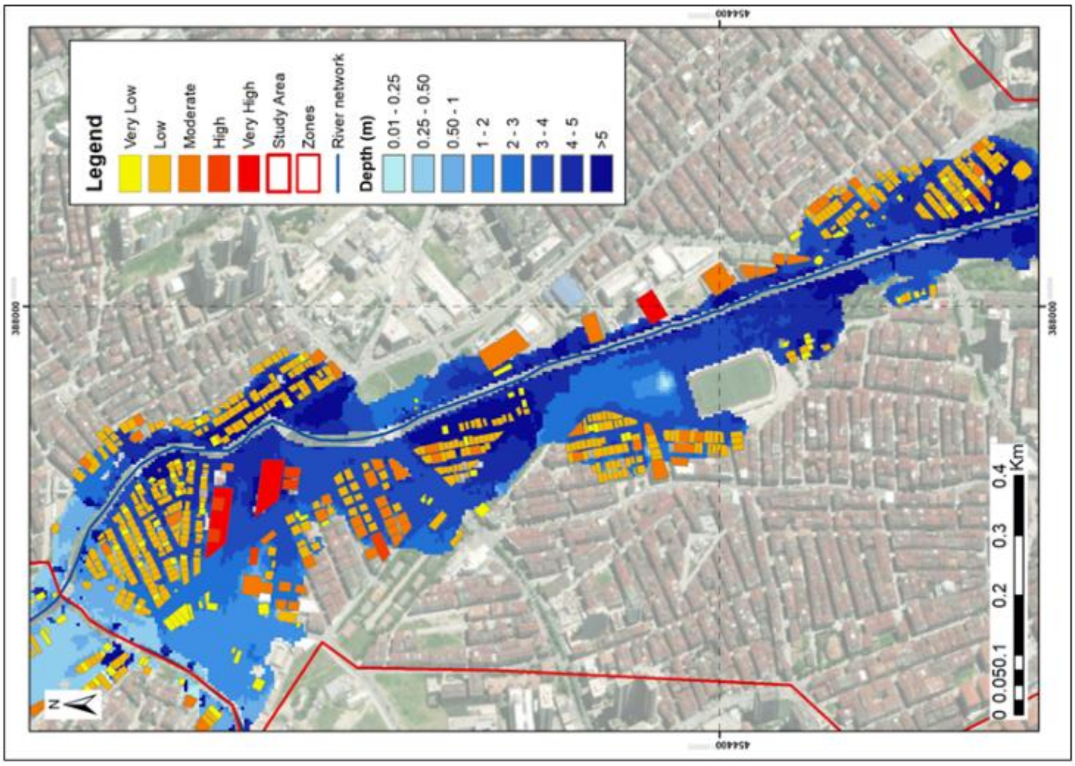

2019

Figure 6.2. Zone-4 urban flood risk maps (2020- 2019)

APPENDIX-6. (continued) Zone-4 urban flood risk maps

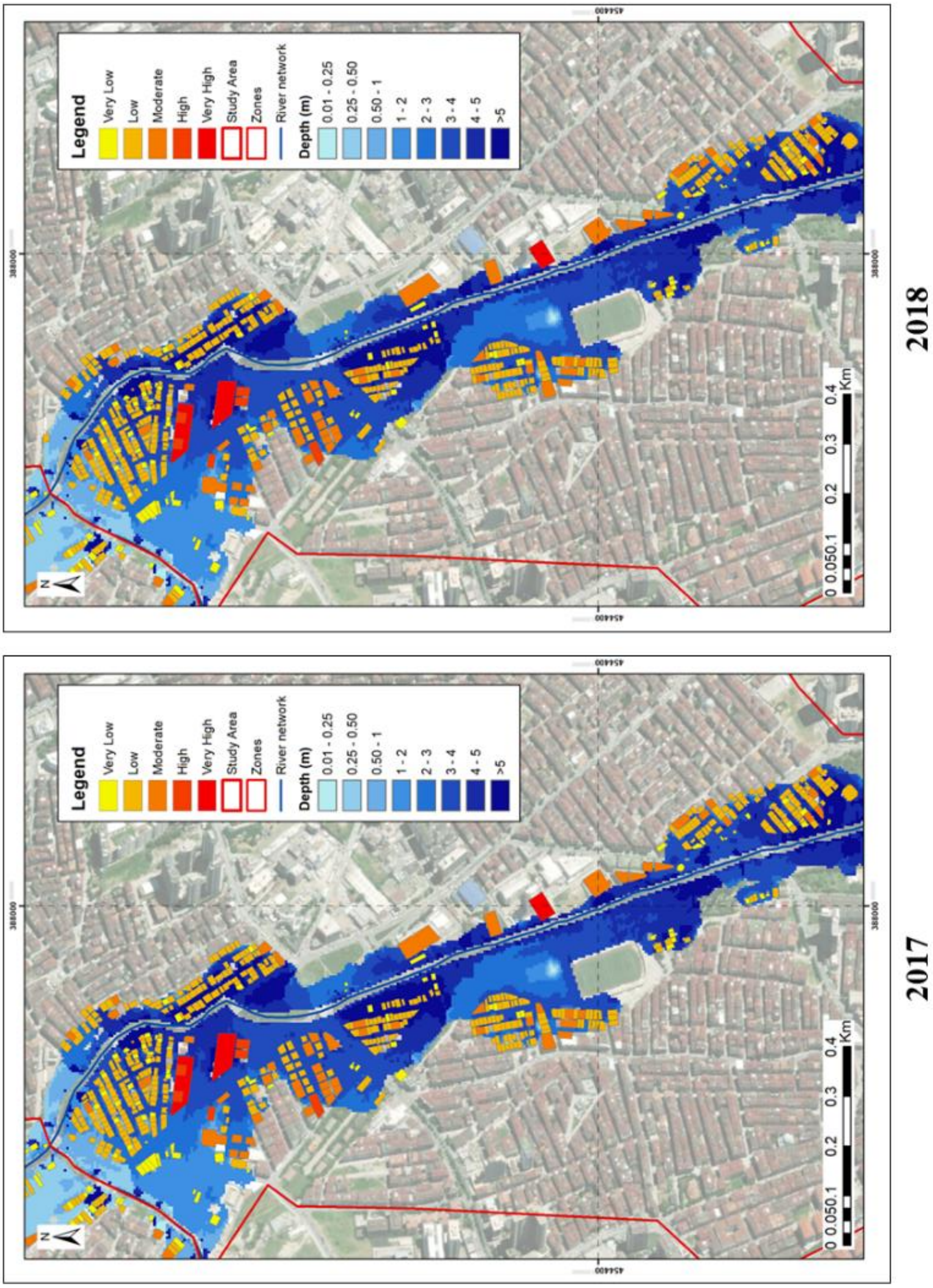

Figure 6.3. Zone-4 urban flood risk maps (2018- 2017)

APPENDIX-6. (continued) Zone-4 urban flood risk maps

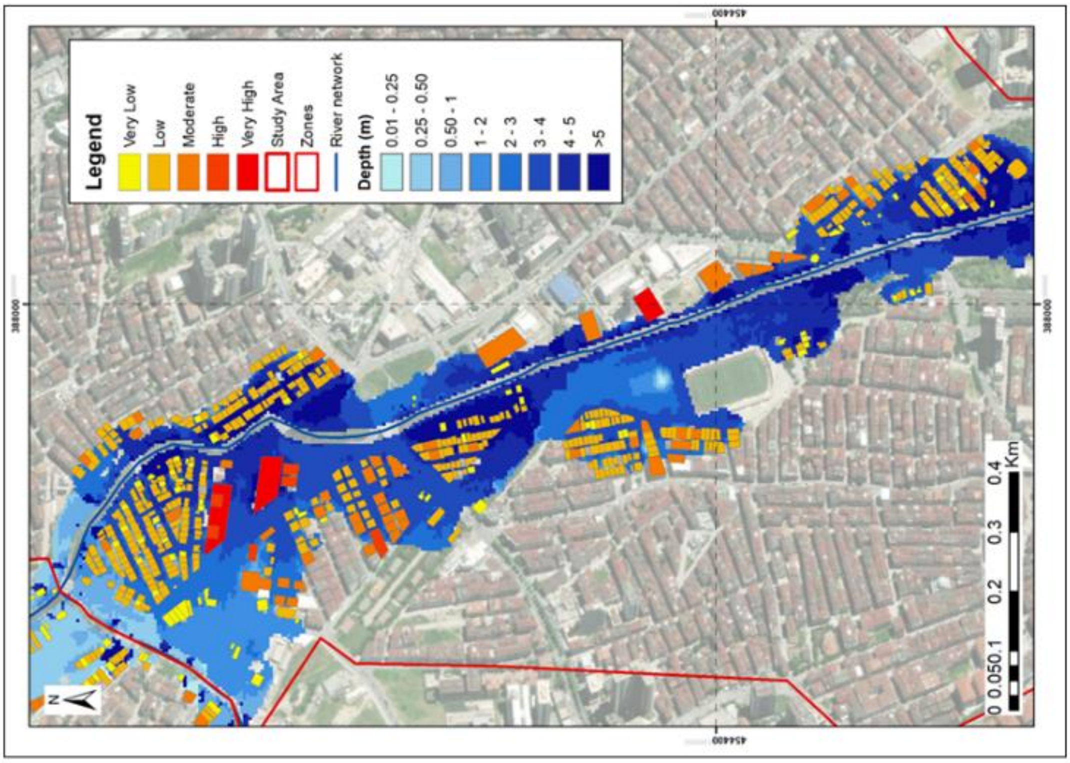

2016

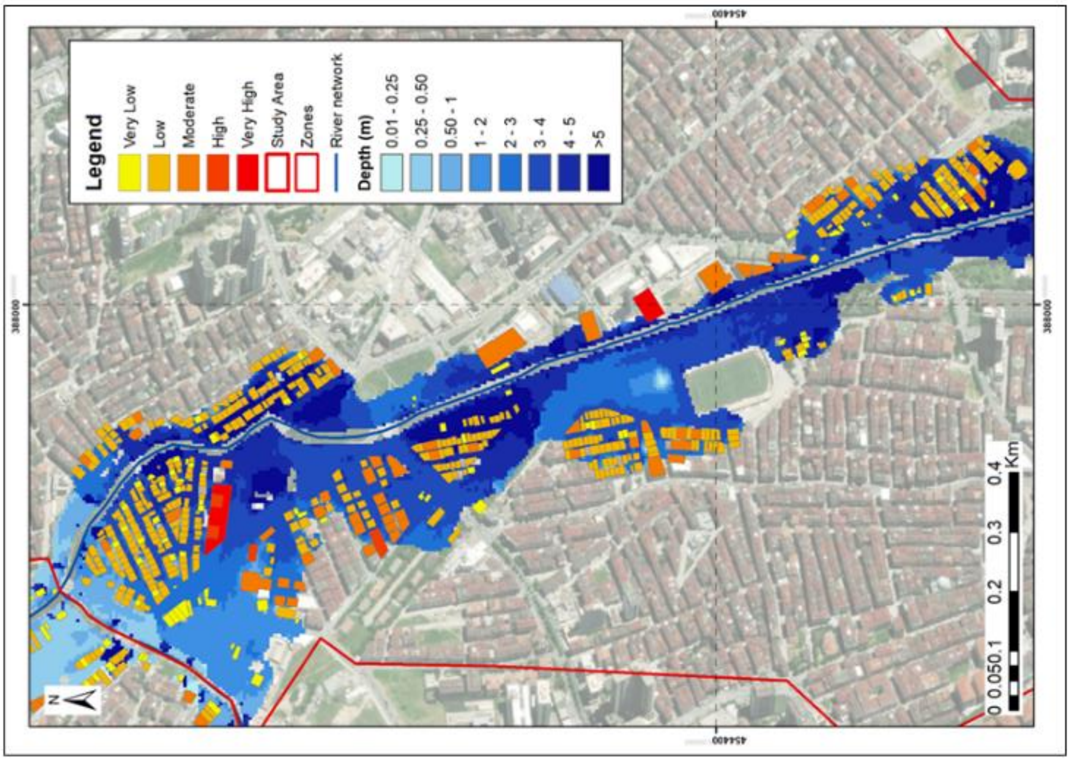

2015

Figure 6.4. Zone-4 urban flood risk maps (2016- 2015)

APPENDIX-6. (continued) Zone-4 urban flood risk maps

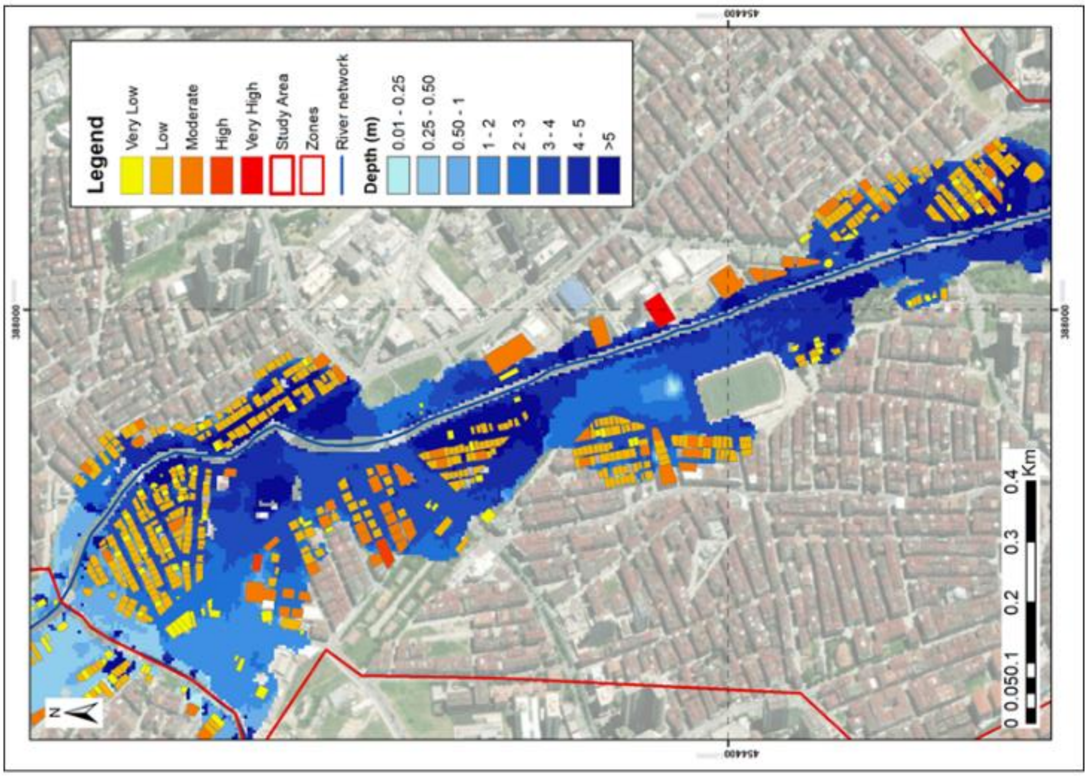

2014

Figure 6.5. Zone-4 urban flood risk maps (2014)

APPENDIX-7. Zone-5 urban flood risk maps

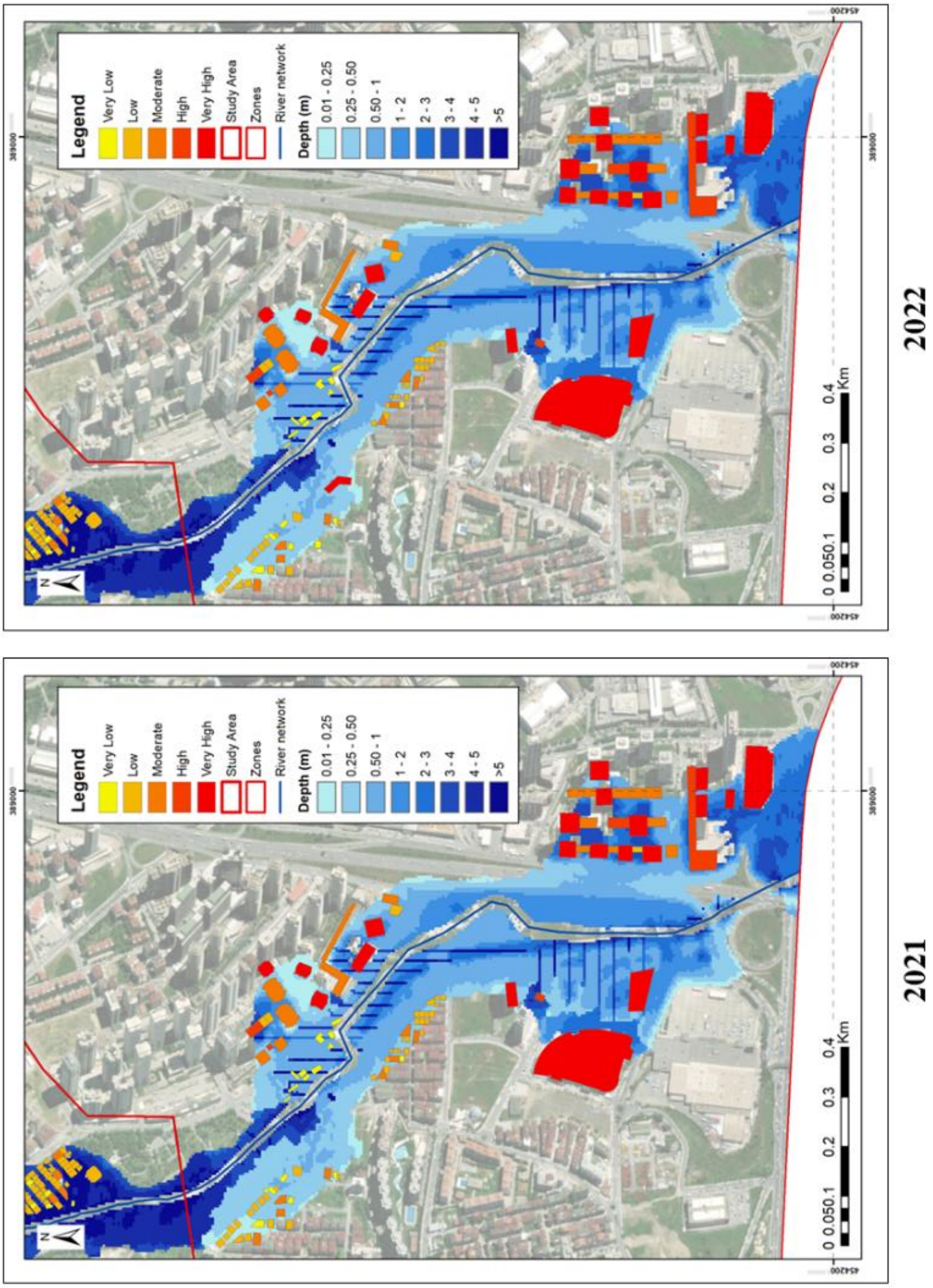

Figure 7.1. Zone-5 urban flood risk maps (2022- 2021)

APPENDIX-7. (continued) Zone-5 urban flood risk maps

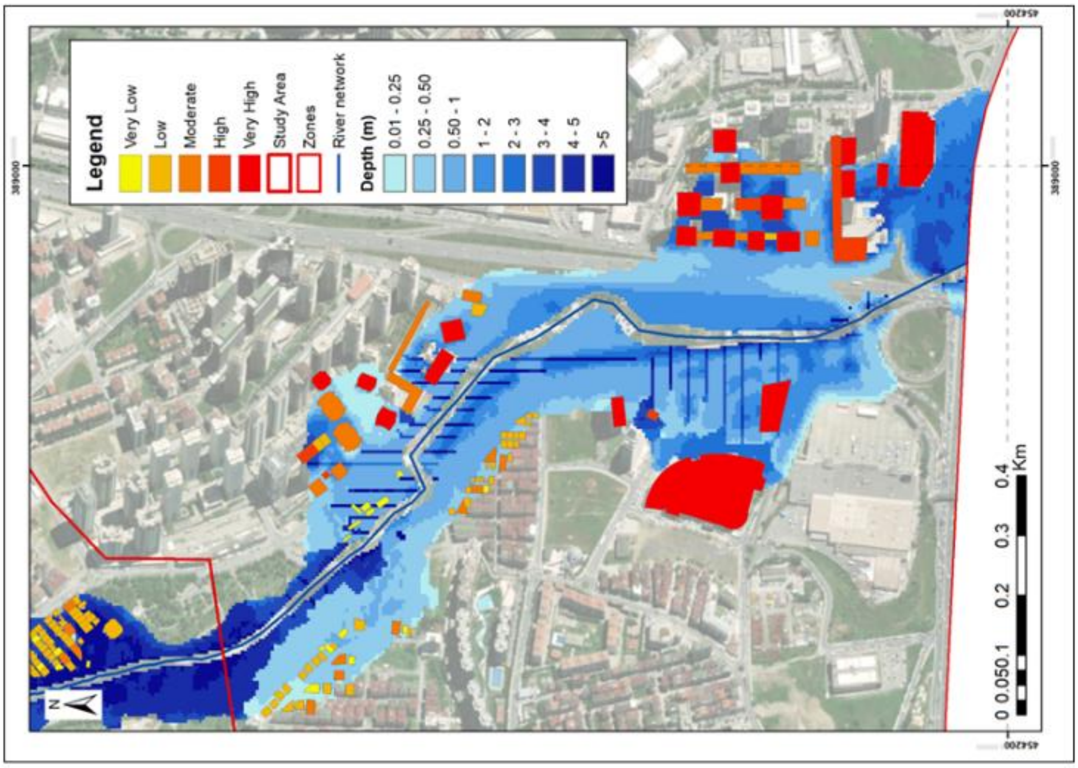

2020

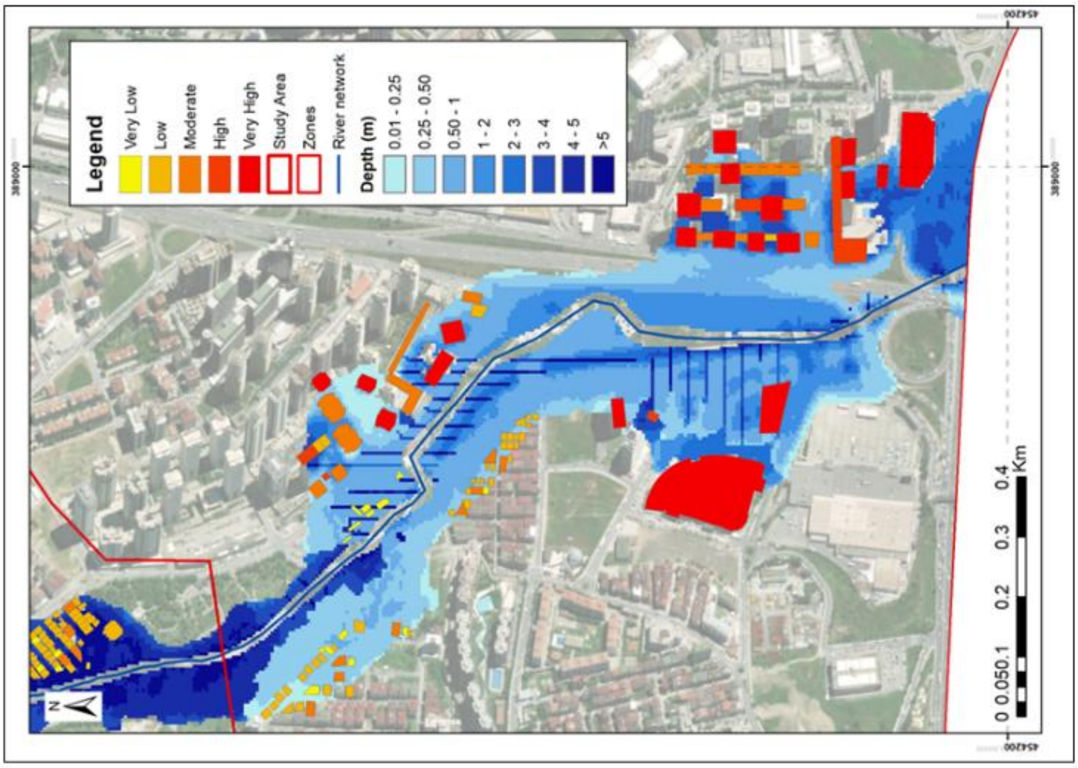

2019

Figure 7.2. Zone-5 urban flood risk maps (2020- 2019)

APPENDIX-7. (continued) Zone-5 urban flood risk maps

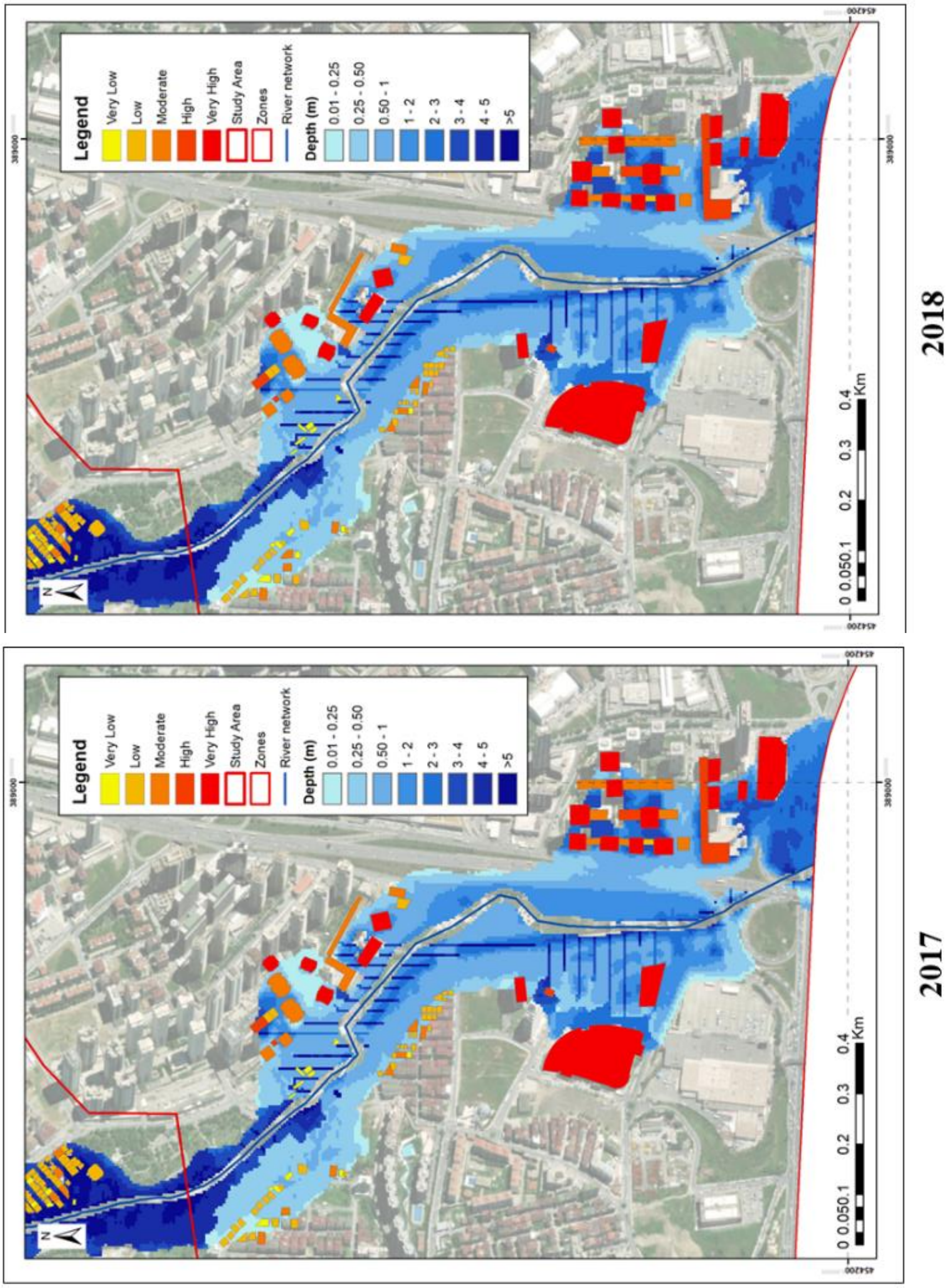

Figure 7.3. Zone-5 urban flood risk maps (2018- 2017)

APPENDIX-7. (continued) Zone-5 urban flood risk maps

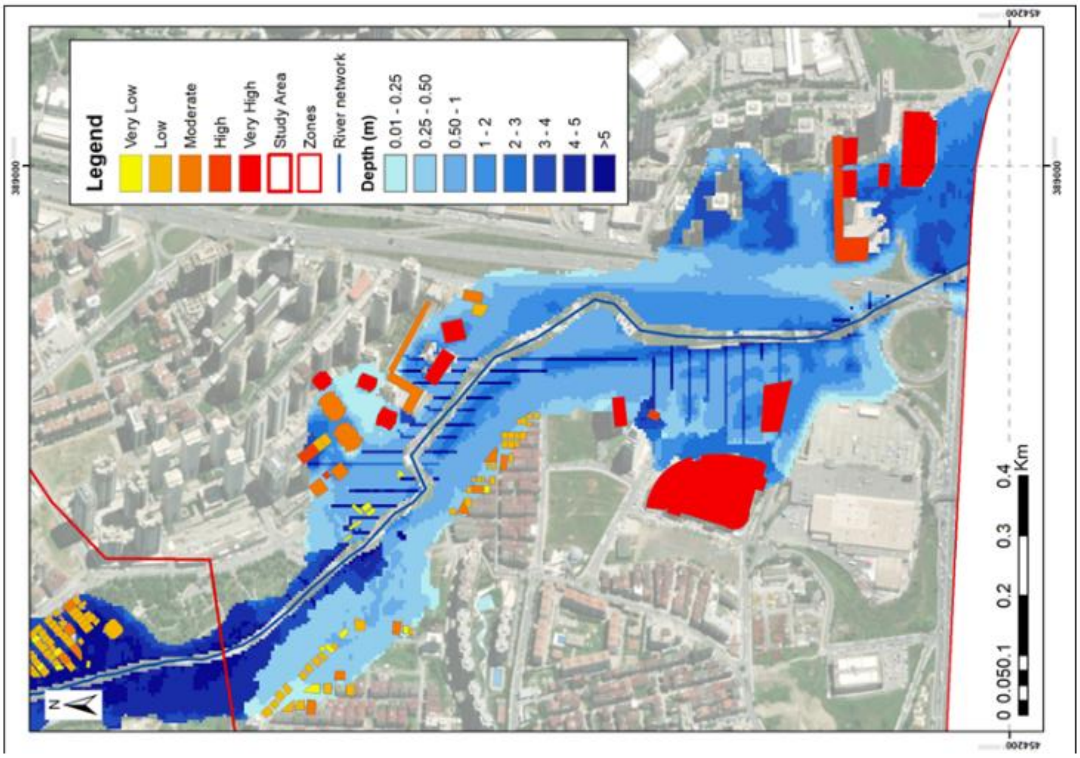

2016

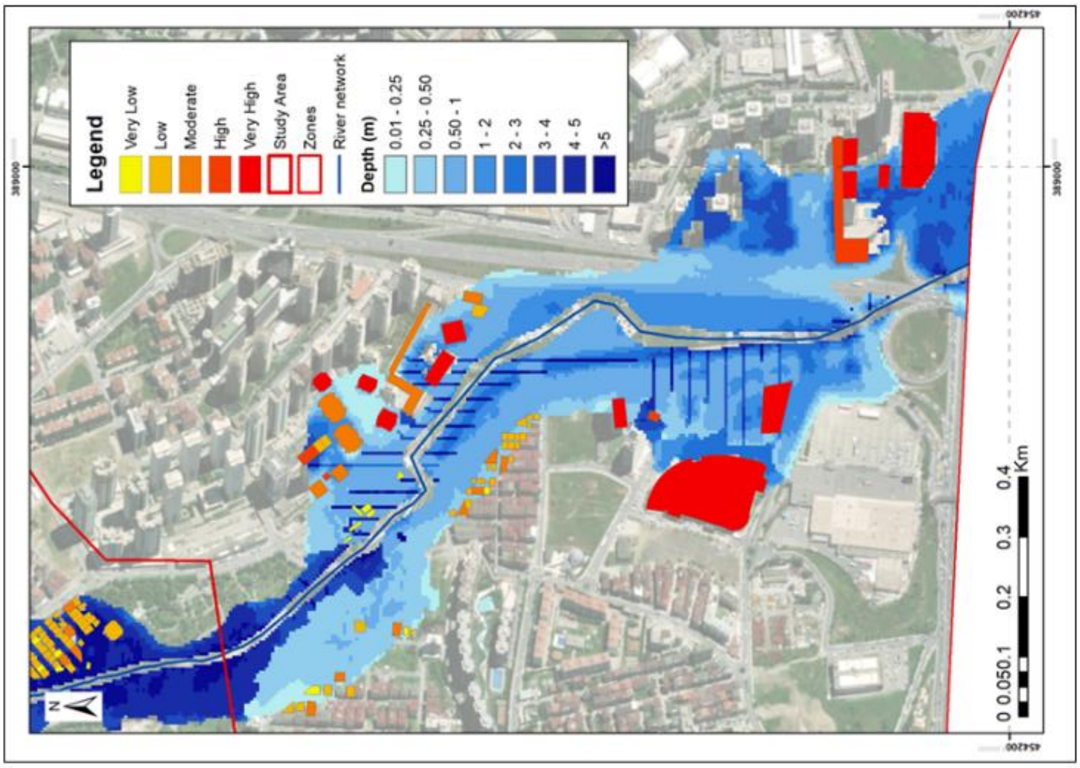

2015

Figure 7.4. Zone-5 urban flood risk maps (2016- 2015)

APPENDIX-7. (continued) Zone-5 urban flood risk maps

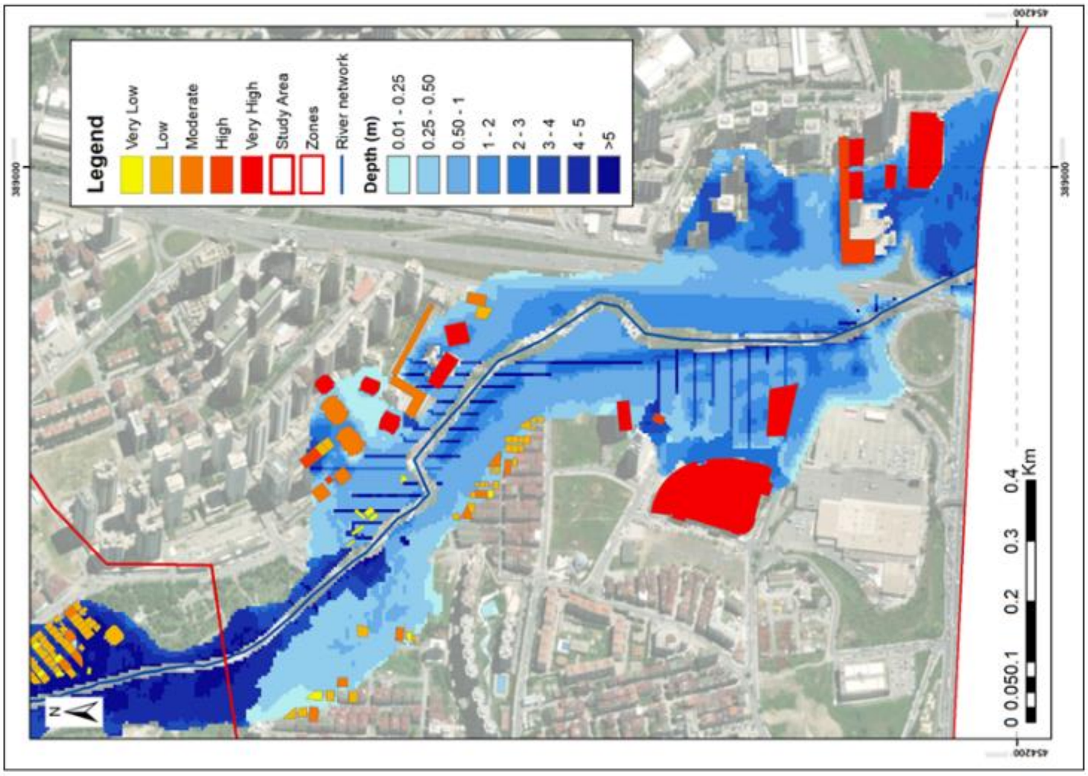

2014

Figure 7.5. Zone-5 urban flood risk maps (2014)

Gazili olmak ayrıcalıktır